

**People's Democratic Republic of Algeria**  
Ministry of Higher Education and Scientific Research



**Batna 2 University – Mostefa Ben Boulaïd**  
**Faculty of Technology**  
**Department of Mechanical Engineering**



## **Thesis**

Performed at  
(Mechanical Structures and Materials Laboratory - LaMSM))

Presented for the degree of:  
**LMD Doctor in Mechanical Engineering**  
**Option: Mechanical Construction**

Theme :

---

**Topological Optimization for Multi-Scale Modeling of  
Porous and Architectural Structures**

---

Defended by:

**AL-Kebssi Ebrahim Ahmed Ali**

**Before the Jury Composed of:**

Mr MADANI Salah	Professeur	Université de Batna2	Président
Mr OUTTAS Toufik	Professeur	Université de Batna2	Rapporteur
Mr AMEDDAH Hacène	Professeur	Université de Batna2	Co-Rapporteur
Mr BENHIZIA Abdennour	MCA	Université de Batna2	Examineur
Mr DJEBARA Abdelhakim	MCA	ENP Constantine	Examineur
Mr HECINI Mabrouk	Professeur	Université de Biskra	Examineur

**March 2022**

بِسْمِ اللّٰهِ الرَّحْمٰنِ الرَّحِیْمِ  
{ وَمَا أُوتِیْتُمْ مِّنَ الْعِلْمِ إِلَّا  
قَلِیْلًا }

صدق الله العظيم

*Dedication*

*I dedicate this work to:*

*My dear parents*

*My brothers*

*My fiancée*

*All family members*

*All my friends*

***AL-KEBSI Ebrahim Ahmed Ali***

## *Acknowledgement*

First of all, thanks to Allah, the Almighty, for giving me so much courage, patience and will to achieve this goal. I took a step back to reflect and try to list in the space of a few lines the people whose influence has shaped this work. I will certainly fail to quote people and I would apologize to them in advance.

I would like to express my gratitude and warm thanks to my Thesis Director, Professor **Outtas Toufik** and Professor **Ameddah Hacene**, my thesis co-supervisor, who have followed this work with particular interest, the confidence they have in me, their advice and constant support.

I would also like to address my thanks to Dr **Almutawakel Abdallah** who opened the doors of research to me by having assisted me throughout this work with not only his interventions in difficult times but also for his kindness and his nobility.

I would like to thank Professor **Madani Salah** for agreeing to chair the jury responsible for evaluating my work also I would like to thank the members of the jury Professors: **Hecini Mabrouk**, **Benhizia Abdennour**, **Djebara Abdelhakim** for having honoured me with their presence and accepted to judge my work.

I would like to thank the Director of the **Laboratory of Mechanical Structures and Materials (LaMSM)**, Professor **Toufik Outtas** for providing us with everything we need to complete this work.

I would also like to extend my warm thanks to Professor **Mohamed Masmoudi** for encouraging me to complete my work through his advices, conduct, simplicity and competence.

I want to thank my family for the continued support they have given me throughout these years of study. I would like to thank my colleagues and friends at the University of Batna 2.

**I will not forget either all those who, from near or far, by their competence, their technical assistance and their advice contributed to the realization of this work.**



**Contents**

*Dedication*..... **i**

*Acknowledgement*..... **ii**

**Contents**..... **iii**

**List of Figures** ..... **vii**

**List of Tables**..... **xi**

**General Introduction** ..... **1**

**Chapter I.** ..... **6**

**Literature review** ..... **6**

I.1 INTRODUCTION ..... 7

I.2 RECENT DEVELOPEMENT ..... 7

I.3 THE HETEROGENEOUS MATERIALS ..... 8

*I.3.1 Composite materials* ..... 9

        I.3.1.1 Classification of composite materials ..... 10

        I.3.1.2 The advantages and disadvantages of composite materials for different applications ..... 11

            a) Aeronautical applications ..... 11

            b) Military applications ..... 12

            c) Space applications (satellites) ..... 13

*I.3.2 Bio Mimetics materials*..... 13

*I.3.3 Porous materials*..... 16

        I.3.3.1 Definition of porosity..... 16

        I.3.3.2 Types of porosities..... 17

            a) According to the shape and origin of the pores..... 17

            b) According to pore size ..... 17

*I.3.4 Architectural materials* ..... 17

        I.3.4.1 Introduction..... 17

        I.3.4.2 Lattice structure ..... 18

        I.3.4.3 History of lattice structures ..... 19

        I.3.4.4 Importance of lattice structures ..... 20

        I.3.4.5 Types of lattice structures ..... 20

            a) Lattice structures in nature..... 20

            b) Prismatic and lattice structures ..... 21

            c) Lattice structure patterns ..... 22

            d) The implicit surfaces ..... 22

        I.3.4.6 Lattice structure properties..... 24

            a) Influences of a structure's property..... 24

            b) Stretching and bending-dominated structures..... 25

I.4 MULTI-SCALE IN HETEROGENEOUS MATERIALS ..... 27

*I.4.1 Multi-scale definition* ..... 28

        I.4.1.1 Macroscopic ..... 28

        I.4.1.2 Mesoscopic..... 28

        I.4.1.3 Microscopic ..... 28

*I.4.2 Finite element modeling* ..... 29

        I.4.2.1 Macroscopic scale modeling..... 29

I.4.2.2 Mesoscopic scale modeling .....	30
I.4.2.3 Microscopic scale modeling .....	30
a) Hexachiral lattice .....	30
b) Anti-tetrachiral lattice .....	31
c) Rotachiral lattice .....	31
d) Honeycomb lattice.....	32
I.5 CONCLUSION .....	33
<b>Chapter II.....</b>	<b>34</b>
<b>Topology optimization .....</b>	<b>34</b>
II.1 CONTEXT OF THE PROBLEM.....	35
II.2 INTRODUCTION .....	35
II.3 SIGNIFICANCE AND HISTORY .....	35
II.4 OPTIMIZATION OF STRUCTURES .....	36
<i>II.4.1 Types of discretization of a structure .....</i>	<i>38</i>
II.4.1.1 Lattice structures .....	39
II.4.1.2 Continuous structures.....	39
<i>II.4.2 Types of optimization of structures .....</i>	<i>40</i>
II.4.2.1 Dimensional optimization .....	40
II.4.2.2 Shape optimization .....	41
II.4.2.3 Topological optimization.....	41
II.5 METHOD OF TOPOLOGY OPTIMIZATION (TO).....	43
<i>II.5.1 Application of the topological optimization method.....</i>	<i>45</i>
The procedure for TO depend of the following fundamental steps: .....	45
a) Define and describe the problem .....	45
b) Select the element types. ....	45
c) Specify optimized and non-optimized regions.....	45
d) Define and control the load cases. ....	45
e) Define and control the optimization process. ....	45
f) Review results. ....	46
<i>II.5.2 The topology optimization methods developed in additive manufacturing applications .....</i>	<i>46</i>
II.5.2.1 Homogenization optimization (Solid Isotropic Microstructure with Penalization (SIMP)) method .....	46
II.5.2.2 Evolutionary Structural optimization ESO-BESO method.....	47
II.5.2.3 Level set method (LSM) .....	48
II.5.2.4 Lattice structure topology optimization (LSTO) method.....	49
a) Cell structure .....	50
b) Cell size and density.....	50
c) Cell orientation .....	50
d) Material selection .....	50
<i>II.5.3 Modeling techniques for porosity gradients.....</i>	<i>50</i>
II.5.3.1 Library of cells of uniform size .....	51
II.5.3.2 Parameterized cells of uniform size .....	51
II.5.3.3 Gradients for implicit surfaces .....	52
II.5.3.4 Cells of variable sizes .....	53
II.6 CONCLUSION .....	53
<b>Chapter III.....</b>	<b>54</b>
<b>Additive Manufacturing .....</b>	<b>54</b>
III.1 INTRODUCTION.....	55
III.2 ADDITIVE MANUFACTURING MATERIALS .....	56
III.3 ADDITIVE MANUFACTURING TECHNOLOGIES .....	57

<b>III.3.1 Vat Photopolymerization</b> .....	58
<b>III.3.1.1 Stereolithography (SLA)</b> : .....	59
<b>III.3.1.2 Digital Light Processing (DLP)</b> : .....	60
<b>III.3.1.3 Continuous Digital Light Processing (CDLP)</b> : .....	61
<b>III.3.2 Material Extrusion</b> .....	61
<b>III.3.3 Material jetting (MJ)</b> .....	63
<b>III.3.3.1 Single Material jetting (SMJ)</b> : .....	64
<b>III.3.3.2 Nanoparticle Jetting (NPJ)</b> : .....	65
<b>III.3.3.3 Drop-On-Demand (DOD)</b> : .....	65
<b>III.3.4 Binder Jetting (BJ)</b> .....	66
<b>III.3.5 Powder Bed Fusion</b> .....	67
<b>III.3.5.1 Multi Jet Fusion (MJF)</b> : .....	69
<b>III.3.5.2 Selective Laser Sintering (SLS)</b> : .....	69
<b>III.3.5.3 Direct Metal Laser Sintering (DMLS/ SLM)</b> : .....	70
<b>III.3.5.4 Electron Beam Melting (EBM)</b> : .....	71
<b>III.3.6 Direct Energy Deposition</b> .....	71
<b>III.3.6.1 Laser Engineering Net Shape (LENS)</b> :.....	72
<b>III.3.6.2 Electron Beam Additive Manufacturing (EBAM)</b> : .....	72
<b>III.3.7 Sheet lamination</b> .....	73
<b>III.4 APPLICATIONS FIELDS OF ADDITIVE MANUFACTURING</b> .....	74
<b>III.4.1 Civil Engineering Construction</b> .....	75
<b>III.4.2 Manufacturing</b> .....	75
<b>III.4.2.1 Additive manufacturing in the aircraft industry</b> .....	76
<b>III.4.3 Medicine</b> .....	77
<b>III.4.3.1 Bio-printers</b> .....	77
<b>III.4.3.2 Digital dentistry</b> .....	77
<b>III.4.3.3 Prostheses</b> .....	78
<b>III.4.3.4 Artificial organs</b> .....	78
<b>III.4.4 Domestic use</b> .....	79
<b>III.4.5 Clothes</b> .....	79
<b>III.4.6 Academic</b> .....	79
<b>III.5 CONCLUSION</b> .....	79
<b>Chapter IV</b> .....	<b>81</b>
<b>Case Study</b> .....	<b>81</b>
<b>IV.1 INTRODUCTION</b> .....	82
<b>IV.2 THE FIELD OF AEROSPACE</b> .....	82
<b>IV.2.1 Designing Lattice Structures</b> .....	82
<b>IV.2.2 General Architecture of the Proposed Procedure</b> .....	82
<b>IV.2.3 Design of Equivalent CAD Model for Turbine Blade. (Initialization)</b> .....	83
<b>IV.2.3.1 Properties of Material</b> .....	84
<b>IV.2.3.2 Boundary Conditions</b> .....	84
<b>IV.2.4 Topology Optimization of Lattice Structures Design</b> .....	86
<b>IV.2.4.1 Optimization</b> .....	87
<b>IV.2.5 Triply periodic minimal surface (TPMS) -based Lattice Structures Design</b> .....	88
<b>IV.2.6 Manufacturability of Lattice Structures</b> .....	89
<b>IV.2.7 The effectiveness of the proposed method</b> .....	91
<b>IV.3 THE FIELD OF BIOMECHANICAL</b> .....	92
<b>IV.3.1 General Architecture of the Proposed Procedure for the cancellous bone</b> .....	92
<b>IV.3.2 Material</b> .....	92
<b>IV.3.2.1 The Design of the human bone with Porous Lattice Structures</b> .....	92
<b>IV.3.2.2 Design 3D Lattice structures for Cancellous Bone TPMS-based</b> .....	93

<i>IV.3.3 Method</i> .....	96
<b>IV.3.3.1</b> The study of numerical simulations of lattice structures.....	96
<b>IV.3.3.2</b> Predict the Stiffness of the lattice structure of the porous model by using Gibson and Ashby classical method .....	98
<b>IV.3.3.3</b> Mechanical testing.....	99
<b>a)</b> Fused Filament Fabrication (FFF) Technology.....	99
<b>b)</b> Stiffness Performance Testing of Lattice Structures.....	100
<b>IV.3.4</b> <i>The effectiveness of the proposed method</i> .....	101
IV.4 CONCLUSION .....	101
<b>Chapter V</b> .....	<b>102</b>
<b>Numerical and experimental results</b> .....	<b>102</b>
V.1 INTRODUCTION .....	103
V.2 AEROSPACE APPLICATION.....	103
<b>V.2.1 Results and Discussion</b> .....	<b>103</b>
<b>V.2.1.1</b> Designing and Validation.....	103
<b>a)</b> The first stage (the finite element analysis (FEA)) .....	103
<b>b)</b> The second stage is a lattice structure topology optimization (LSTO).....	105
<b>c)</b> The third stage (the finite element validation analysis (FEVA)) .....	106
<b>V.2.1.2</b> Results discussion.....	108
V.3 BIOMECHANICAL APPLICATION .....	111
<b>V.3.1 Results and Discussion</b> .....	<b>111</b>
<b>V.3.1.1</b> Modelling Structural for the proposed lattice Structures .....	111
<b>a)</b> Finite Element Simulation Results .....	113
<b>V.3.1.2</b> Result of Effective Stiffness of lattice structures Porous by (Gibson and Ashby) Method .....	114
<b>V.3.1.3</b> Experimental Method Results .....	115
<b>V.3.1.4</b> Results discussion.....	119
V.4 CONCLUSIONS .....	120
<b>General Conclusion</b> .....	<b>121</b>
<b>Bibliography</b> .....	<b>124</b>
<b>Annex: Scientific Publications</b> .....	<b>135</b>
<b>ملخص</b> .....	Erreur ! Signet non défini.

**List of Figures**

FIGURE I.1 REPRESENTATION OF POROUS MATERIALS WITH ORDERED (LEFT) AND RANDOM (RIGHT) POROSITIES [24]..... 8

FIGURE I.2 EXAMPLE OF MULTIPHASIC HETEROGENEOUS MATERIALS OBTAINED BY TOMOGRAPHY [28] ..... 9

FIGURE I.3 MICROSTRUCTURE OF HETEROGENEOUS MATERIALS [29]..... 9

FIGURE I.4 HETEROGENEOUS REINFORCING COMPOSITES: (A) FIBERS AND (B) PARTICLES [30]..... 10

FIGURE I.5 COMPOSITE PARTS ON AIRCRAFT STRUCTURES - BOEING 787 (SOURCE BOEING) [35] ..... 12

FIGURE I.6 CARBON / EPOXY COMPOSITE PARTS ON AIRCRAFT STRUCTURES - MIRAGE 2000 [36]..... 12

FIGURE I.7 MISSILE GUIDE VANES [37] ..... 12

FIGURE I.8 EXAMPLE OF A SATELLITE [38] ..... 13

FIGURE I.9 TYPICAL BIOMIMETIC EXAMPLES [39]..... 14

FIGURE I.10 NATURAL AND ARTIFICIAL CELLULAR STRUCTURE [41]..... 15

FIGURE I.11 DIFFERENT TYPES OF PORES [42] ..... 16

FIGURE I.12 DIFFERENT TYPES OF POROUS MEDIUM OF COMPLEX MICROSTRUCTURE: A) CLOSED-CELL METAL FOAM; B) HOLLOW ALUMINA SPHERES EMBEDDED IN A MAGNESIUM MATRIX; C) HOLLOW SPHERE FOAM Fe088.CR012 [44] ..... 17

FIGURE I.13 ARCHITECTURED MATERIALS [46]..... 18

FIGURE I.14 EXAMPLES OF ARCHITECTURE MATERIALS [47]..... 18

FIGURE I.15 LATTICE STRUCTURES IN NATURE [49] ..... 21

FIGURE I.16 STOCHASTIC, PERIODIC: PRISMATIC, AND LATTICE STRUCTURES [49]..... 21

FIGURE I.17 THE DIFFERENT TPMS TOPOLOGIES USED TO CREATE IPCs. A) A SINGLE UNIT CELL B) A 3X3X3 REPETITION OF THE TPMS C) THE DESIGNED IPC D) A (111) PLANE CUT THAT REVEALS THE INTERCONNECTIVITY OF THE TPMS E) A SAMPLE FABRICATED USING 3D PRINTING [53]..... 23

FIGURE I.18 YOUNG'S MODULUS-DENSITY SPACE MATERIALS DIAGRAM [47]..... 24

FIGURE I.19 THREE MAIN LATTICE STRUCTURE DESIGN VARIABLE INFLUENCE [48]..... 25

FIGURE I.20 SCALES AND SIZES OF CONSTITUENTS IN A BUILDING MATERIAL [55]..... 28

FIGURE I.21 REPRESENTATION OF MODELING OF MULTISCALE BRAIDED STRUCTURES. (A) MICRO-SCALE MODEL; (B) MESOSCALE MODEL; (C) FULL-SCALE MODEL; (D) MACRO-SCALE MODEL [57]..... 29

FIGURE I.22 (A) PERIODIC CELL WITH GEOMETRIC PARAMETERS, (B) HEXACHIRAL LATTICE WITH UNIT-CELL (BLUE) AND PERIODICITY VECTORS  $v_1$  AND  $v_2$  (RED) [59]..... 31

FIGURE I.23 (A) PERIODIC CELL WITH GEOMETRIC PARAMETERS, (B) ANTI-TETRACHIRAL LATTICE WITH UNIT-CELL (BLUE) AND PERIODICITY VECTORS  $v_1$  AND  $v_2$  (RED) [60]..... 31

FIGURE I.24 (A) PERIODIC CELL WITH GEOMETRIC PARAMETERS, (B) ROTACHIRAL LATTICE WITH UNIT-CELL (BLUE) AND PERIODICITY VECTORS  $v_1$  AND  $v_2$  (RED) [62]..... 32

(A) HONEYCOMB UNIT-CELL (B) HONEYCOMB LATTICE ..... 32

FIGURE I.25 (A) PERIODIC CELL WITH GEOMETRIC PARAMETERS. (B) HONEYCOMB LATTICE WITH UNIT-CELL (BLUE) AND PERIODICITY VECTORS $v_1$ AND $v_2$ (RED) [62].....	32
FIGURE II.1 THE OPTIMIZATION OF STRUCTURES [70].....	38
FIGURE II.2 DIFFERENT TYPES OF FINITE ELEMENTS [69].....	38
FIGURE II.3 EXAMPLE OF A TRUSS STRUCTURE AND A CROSS SECTION [69].....	39
FIGURE II.4 DIFFERENT REPRESENTATIONS OF CONTINUOUS STRUCTURES [69].....	40
FIGURE II.5 PARAMETRIC OPTIMIZATION OF A LATTICE[69].....	41
FIGURE II.6 SHAPE OPTIMIZATION OF A PLATE [69].....	41
FIGURE II.7 TOPOLOGICAL OPTIMIZATION OF A TRELIS [71].....	42
FIGURE II.8 TOPOLOGICAL OPTIMIZATION OF A CONTINUOUS STRUCTURE [71].....	42
FIGURE II.9 CATEGORIES OF OPTIMIZATION A) SIZING B) SHAPE C) TOPOLOGY [64].....	43
FIGURE II.10 A)GYROID B)PRIMITIVE C)DIAMOND D)IWP E)LIDINOID F)NEOVIVUS G)OCTO H)SPILT [93].....	50
FIGURE II.11 INTERPOLATION FUNCTIONS AND CELL LIBRARY FOR THE GENERATION OF ARCHITECTURAL MATERIALS A) VISUALIZATION OF LINEAR INTERPOLATION B) LIBRARY CELLS ADDED TO THE DISCRETE BODY.....	51
FIGURE II.12 MODELING OF A LINEAR GRADIENT WITH REPRESENTATION BY FUNCTIONS [98].....	52
FIGURE II.13 TOPOLOGICAL OPTIMIZATION PRODUCED WITH PARAMETERIZED CELLS [100].....	52
FIGURE III.1 ADDITIVE MANUFACTURING TECHNOLOGIES [111].....	58
FIGURE III.2 SOME SLA METHODS PRINT PARTS UPSIDE DOWN AS THEY ARE PULLED FROM THE RESIN [108].....	59
FIGURE III.3 FORM LABS MACHINE FROM STL[116].....	60
FIGURE III.4 DLP ENVISION TEC MACHINE [117].....	61
FIGURE III.5 CDLP CARBON 3D MACHINE [118].....	61
FIGURE III.6 FDM EXTRUDES THERMOPLASTIC FROM A HEATED NOZZLE ALONG A PREDETERMINED PATH TO ACCUMULATE PARTS [120].....	62
FIGURE III.7 ZORTRAX MACHINE FROM FDM [122].....	63
FIGURE III.8 AN INKJET PRINTER ILLUSTRATING THE SIZE OF THE MACHINES [108] [123].....	64
FIGURE III.9 MJ'S STRATASYS MACHINE [123].....	65
FIGURE III.10 : NPJ XJET MACHINE [124].....	65
FIGURE III.11 DOD SOLIDSCAAPE MACHINE [125].....	66
FIGURE III.12 A BINDER PROJECTION PART AFTER REMOVING THE PRINTING POWDER [102].....	66
FIGURE III.13 BJ'S EXONE MACHINE [126].....	67
FIGURE III.14 POWDER PIN REMOVAL FROM THE SLS PROCESS WITH THE PRINTED PARTS STILL ENCLOSED IN THE UNSINTERED POWDER [127] [108].....	68
FIGURE III.15 HP JET FUSION 4200 MACHINE FROM MJF [128].....	69

FIGURE III.16 SINTERIT MACHINE FROM SLS [129] .....	70
FIGURE III.17 SLM MACHINE FROM SLM [130] .....	70
FIGURE III.18 EBM ARCAM Q10 PLUS MACHINE [131] .....	71
FIGURE III.19 LENS OPTOMECH MACHINE [133].....	72
FIGURE III.20 EBAM SCIAKY MACHINE [134] .....	73
FIGURE III.21 LOM's MCOR MACHINE (FOR PAPER) AND IMPOSSIBLE OBJECTS MACHINE FROM LOM (FOR COMPOSITES) [135].....	74
FIGURE III.22 3D PRINTING APPLICATIONS .....	74
FIGURE III.23 3D CONSTRUCTION [136].....	75
FIGURE III.24 3D MODEL OF TURBINE [138] .....	75
FIGURE III.25 APPLICATIONS OF ADDITIVE MANUFACTURING IN THE AERONAUTICS SECTOR - SOURCE STRATASYS [139] .....	76
FIGURE III.26 FIRST TOTAL AND AUTONOMOUS ARTIFICIAL HEART [141] .....	77
FIGURE III.27 3D PRINTING AND THE DENTAL WORLD [142] .....	78
FIGURE III.28 HAND PROSTHESES [141].....	78
FIGURE III.29 ARTIFICIAL ORGANS FOR THE STUDY OF MEDICINE [143].....	79
FIGURE IV.1 GENERAL ARCHITECTURE OF THE PROPOSED PROCEDURE.....	83
FIGURE IV.2 3D MODEL TO TURBINE BLADE.....	83
FIGURE IV.3 BOUNDARY CONDITIONS OF THERMO-MECHANICAL LOADS APPLIED ON BLADE .....	86
FIGURE IV.4 STANDARD TOPOLOGY OPTIMIZATION DESIGN FOR A PART OF BLADE .....	87
FIGURE IV.5 SELECTIVE LASER MELTING (SLM): (A) TECHNOLOGY PRINCIPLE, (B) PROCESS DURING OPERATION AND (C, D) MOLYBDENUM DEMONSTRATOR PARTS FABRICATED BY SLM AT PLANSEE SE .....	91
FIGURE IV.6 GENERAL ARCHITECTURE OF THE PROPOSED PROCEDURE.....	92
FIGURE IV.7 A THREE-DIMENSIONAL IMAGE OF A 4-MILLIMETRE-CUBE OF BONES (A) A 30-YEARS-OLD PERSON WITH ARCHITECTURE AND NORMAL DENSITY (B) A 63 YEARS OLD PERSON WITH FRAGILE ARCHITECTURE AND LOW NORMAL DENSITY .....	93
FIGURE IV.8 3D MODEL TO THE CUBE OF THE LATTICE STRUCTURE (A) GYROID, (B) PRIMITIVE AND (C) DIAMOND.....	95
FIGURE IV.9 THE UNIT CELLS OF THE LATTICE STRUCTURES WITH THE VARIOUS REGULARLY FOR THE LATTICE STRUCTURES.....	96
FIGURE IV.10 BOUNDARY CONDITIONS AND THE FINITE ELEMENT MESH OF THE LATTICE STRUCTURES .....	97
100	
FIGURE IV.11 (A) 3D PRINTER ZORTRAX M200+, (B) GYROID, (C) PRIMITIVE AND (D) DIAMOND WITH THE POROSITY 70%, 50% AND 30%, RESPECTIVELY FOR EACH TYPE .....	100

---

FIGURE IV.12 THE UNIAXIAL COMPRESSION TEST MACHINE (JINAN UNIVERSAL TESTING MACHINE MODEL WDW-100S).....	101
FIGURE V.1 FINITE ELEMENT MESH OF THE INITIAL DESIGN.....	104
FIGURE V.2 DISTRIBUTION OF TOTAL HEAT FLUX, STRESS AND DEFORMATION IN THE THERMO MECHANICAL STATE OF THE INITIAL DESIGN.....	104
FIGURE V.3 OPTIMAL DENSITY DISTRIBUTION.....	105
FIGURE V.4 (A) THE UNIT CELLS OF EACH TPMS; (B) THE INITIAL DESIGN; (C) A DIFFERENT FILLING DENSITIES; (D) THE INTERNAL BLADE STRUCTURE BUILT WITH LATTICE STRUCTURES (GYROID, DIAMOND AND PRIMITIVE).....	106
FIGURE V.5 FINITE ELEMENT MESH OF THE FINAL OPTIMIZED DESIGNS.....	107
FIGURE V.6 RATE OF REDUCED WEIGHT.....	109
FIGURE V.7 RATE OF LOW STRESS.....	110
FIGURE V.8 RATE OF LOW DEFORMATION.....	110
FIGURE V.9 DISTRIBUTION OF STRESS AND STRAIN IN SIMULATION NUMERICAL FOR THE THREE DESIGNS: A) GYROID, B) PRIMITIVE, C) DIAMOND.....	112
FIGURE V.10 VARIATION OF EQUIVALENT ELASTIC MODULUS IN FACT OF $(1-\Delta)$ POROSITY FOR THE THREE TYPES OF LATTICE STRUCTURES.....	113
FIGURE V.11 COMPARISON OF THE TWO METHODS OF THE EQUIVALENT ELASTIC MODULUS FOR THE LATTICE STRUCTURES.....	115
FIGURE V.12 THE COMPRESSIVE STRESS-STRAIN CURVE OF THREE MODELS BY THE UNIAXIAL COMPRESSION.....	117
FIGURE V.13 EFFECT OF RATIO POROSITY ON EQUIVALENT ELASTIC MODULUS IN THE PHYSICAL TEST.....	118
FIGURE V.14 COMPARISON OF EQUIVALENT ELASTIC MODULUS FOR THE LATTICE STRUCTURES BY THE THREE METHODS.....	119



**List of Tables**

TABLE I.1 DEFINITION OF ELEMENTARY AND LATTICE STRUCTURE [49] ..... 22

TABLE I.2 OCTET-TRUSS, TETRAKAIDECAHEDRON AND OPEN-CELL FOAM ELEMENTARY  
STRUCTURES [48]..... 22

TABLE I.3 TYPES OF DEFORMATION FOR LATTICE STRUCTURES [54] ..... 26

TABLE I.4 INFLUENCE OF STRETCHING AND BENDING-DOMINATED STRUCTURES ON  
MECHANICAL PROPERTIES [48]..... 27

TABLE III.1 COMMERCIAL MATERIALS USED IN THE MANUFACTURING OF AM..... 57

TABLE III.2 CELL PHOTOPOLYMERIZATION TECHNOLOGIES, ITS MANUFACTURERS, AND THE  
MATERIALS USED ..... 59

TABLE III.3 MATERIAL EXTRUSION TECHNOLOGIES, MANUFACTURERS, AND MATERIALS USED  
..... 63

TABLE III.4 JET TECHNOLOGIES OF MATERIALS, MANUFACTURERS, AND ITS MATERIALS USED. 64

TABLE III.5 BINDING JET TECHNOLOGIES, ITS MANUFACTURERS, AND MATERIALS USED ..... 67

TABLE III.6 POWDER BED FUSION TECHNOLOGIES, ITS MANUFACTURERS, AND MATERIALS  
USED..... 68

TABLE III.7 DIRECT ENERGY DEPOSIT TECHNOLOGIES, THEIR MANUFACTURERS, AND THE  
MATERIALS USED ..... 72

TABLE III.8 LAMINATED OBJECT MANUFACTURING TECHNOLOGIES, ITS MANUFACTURERS, AND  
THE MATERIALS USED ..... 73

TABLE IV.1 PHYSICAL AND MECHANICAL PROPERTIES OF INCONEL 718 ..... 84

TABLE IV.2 STEADY-STATE BOUNDARY CONDITION FOR THE THERMO-MECHANICAL ANALYSIS  
..... 85

TABLE IV.3 THE UNIT CELLS OF EACH TPMS ..... 89

TABLE IV.4 THE UNIT CELLS FOR EACH LATTICE STRUCTURE OF TPMS ..... 94

TABLE IV.5 ELEMENTAL DISTRIBUTION OF MESH..... 97

TABLE V.1 DISTRIBUTION OF TOTAL HEAT FLUX, STRESS AND DEFORMATION IN THE THERMO  
MECHANICAL STATE OF THE FINAL OPTIMIZED DESIGNS..... 108

TABLE V.2 RESUME OF NUMERICAL SIMULATION RESULTS ..... 113



# **General Introduction**



## 1. Context

In recent years, rapid developments in the field of computing and manufacturing techniques have made significant progress in the development of designs with smart engineering character in terms of high accuracy and complex internal configurations [1]. Many modern technologies use materials with properties that traditional materials cannot. This is the case for certain materials used in the automotive, naval aviation, aerospace industries and medical...etc. Therefore, engineers are increasingly looking for materials that are robust, rigid and capable of withstanding impact, abrasion and corrosion. Particularly, in aerospace and aviation, designing parts that maximize stiffness and minimize structure size has recently gained increasing attention mainly because it reduces fuel consumption and increases products quality and carrying capacity [2]. Also, In the biomechanical, significant progress has been observed in processes of bone remodeling and relying on useful grafts to replace lost cancellous bone due to several factors related to bone remodeling deficiency, increased pore space and osteoporosis [3]. For bone transplantation, it is ideal to seek a natural bone replacement or an endoprosthesis biocompatible able to replace the bone structure with an artificial structure with mechanical properties are similar to those of the original bone [4][5].

Therefore, cellular and lattice structures are widely used in designing engineering applications thanks to their lightweight structures with complex engineering character and the availability of manufacturing techniques that allow their production [6], [7]. Thus, the use of single-scale lattice structures helps to design and manufacture them with desirable mechanical and physical properties (low mass density, highest stiffness possible and efficiency in resisting high temperatures) due to their useful mechanical properties (lightweight with relatively high stiffness, high porosity, better local buckling resistance, good absorption of energy and high capabilities in heat transfer)[8]. The incorporation of lattice materials with graded microstructures into macrostructures under multiple loading conditions necessitate choosing the suitable type of:

- (1) The technique that achieves optimum design (i.e. finding the optimal density distribution of lattice structures in the design space (low mass density with maximum stiffness possible)).
  - (2) Materials that gives design high efficiency under hard boundary conditions.
  - (3) The manufacturing design technique takes into account their complex internal architecture.
-

To find the optimum mechanical properties of the lattice structures in order to increase designs endurance of high stresses effects and resist lateral effects relying on three basic parameters: unit cell microstructure, relative density and the appropriate type of material. The microstructure design of the unit cell is considered one of the most essential factors affecting the improvement of mechanical properties [7]. To generate the unit cell, we will design a graded lattice structure using the Lattice Structure Topology Optimization (LSTO) method. The graded lattice structure is built by repeatable unit cells in a 3D framework by using the implicit surfaces derived from the triply periodic minimal surface (TPMS) particularly: Diamond, Gyroid and Primitive. These surfaces present considerable advantages such as: the ease of representing complex topologies, providing at the same time a flexible and robust technical representation of the mathematical formulations considered compared to other representations of surfaces [9]. At the same time, the topology optimization technique provides an optimal distribution for lattice structures under specific constraints to realize maximum stiffness and minimum structure size [1]. Relative density is another affecting factor in the improvement of mechanical properties as it determines the strength of lattice structures [10], [11]. For graded lattice structures, the relative density has a great influence on the mechanical properties of the unit cell, so the density of each unit of finite element is determined by design variable (i.e. relative density).

## **2. Problem and Objectives of the thesis**

This research work focuses on understanding structural morphologies at different scales and studying their mechanical behavior in the context of the development of optimal topology and is motivated by the concern for the creation and enhancement of new porous and architectural materials in the fields of industrial, aerospace, and even medical applications. Two issues will be highlighted that concerning the aerospace and medical field.

In gas turbine engines, designing and manufacturing blades play an important role in achieving the highest levels of efficiency, performance and operational flexibility. When designing turbine blades, it is important to put into consideration that they will operate under harsh conditions [12].

bone defects are among the major problems caused by external trauma, bone tumor, fractures or during normal ageing [5][13]. Also, the inner bone structure changes and deterioration over time due to Osteoporosis the microstructure for bone mass and changes in material properties through reorientation of trabecular [3][13]. For bone transplantation, it is ideal to seek a natural

---

bone replacement or an endoprosthesis biocompatible able to replace the bone structure with an artificial structure with mechanical properties are similar to those of the original bone [4][5].

### **3. Contributions**

In the aerospace field for the sake of reducing fuel consumption, decreasing the manufacturing cost and increasing the carrying capacity in the aviation field, manufacturers have recently used lattice structures as an emerging solution for reducing weight and manufacturing time. This thesis pays special attention to the design of graded density lattice structures for dense materials with thermomechanical behavior in turbine blades.

The major contribution is manifested in the combined use of implicit surfaces, deformable modelling, finite element analysis and topology optimization to create optimized designs for graded density lattice structures that replace the internal solid volume of the turbine blade.

In the medical field, the major contribution of this work is to get a prediction for the effective mechanical properties of lattice structures by the finite element simulation and Gibson and Ashby method calculation and uniaxial compression. This contribution helps to determine the effective stiffness of three lattice structures (Gyroid, Primitive and Diamond) with different porosity by adjusting the structural parameters for the samples manufactured when tested.

After a general conclusion describing the context of the work, the problematic and the contribution, this thesis is organized as follows:

In chapter one, we aim to expose generalities on heterogeneous materials and mentioned their types including composite materials, porous materials and architectural materials taken from bio-mimetics materials, questions related to their scales and the problem related to the passage between a microstructural and macrostructural behavior. In addition to the interest of a porous and architectural materials approach making it possible to predict the global behavior from that of heterogeneities, we also present the approach of characterizing multiscale modeling for the architectural materials (lattice structures) and mention their properties, types.

In chapter 2, after having defined the general notions of an optimization problem, we present the classical process of structure optimization. Subsequently, we highlight the category of structures, and we detail the different types of optimization (dimensional, shape and topological). Finally, after having raised the scientific obstacles linked to the mechanical constraints considered, we present the various contributions in the topology optimization in this work.

The chapter three is interested to "additive manufacturing", the technologies of this process, its machines, its common manufacturers and the materials used and the applications and fields of use of each process and in particular the processes (PBF, FFF).

The fourth chapter describes the method of our proposed approach and designing the lattice structures with a different architecture in two fields (Aerospace, Biomechanical).

In the final and fifth chapter, the results obtained are presented and describe the validation phase of our proposed approach for the designs of the lattice structures with a different architecture in two fields (Aerospace, Biomechanical).

## **Chapter I.**

# **Literature Review**





## I.1 Introduction

In this chapter, we aim to expose generalities on heterogeneous materials and mentioned their types including a composite materials, porous materials and architectural materials taken from bio-mimetics materials, questions related to their scales and the problematic related to the passage between a microstructural and macrostructural behavior. In addition to the interest of a Porous and architectural materials approach making it possible to predict the global behavior from that of heterogeneities, we also present the approached of characterizing a multiscale modeling for the architectural materials (lattice structures) and mention their properties, types.

## I.2 Recent developpement

The development of new materials is address to the needs of users (builders) who always want materials that are more efficient, more economical and last longer. Researchers are often called upon to optimize solutions already in use. However, in some cases, they have to completely rethink the problem and consider "new materials". Indeed, we no longer discover new materials, but rather we create new associations of materials.

One of the great needs of mechanical researchers is to be able to predict the properties of materials without even producing them, from the properties of elementary constituents. This quest has led to the recent growth of theoretical models making it possible to find the homogenized behavior of a heterogeneous material. Their development requires an in-depth reflection on the boundary conditions, on the influence of the volume fraction of the phases, their volume distribution and their morphology. We are faced with complex multi-physical phenomena, the essential tool for modeling these phenomena at all scales is numerical simulation, it integrates several scales of representation in the same model in order to predict the influence of the behavior of small scales on the behavior of the whole structure at the macroscopic scale.

Today, the evolution of numerical simulation has also authorized the deployment of a large number of new materials, known as Porous and architectural materials. Because it is a more flexible material with controlled porosity. A major challenge, however, is to adjust the porosity to ensure mechanical compatibility. Indeed, the porosity, as well as the size and interconnectivity of the pores, are parameters that will significantly affect the mechanical and physical properties [1][2].

Several manufacturing processes can control these properties, but these are generally used for the production of metallic foams having a random pore distribution [16]. The development of new processes such as additive manufacturing (AM) has, however, made it possible to

generate materials with an organized pore distribution and varied cellular structures. Figure I.1. presents an example of two types of porous materials, namely an architectural material with ordered porosity and a metallic foam with random porosity. In the context of the work presented in this work, porous materials with an organized structure are treated. Architectural structures are formed by a network of members fixed together [17]. A chord network is generated by the repetition of a cell in space which can also be used to characterize the structure. When the dimensions of the cell are significantly smaller than those of the structure, the network of members can also be designated as an architectural material. Architected materials, which have a certain porosity, are particularly interesting [1][5 - 6].

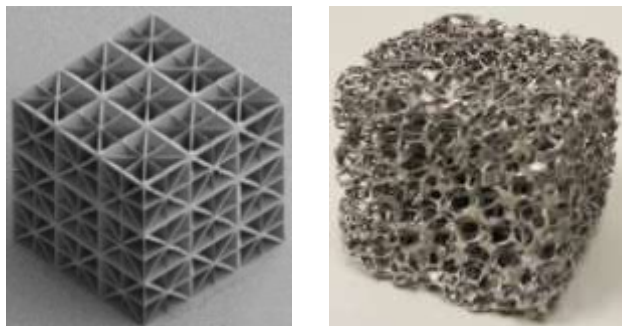


Figure I.1 Representation of porous materials with ordered (left) and random (right) porosities [17]

### I.3 The Heterogeneous Materials

Heterogeneous materials can be defined as materials with dramatic heterogeneity in strength from one domain area to another. It has two (two-phase) or several phases (multi-phase). This strength heterogeneity can be caused by microstructural heterogeneity, crystal structure heterogeneity or compositional heterogeneity. Figure I.2.

The essential advantage of this type of material is the important structural properties, which their elementary constituents do not individually possess, to enable them to fulfill many technical functions. The examples are numerous: fibrous or particulate composites, porous materials, granular materials, metallic or ceramic foams, construction materials in civil engineering and living materials. Figure I.3.

Almost all heterogeneous materials are made up of discontinuous elements called heterogeneities, embedded in a continuous phase called matrix [20].

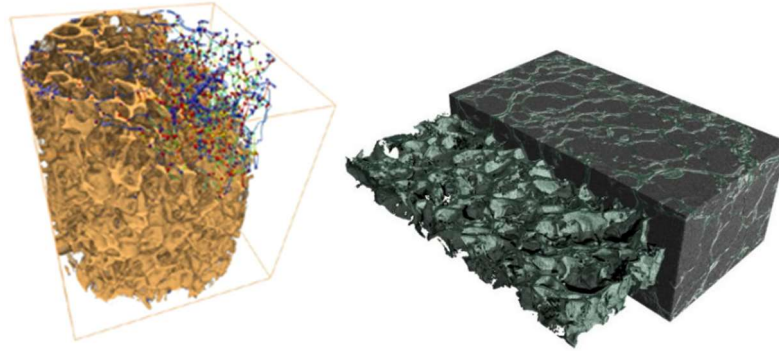


Figure I.2 Example of multiphase heterogeneous materials obtained by tomography [21]

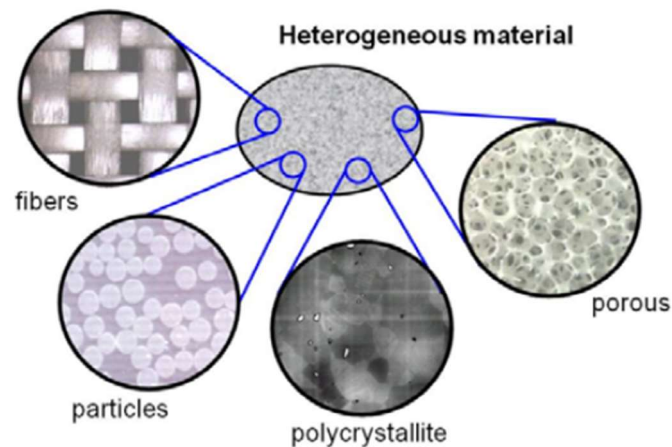


Figure I.3 Microstructure of heterogeneous materials [22]

### I.3.1 Composite materials

This type of material consists of combining several materials with different properties. Therefore, they improve one another but keep distinct and separate identities in the final product. Called phases. A matrix phase, generally continuous, the others, called reinforcements, are usually hard, of different shape. Figure I.4. Schematizes an example of two-phase heterogeneous composites with different forms of reinforcements. In a composite, there are two types of reinforcements, fiber or in particle form. They have the character of being compatible with the matrix in order to have a homogeneous overall behavior. These composite materials have simple or complex microstructures covering a wide spectrum of length scales, which determine their properties and macroscopic performance [23].

Composites improve the quality of materials for a certain use, due to their lightness, rigidity, etc. Due to the wide use of these composites, special effort is made to reduce costs, increase service life, prevent breakage and optimize wear properties. Also the growing demands for universal sustainability, safety and renewable energies have raised great challenges in the

development of multifunctional materials that can achieve optimum performance under extreme conditions [24].

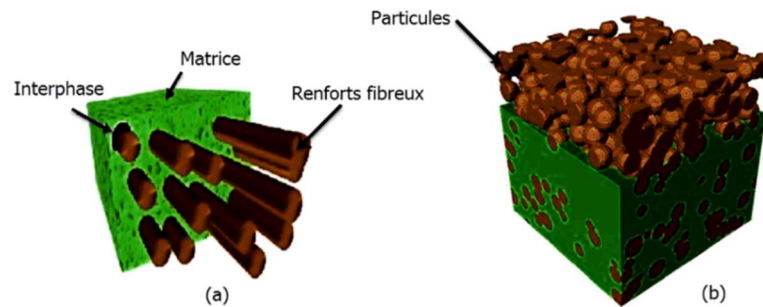


Figure I.4 Heterogeneous reinforcing composites: (a) fibers and (b) particles [23]

### I.3.1.1 Classification of composite materials

The nature of the material constituting the matrix makes it possible to list three main classes of composites, considered here in increasing order of temperature resistance: composites (Organic Matrix Composites), composites (Metal Matrix Composites) and composites (Matrix Composites Ceramic). It is then possible to associate with these three types of matrix either discontinuous reinforcements, all of the dimensions of which are much smaller than the dimensions of the part or continuous reinforcements of which at least one dimension is of the same order of magnitude as one. Dimension of the room. The materials used as reinforcements have good intrinsic mechanical properties (carbon, alumina, silica, boron, kevlar. Steel, silicon nitride and carbide, etc.). Among the discontinuous reinforcements, there are short monocrystalline fibers with a length of between 20 and 100 micrometers and particles (balls, platelets, chips, etc.) characterized by a slenderness ratio of less than 5 and a size which can vary. From micrometer to a few hundred micrometers. The continuous reinforcements or long fibers have a diameter which varies according to their nature between a few micrometers to more than a hundred micrometers [25].

Depending on the intended application, the assembly of these long fibers can be one-dimensional (unidirectional folds). Two-dimensional (woven folds, mats with staple fibers of a few centimeters or continuous fibers) or three-dimensional (multidimensional fabrics). The manufacture of composites (Organic Matrix Composite) uses two types of matrices: thermosetting resins which represent 75% of current (Organic Matrix Composites) (epoxy, polyester, vinyl ester. Polyurethane, etc.), and thermoplastic resins (polypropylene , polyamide ...) which are less used. Polymer matrices reinforced with glass fibers, used in particular in mass market products, are of great industrial importance. Carbon and Kevlar

fibers are used to a lesser extent for high performance applications in aeronautics and aerospace. Other types of reinforcement are used such as balls (glass, elastomer, etc.) and fillers (crushed fibers, scales, powders, etc.). The use of (Organic Matrix Composites) remains limited to the temperature range below 200 ° C. For higher temperature applications, composites (Metal Matrix Composites) up to 600 ° C are used. The metals or metal alloys used in the manufacture of (Metal Matrix Composites) are generally chosen according to their specific properties in the unreinforced state. Thus, aluminum, titanium and magnesium are the most commonly used metals. (Metal Matrix Composites) have good specific mechanical characteristics, good resistance to temperature and thermal shock as well as good resistance to wear and abrasion. All these skills are put to good use in the manufacture of structural parts ( housings, inserts, etc.) and functional components (connecting rods, valves, etc.) working at high temperature.

Finally, when the operating temperatures are above 1000 ° C, ceramic matrix composites are used. In this type of behavior, the reinforcement generally consists of long fibers made of carbon, silica or silicon carbide assembled by multidimensional weaving. This porous reinforcement is infiltrated by the matrix (carbon, silica, silicon carbide) which is either in the liquid phase or in the gas phase. The last stage of production consists in densifying the composite by sintering under high pressure at high temperature. These materials are mainly developed in the aerospace field as a thermal structure (brake discs, nozzles, flaps, ablative tiles, etc.) due to their high specific thermomechanical resistance [26].

### *1.3.1.2 The advantages and disadvantages of composite materials for different applications*

#### *a) Aeronautical applications*

The main motivation in the use of composite materials for the production of aeronautical structures is essentially the saving in mass while maintaining excellent mechanical characteristics, Figure I.5. Composite materials also exhibit virtually insensitivity to fatigue, compared to metallic materials, which require maintenance and regular monitoring of crack propagation. They are not as prone to corrosion, but they require good electrical insulation when assembling with light alloy parts between the composite and the metal to avoid galvanic corrosion of the aluminum (if the reinforcing fiber is carbon for example). The manufacturing techniques used make it possible to obtain complex shapes directly by molding with the possibility of making an assembly in one piece, Figure I.6, which is made of metal and requires several sub-elements. This significantly reduces assembly costs [27].

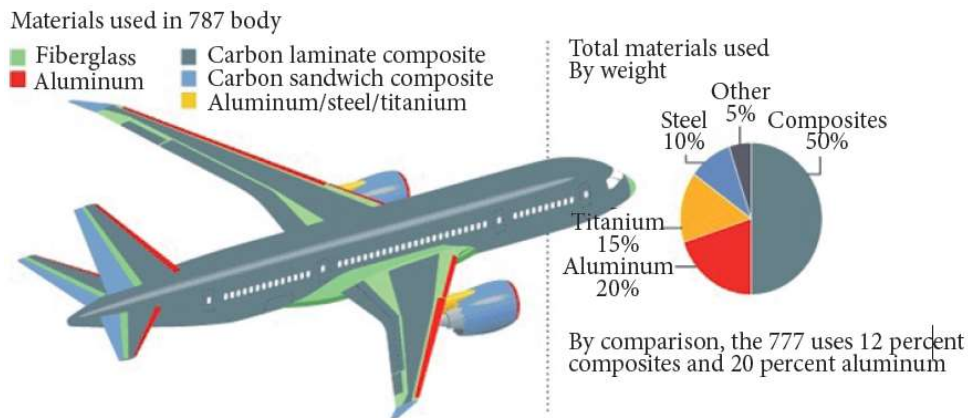


Figure I.5 Composite parts on aircraft structures - Boeing 787 (Source Boeing) [28]

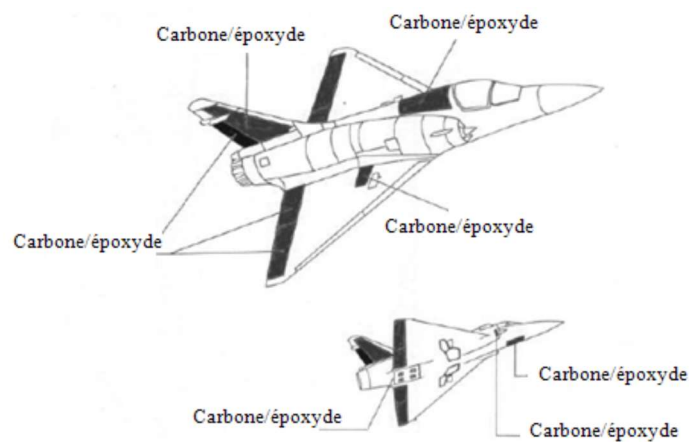


Figure I.6 Carbon / epoxy composite parts on aircraft structures - Mirage 2000 [29]

#### b) Military applications

For military products (missiles), the first advantage is the performance of composite materials, and then the use of composites on the missile guide fins makes it possible to maintain good control of the trajectory to the final target at the cause of the kinetic heating caused by the friction of the structure of the missile fins as Figure I.7. at the end of the trajectory the aluminum alloy fins can lightning under certain conditions and the missiles continue on its trajectory without control, which results in a precise loss of shot [27].

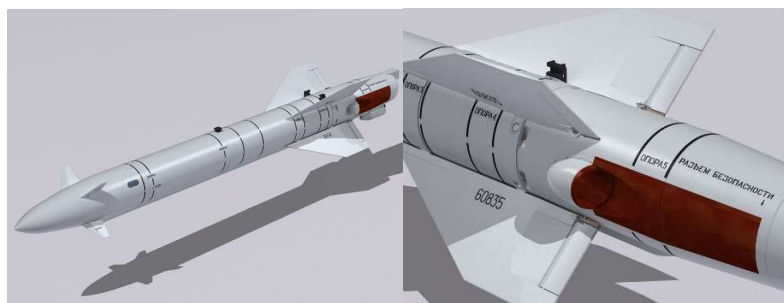


Figure I.7 Missile guide vanes [30]



### c) *Space applications (satellites)*

The deformations of the structure can have a thermal origin, with temperature exposures varying between  $-180^{\circ}\text{C}$  when the satellite is in the shade and  $+160^{\circ}\text{C}$  when the satellite is exposed to the sun, Figure I.8. In addition, on the same structure, between the illuminated side and the shadow side, the temperature gradient can be significant. Structures made of composite materials with an organic matrix, due to the negative value of the coefficient of thermal expansion of carbon fibers and the positive value of the coefficient of thermal expansion of the matrix. An optimized orientation of the various layers constituting the structure presents overall a thermal expansion coefficient close to zero for the whole of the structure. The geometric stability of the structure also provided by the overall stiffness of the structure. The use of very high modulus carbon fibers in composites addresses this concern. The main disadvantage of organic matrix composites for satellite applications is undoubtedly moisture pick-up, during assembly operations and during pre-launch storage [27].



Figure I.8 Example of a satellite [31]

### I.3.2 Bio Mimetics materials

The study of the formation, structure, or function of biologically produced substances and materials (such as enzymes or silk) and biological mechanisms and processes (such as protein synthesis or photosynthesis) especially for synthesizing similar products by artificial mechanisms which mimic natural ones is Bio Mimetics. Living organisms have evolved well-adapted structures and materials over geological time through natural selection. Biomimetics has given rise to new technologies inspired by biological solutions at macro and nanoscales. Humans have turned to nature for solutions to their problems since the dawn of time.

Millions of years of “trials and errors” in nature have resulted in a vast database of optimized solutions to technical problems with the survival of biological organisms. Integration of design in nature with artificial materials has greatly benefited humankind as indicated by

biomimetic paradigms such as shark skin, gecko tape, lotus effect and moth eye. As shown in Figure I.9. (a) The riblets on shark skin. (b) led to trials on an aircraft coated with a plastic film with the same microscopic texture. (c) The lizard *G. gecko*. (d) employs setal structures on foot (background) for attachment and resulted in microfabricated mimetic materials with polyimide hairs (the inset). Water droplets on a wood surface treated with “Lotus Spray”. (e) resembling those rolling down the surface of lotus leaf (the inset) demonstrate the superhydrophobicity of the surface. Compound eyes of *Calliphora* sp. in show antireflection effects via subwavelength structures on the surface of the ommatidium (f). Applying the surface geometric patterning of moth eye to glass by sol–gel methods resulted in the handheld glass pane in (g) that has a porous sol–gel anti-reflection coating in its lower section and no such coating in the section nearer the upper edge.

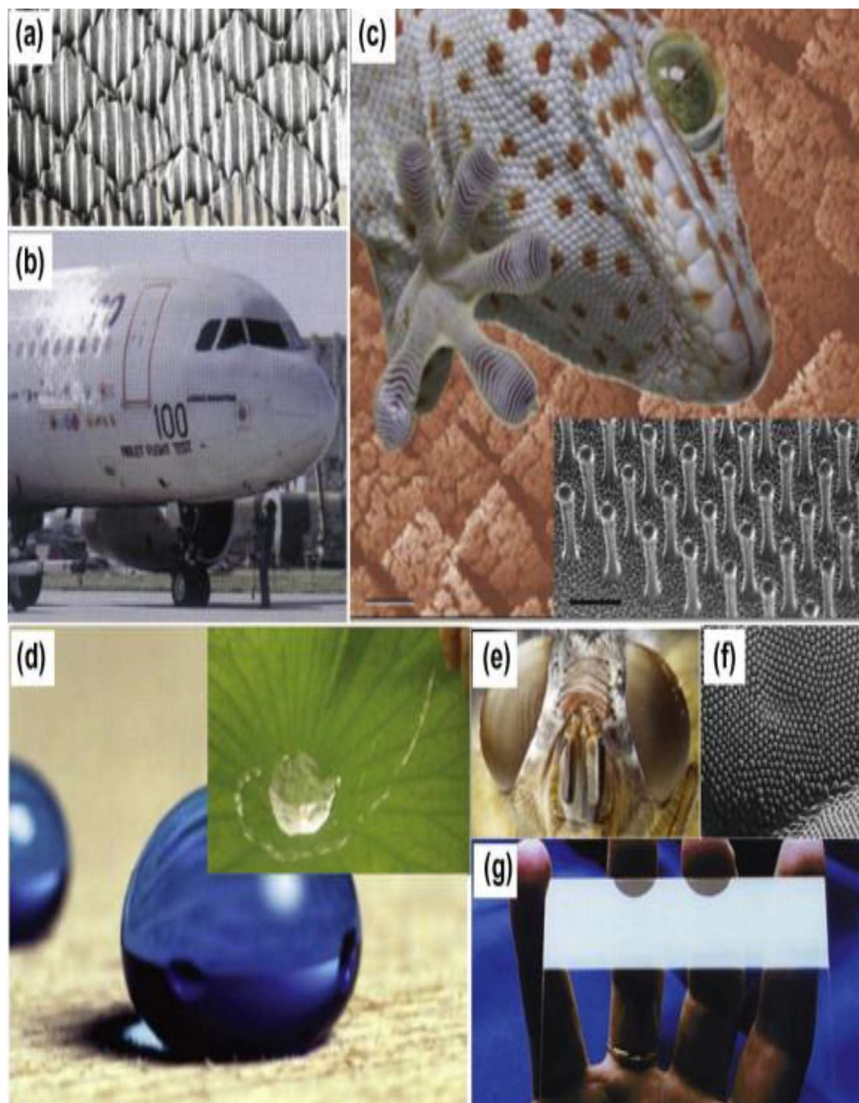


Figure I.9 Typical biomimetic Examples [32]



Structures that we see in nature has evolved over several years such that it becomes strong and adaptive to given environment. Nature inspired architecture is becoming more famous and excellent way to sort the sustainable structures. As shown in Figure I.10.

Cellular materials offer high strength to-weight proportion, high stiffness, high porousness, good impact-absorption, and thermal and acoustic protection. Lightweight cellular composites, made from an interconnected system of solid struts that shape the edges or face of cells, are a rising class of elite structural materials that may discover potential application in high firmness sandwich panels, energy absorbents, catalyst support, vibration damping, and insulation.

Cellular composites give favorable position of having a permeable structure design and capacity to adjust our own property as a composite. Cellular composites are of critical enthusiasm because of their wide applications in lightweight structural parts and thermal auxiliary materials and can possibly upset aviation industry and capability [33].

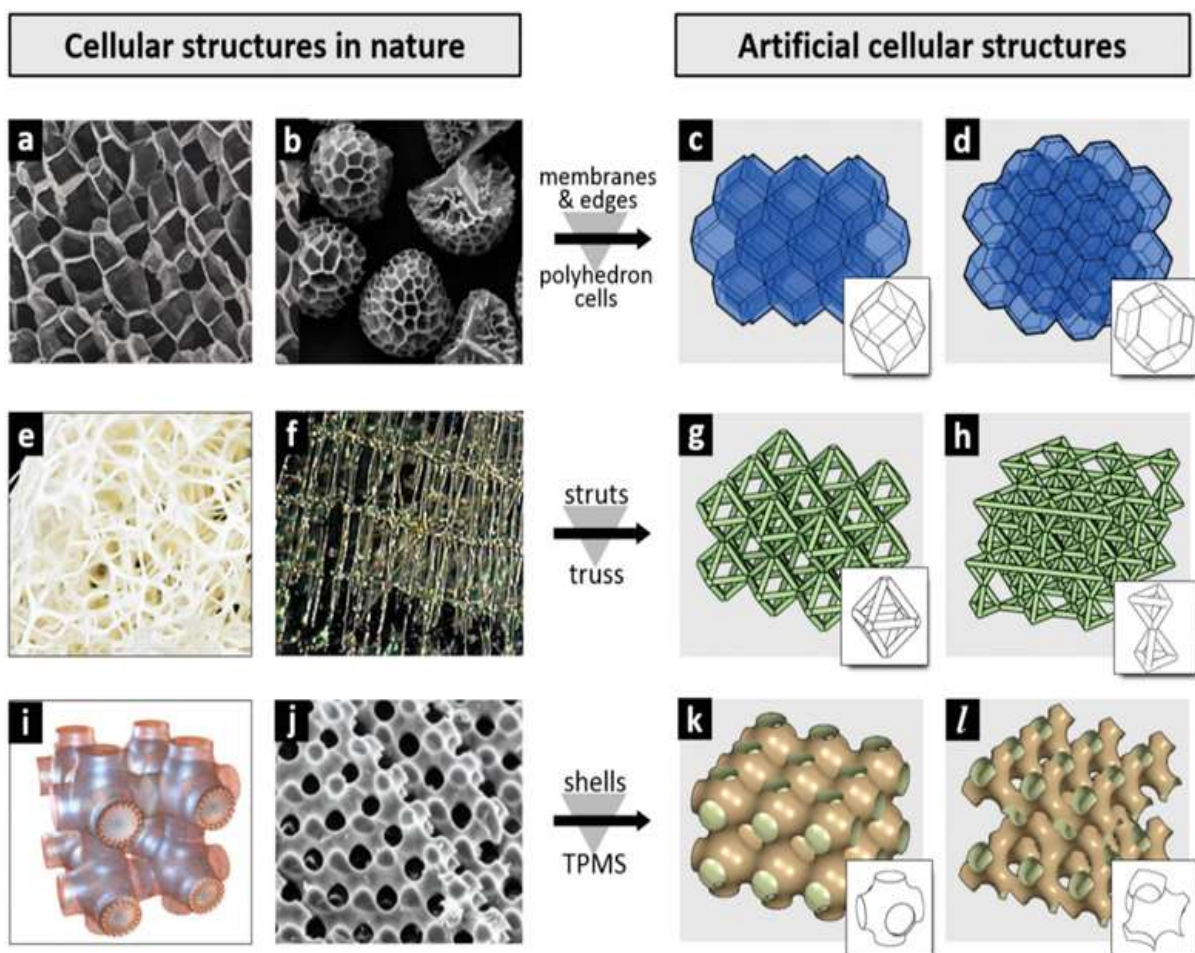


Figure I.10 Natural and artificial cellular structure [34]

### I.3.3 Porous materials

#### I.3.3.1 Definition of porosity

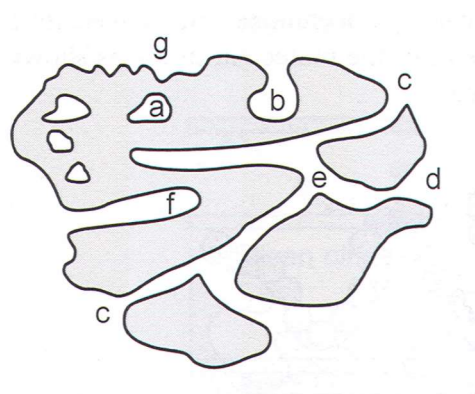
A porous medium is a rigid solid matrix which has voids (pores) which can communicate with each other. It can be defined as the property of a medium, soil or rock to have pores, that is to say interstitial voids, interconnected or not. It can be expressed as the ratio of the volume of these voids to the total volume of the medium. A porous medium can generally be in the following two forms:

- Consolidated porous medium in which the solid phase is formed from cement grains (limestone, sandstone, clays, wood, ceramics, sintered powders, plant and animal tissue, etc.).
- Unconsolidated porous medium in which the solid phase is formed of grains or fibers not welded together (gravel, sand, glass and steel balls, silt, various materials). Porous materials are often used because their many properties position them in large industrial sectors in all fields of mechanical engineering, mainly in terms of dissipation of acoustic and vibratory energy [35]. Porosity is therefore defined both as a characteristic property of a porous medium and as a parameter which expresses it quantitatively (volume ratio, dimensionless). We can find two categories of pores:

- Open porosities made up of intercommunicating voids connected to the exterior part of the material.

- Closed porosities, isolated inside the material and not allowing any permeability.

Penetrating pores are open pores which have the particularity of connecting at least two faces of the porous material. As shown on Figure I.11.



#### Accessibility:

a: closed pores

b,c,d,e,f: open pores

b, f: blind pores (dead-end or saccate)

e: through pores

#### Shape:

c: Cylindrical open

f: Cylindrical blind

b: ink-bottle-shaped

d: funnel shaped

g: roughness

Figure I.11 Different types of pores [35]

It should be noted that in the case of a material with a very high porosity (generally 70 to 95% of the volume), we are dealing with what is called a foam. These heterogeneous foams as a porous medium of complex microstructure with a very high pore volume fraction, which made them ultralight. As shown in Figure I.12. This kind of material retains certain physical properties of its base material [36].

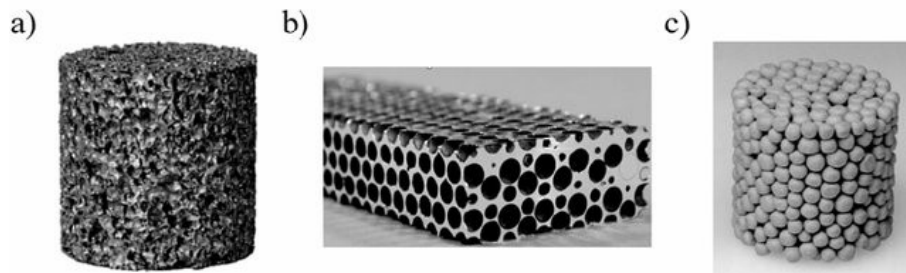


Figure I.12 Different types of porous medium of complex microstructure: a) closed-cell metal foam; b) hollow alumina spheres embedded in a magnesium matrix; c) hollow sphere foam Fe088.Cr012 [37]

### I.3.3.2 Types of porosities

The porosity can have various origins, specific to the material and its evolution over time, which leads to pores of different size and geometry, more or less interconnected.

#### a) According to the shape and origin of the pores

A pore is a space whose dimensions in the three directions of space are similar, it can be the space between the grains of a sedimentary rock (gravel or sand for example) or spaces internal to the material (in coal, shale or charcoal for example).

#### b) According to pore size

We can distinguish pores by size, and thus define several porosities:

- Microporosity: diameter  $\leq 2$  nanometers;
- Mesoporosity: diameter: 2-50 nanometers;
- Macroporosity: diameter  $\geq 50$  nanometers [38].

## I.3.4 Architectural materials

### I.3.4.1 Introduction

Architected materials are known as cellular structures. The word "cell" originates from a Latin word called "cella", which means a small compartment or an enclosed space. The term architected materials encompass any microstructure designed in a thoughtful fashion, that some of its materials properties have been improved in comparison to those of its constituents

[39]. Figure I.13. Illustrates the two combinations and categories of architecture material.

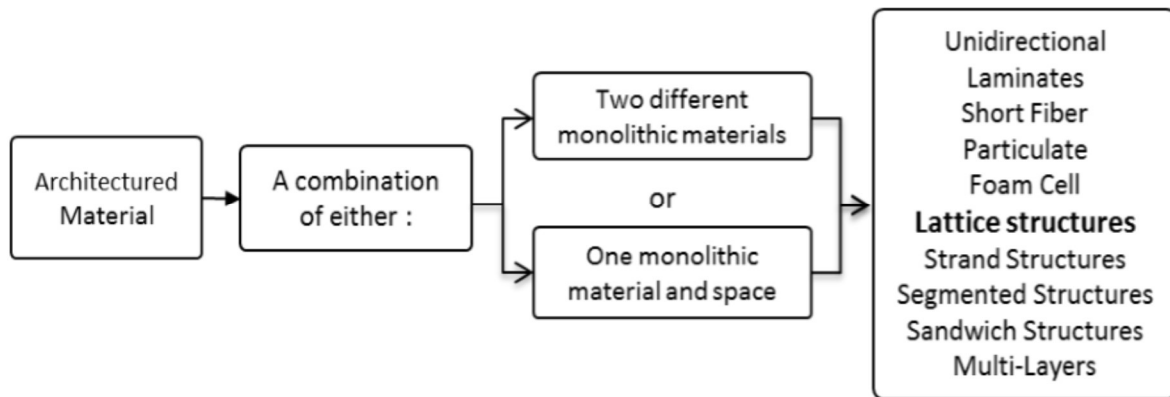


Figure I.13 Architected materials [39]

### I.3.4.2 Lattice structure

Lattice structure is a type of architected material, which is a combination of a monolithic material and space to generate a new structure which has the equivalent mechanical properties of a new monolithic material. It is a rising class of materials that bring new possibilities in terms of functional properties, filling the gaps and pushing the limits of Ashby's materials performance maps. Many examples of architected material exist : particulate and fibrous composites, foams, sandwich structures, woven materials, lattice structures, etc. Most of them are shown on Figure I.14. [40].

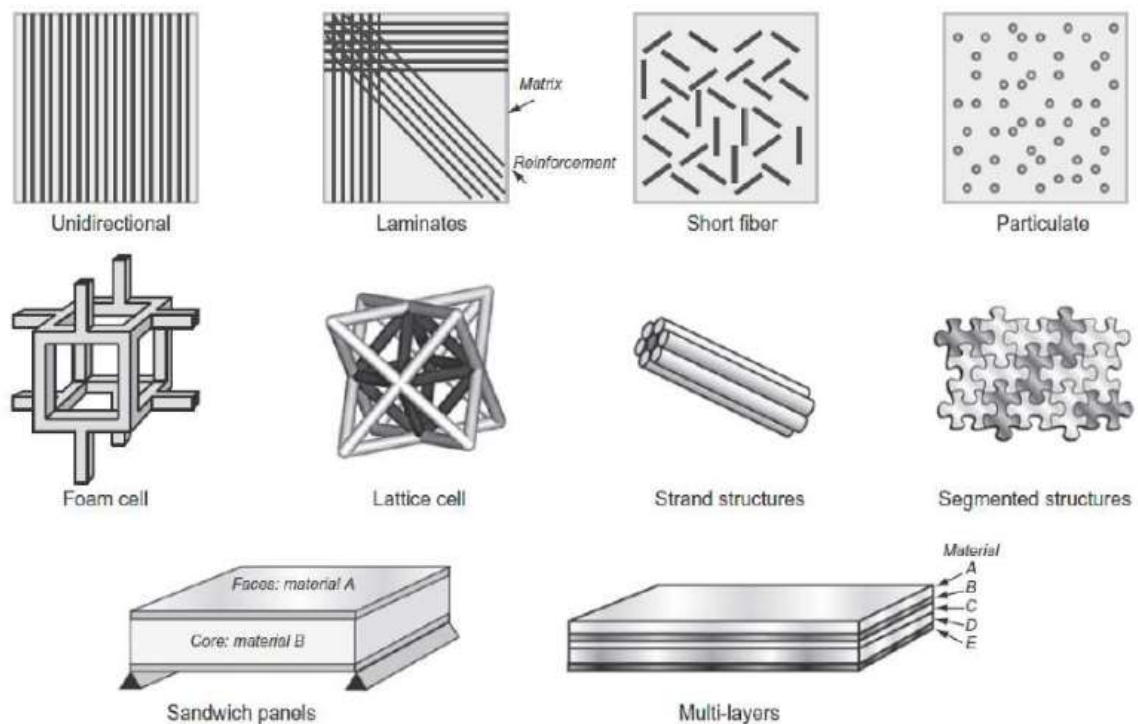


Figure I.14 Examples of architecture materials [40]

Many parameters permit to obtain architected materials, but all of them are related either to the microstructure or the geometry. Parameters related to the microstructure can be optimized for specific needs using a materials-by-design approach, which has been thoroughly developed by chemists, materials scientists and metallurgists. For instance, it is well-known among metallurgists that mechanically decreasing the average grain size of an alloy, as well as increasing the dislocation density, results in a higher yield strength. Stronger polymers can be engineered by changing interchain bounds or by optimizing the chain design. These improvements are intrinsically related to the synthesis and processing of materials and are therefore due to microand nanoscale phenomena, taking place at a scale ranging from 1 nm to 10  $\mu\text{m}$ . Architected materials thus lie between the microscale and the macroscale. This class of materials involves geometrically engineered distributions of microstructural phases at a scale comparable to the scale of the component, thus calling for new models in order to determine the effective properties of materials. One aim of the present work is to provide such models, in the case of mechanical and thermal properties [41].

#### *1.3.4.3 History of lattice structures*

Cellular structures have been known for generations, but it was only in the last 30 years that an understanding of materials with a cellular like structure has emerged. Previously, the process available limited manufacturing lattice structures during that period. It now exists techniques to manufacture lattice structures easily. This has impacted the research in lattice structure properties. Previously, the majority of cellular material research publications were related to the cellular structures which were able to be manufactured at that time. Thus, the majority of research papers published were about material properties of stochastic and prismatic materials only. It was then possible to manufacture these types of structures easily and reliably by manufacturing processes such as foaming solidification.

There were however already some manufacturing processes which were capable of manufacturing lattice structures, but these processes were expensive, complicated and had many limitations. Making it not cost effective and not suitable. This increased cost outweighed the improvements gained in weight reduction of the parts manufactured. Manufacturing stochastic metals were more cheaper than manufacturing periodic lattice structures [42].

The high cost and complexity of titanium investment casting process and limitations of other conventional process to manufacture lattice structures resulted in very limited mechanical



property information for titanium-based lattice structures as a function of their relative density [41].

#### *1.3.4.4 Importance of lattice structures*

As the world becomes more competitive, industries are looking at every viable prospect to stay relevant and be ahead of the competition. Economical and environmental needs are forcing companies to reduce cost, increase performance gains, and reduce wastes. New solutions have to be invented to gain every possible improvement. As the need for energy conservation increases, the need for lightweight parts increases too. The benefits of weight reduction are significant. In the aerospace industry, where it is important to produce parts which are lightweight but have good mechanical properties. Lattice structure is a good solution to achieve this objective. High strength low mass property is a key advantage of lattice structure. Lattice structures can be used to achieve excellent performance and multi functionality while reducing weight. Reduction in the weight of an airplane can contribute to vast amount of savings in fuel expenses. In the automotive industry, reducing a cars weight contributes to fuel economy and lower CO<sub>2</sub> emissions. Studies have shown that a 10% reduction in weight can save around 6-8% in fuel consumption [41].

#### *1.3.4.5 Types of lattice structures*

##### *a) Lattice structures in nature*

There are also many materials in nature which contain lattice structure designs. These materials play a role in lightweight structures. Natural tubular structures often have honeycomb or foam as a core, which supports denser outer cylindrical shell and increases the resistance of the shell to local buckling failure. These materials can be a reference for the configurations of lattice structures in creating lightweight and high strength materials. For example, hexagonal lattice structures have some similarities with cellular structures of wood. The stiffness and strength of a species of wood depends on its density and the direction of the load applied on it. Its stiffness and strength are higher if the direction of the load applied is the same as the longitudinal direction of the wood, compared to if it was applied across it. Another example is the structure of trabecular bone. The structure of the bone is adapted to the loads applied to it. It grows in response to the magnitude and direction of the load applied [43]. Stochastic and periodic structures architected materials can be divided into two categories, stochastic and periodic structures. Materials characterized by a unit cell that can be translated through the structure are referred to as periodic materials [42]. Whereas cellular

materials which cannot be characterized by a single unit cell area are referred to as stochastic foams as shown on Figure I.15.

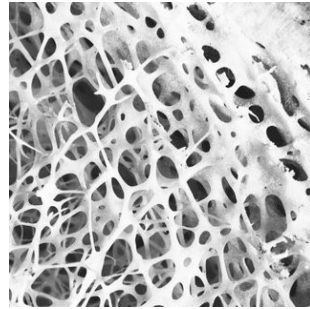


Figure I.15 Lattice structures in nature [42]

b) *Prismatic and lattice structures*

It exists two types of periodic cellular structures. First, periodic materials where the unit cells are translated in two dimensions are known as prismatic cellular materials [42]. An example of a prismatic cellular material is the honeycomb structure, which has very good properties for a high stiffness and low mass structure. The second type, are periodic materials which have three-dimensional periodicity. This means that its unit cells are translated along three axes. These structures are frequently referred to as lattice materials [42]. Therefore, a lattice structure is an example of a cellular structure. In this work, the terms described above are used to identify specific structures and avoid ambiguity. The Venn diagram in Figure I.16. shows the difference between stochastic, periodic, prismatic and lattice structures. In this work, we consider lattice structures as periodic cellular structures. Table I.1. illustrates the definition of the terms used in this chapter for elementary and lattice structures.

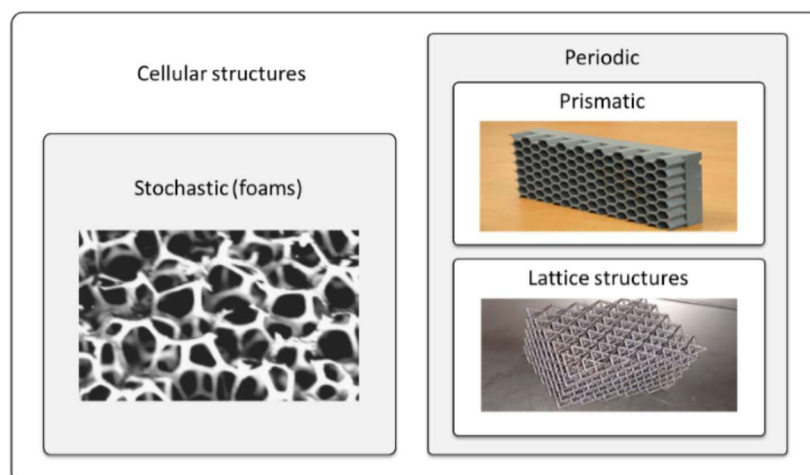

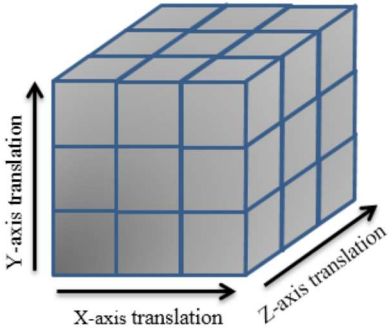


Figure I.16 Stochastic, periodic: prismatic, and lattice structures [42]



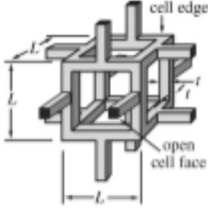
Table I.1 Definition of elementary and lattice structure [42]

Elementary Structure	Lattice structure
	

c) *Lattice structure patterns*

There are many types of lattice structure patterns. A lattice structure pattern depends on the pattern of its elementary structure, as shown in Table I.1. Common lattice structure patterns are octet truss, cubic, tetrakaidecahedron, and open-cell foam lattice structures. Table I.2. Illustrates an octet-truss elementary structure containing an octahedral core surrounded by tetrahedral units, tetrakaidecahedron structure and open cell foam structure. Open-cell foam structures imitate stochastic structures by placing struts connected at the joints. These joints have low connectivity with other joints [41].

Table I.2 Octet-truss, tetrakaidecahedron and open-cell foam elementary structures [41]

Octet-truss	Tetrakaidecahedron	Open cell foam
		

d) *The implicit surfaces*

Another strategy that can be used to represent architectural materials is to model their geometry using mathematical functions. Implicit equations of the form  $F(x, y, z) = 0$  can be used to define surfaces in Euclidean space. In general, it is not possible to define such equations in CAD software, and mathematical function visualization tools may be required to display the structures shown. The modeling of the surfaces of architectural materials is generally done by assembling periodic basic functions. Unlike the surface representation used by CAD software, vertices and edges are not defined and no intersection calculation is

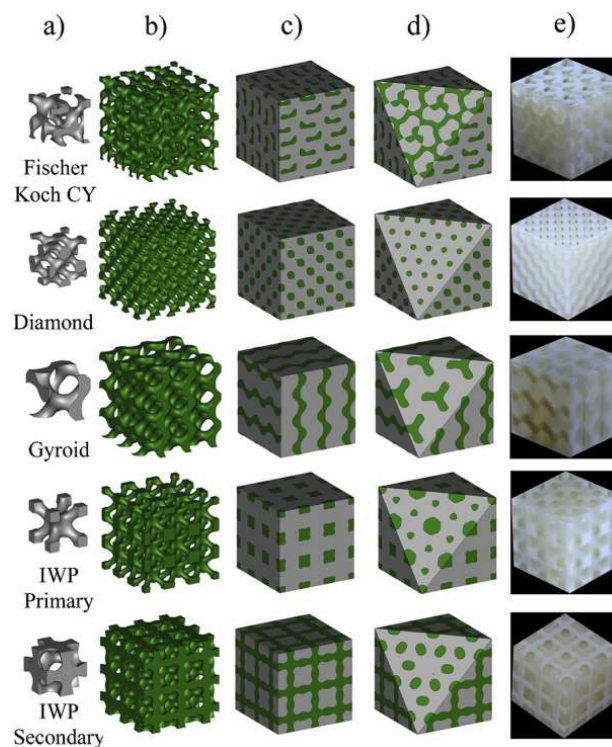


performed. The boundaries of the material being defined by the scope of the function used. Several examples of structures that can be defined in this way are shown in Figure I.17.

Recently, geometric modeling of porous materials using implicit functions has attracted a lot of attention given the ease of representing periodic geometries [14]. One of the main advantages of the approach is the ease with which it is possible to define parameters such as cell geometry or pore size. It has also been demonstrated that the morphology of the geometries thus defined is well suited for bone replacement applications.

For applications where it may be necessary to adapt the architectural material to complex shapes, the approach may however be limited. Indeed, the difficulty in defining the boundary of the architectural material represents a significant disadvantage of the approach [44]. Since geometries are defined by mathematical equations, it can be difficult to define the boundary of any surface. However, approaches have been studied to facilitate this task and to develop tools to automate the modeling process [45].

In this work, the CAD-based representation technique with triangular primitives has been chosen given the ability to generate an STL file without having to convert from another file type [39].



**Figure I.17** The different TPMS topologies used to create IPCs. a) A single unit cell b) A 3x3x3 repetition of the TPMS c) The designed IPC d) A (111) plane cut that reveals the interconnectivity of the TPMS e) A sample fabricated using 3D printing [46]

### I.3.4.6 Lattice structure properties

Material properties can be shown in many possible diagrams. However, they all have one thing in common, which is that they have parts of the diagram filled with materials, and parts which have holes and are empty [40]. For example, Figure I.18. shows the big holes in the top left and bottom right corner in the Young's modulus density space. This means that it does not exist a monolithic material which has high elastic modulus and low density.

Monolithic materials are not able to fill the whole space in material science and are not sufficient to fulfil all required properties, hence creating the need of architected material. With architected material, it is possible to produce parts with high stiffness-to-density ratio and fill these holes of the diagram. These materials such as foams and lattice structures must be seen as a single material with its own properties. If a cellular material outperforms an existing material in the material property diagram, then the material property space has been extended [40]. The possibility to fill the big holes left in the Young's modulus-density diagram with lattice structure is very interesting.

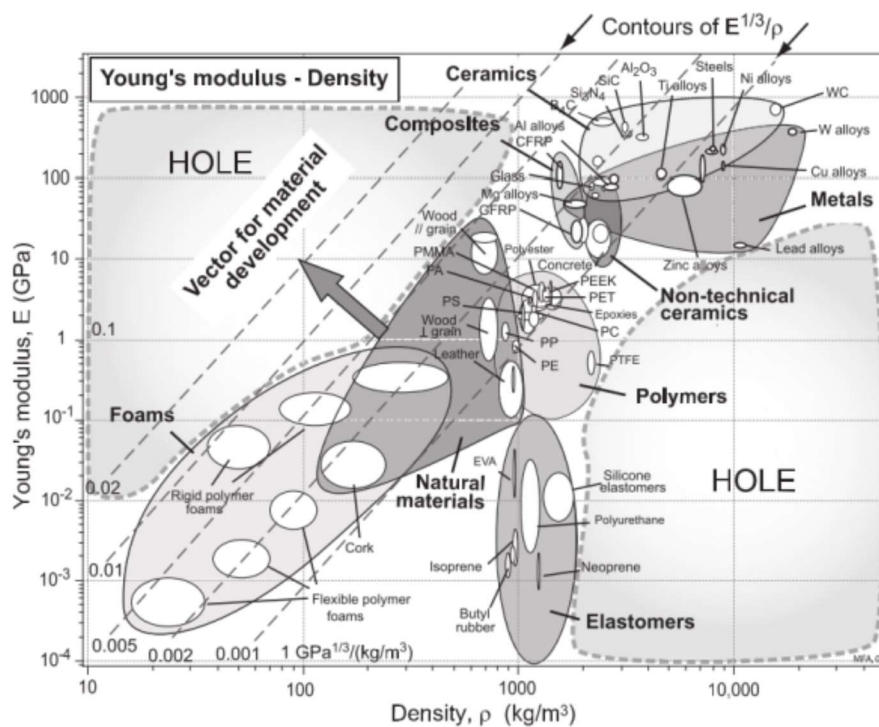


Figure I.18 Young's Modulus-density space materials diagram [40]

#### a) Influences of a structure's property

There are three main factors which influence the properties of a structure, the material of the structure, its cell topology, and its relative density [41]. This is shown in Figure I.19.

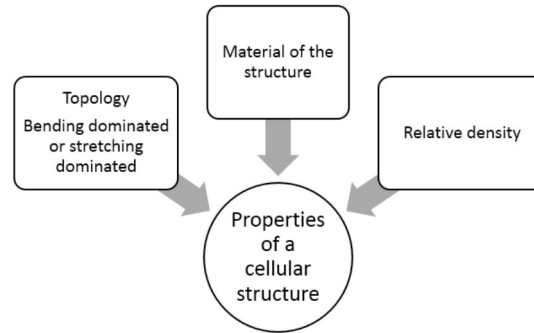


Figure I.19 Three main lattice structure design variable influence [41]

The material of which the lattice structure is made of, influences the mechanical, thermal and electrical properties of the structure. Whereas the elementary structure pattern or topology influences the bending-dominated or stretching-dominated property of the structure. The relative density depends on the struts size and length. The relative Young's modulus of a bending-dominated structure scales with the square of the relative density.

Prismatic structures have single properties which are only in one direction of the part. Whereas lattice structures can have multifunctional properties and along each X, Y and Z axis of the part. Another interesting possibility is to create a lattice structure which has different mechanical properties for each direction of the part, depending on the requirements of the part in each direction [41].

#### b) *Stretching and bending-dominated structures*

To help differentiate the lattice structure mechanical properties and its applications, these structures can be categorized in two different deformation categories: bending dominated and stretching-dominated structures. Stretching-dominated is useful to produce high stiffness and low weight parts, for example cubic and octet-truss lattice structures. By orienting the lattice structures struts in a certain pattern we can obtain a bending dominated structure, it is also possible to manufacture parts suitable for energy absorption. The design pattern of a lattice structure influences its mechanical property [47]. This information is summarized in Table I.3. for each lattice structure pattern.

Table I.3 Types of deformation for lattice structures [47]

<b>Features</b>	<b>Cubic</b>	<b>Octet-truss</b>	<b>Tetrakaidecahedron</b>	<b>Open-cell foam</b>
<b>Type of deformation</b>	Stretching dominated	Stretching dominated	Bending dominated	Bending dominated
<b>Application</b>	For high stiffness low mass parts	For high stiffness low mass parts	For high energy absorption parts	For high energy absorption parts

The difference between stochastic and periodic structure mechanical properties influences their applications. Stochastic foams are bending-dominated structures, thus are well equipped for energy absorption. Table I.4. shows the influence of stretching and bending-dominated structures in mechanical properties [41].

Table I.4 Influence of stretching and bending-dominated structures on mechanical properties [41]

Mechanical properties	Bending-dominated	Stretching-dominated
Examples of elementary patterns	1) Open-cell, 2) Tetrakaidekahedron 	1) Octet-truss 
Relative Young's modulus-relative density graph		
Relative stiffness-relative density		

### I.4 Multi-scale in heterogeneous materials

This section presents the methodology and general concepts of the scaling approach and the constitutive laws between the different scales of a heterogeneous microstructure [35]. A microstructure can be described within the framework of mechanics by three scales:

- Macroscopic scale where the behavior is homogeneous;
- Mesoscopic (intermediate) scale where the behavior is heterogeneous;

- Microscopic scale where the behavior is heterogeneous.

This type of description seems to be particularly suited to heterogeneous materials which are characterized by their multiscale nature which makes it possible to successively distinguish the scale of the structure, the scale of the reinforcement or of the heterogeneity and finally the scale of the constituents, Figure I.20.

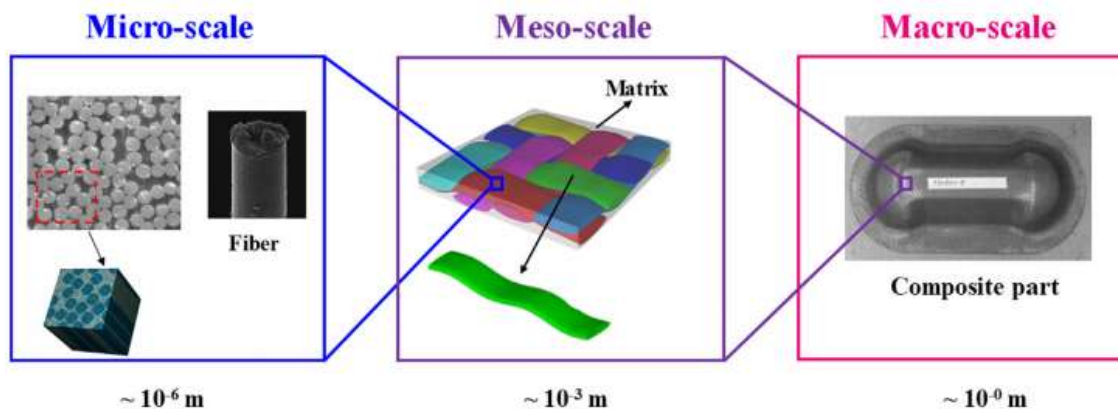


Figure I.20 Scales and sizes of constituents in a building material [48]

In this figure, we present the case of a concrete material with its characterization scales. The constituents and compositions of each scale are also presented. Note that the composition of the heterogeneous material generally depends on the dimensions of the sample. We must first be able to distinguish three scales of variation.

#### I.4.1 Multi-scale definition

##### I.4.1.1 Macroscopic

The macroscopic is the size of the volume from which the macroscopic behavior is calculated taking into account available mesoscopic or microscopic information. This scale is the sample in its natural state.

##### I.4.1.2 Mesoscopic

The mesoscopic is of a mesoscopic nature in which the effect of particles on the overall response remains minor compared to the microscopic scale. At this scale, we find the microstructures in which we speak of grain, fiber, pore or filler.

##### I.4.1.3 Microscopic

This dimension called microscopic, i.e., the local scale. This scale makes it possible to follow the particles in their distributions, orientations, contacts, etc. This scale must be low enough



not to erase the elements of the microstructure responsible for the macroscopic properties. Also, high so that the classic tools of continuous media mechanics can be used. It should be noted that there are no universal criteria to set this dimension.

The passage from one scale to another smaller requires the operation of homogenization. This operation is defined by several stages, each one is governed by a set of equations [35].

### 1.4.2 Finite element modeling

Porous materials are generally more flexible, lighter and have better energy absorption characteristics than dense materials, which makes their use very attractive for the designs. The porosity of the latter must be adjusted in order to allow a compromise between the reproduction and its mechanical resistance [49]. Modeling the mechanical properties of architectural materials, using digital tools, however, represents a significant challenge. Recently approached the modeling approaches of porous metallic materials by categorizing them according to the macro, meso and microscopic scales presented in Figure I.21. The following sections will present the approaches to modeling the porous character of architectural materials at the macroscopic scale, mesoscopic scale and microscopic scale.

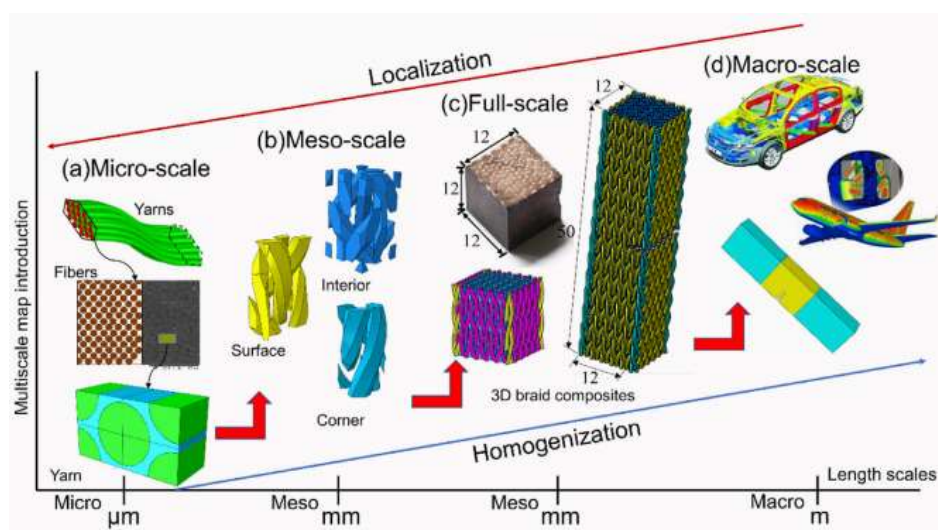


Figure I.21 Representation of modeling of multiscale braided structures. (a) micro-scale model; (b) mesoscale model; (c) full-scale model; (d) macro-scale model [50]

#### 1.4.2.1 Macroscopic scale modeling

Numerical simulation approaches such as the Finite Element Method (FEM) are often used for modeling the mechanical behavior of dense materials. Modeling a porous material at the macroscopic scale, however, may require a large number of elements to correctly represent its mechanical behavior. The approach is often limited to materials with few pores since the

number of elements and the computing power required can increase rapidly with the number of cells. For materials with high porosity (above 90%), it may be possible to model the chords of architectural materials using beam elements, which significantly reduces the amount of elements required for the construction. analysis [49].

#### I.4.2.2 Mesoscopic scale modeling

When the number of cells in the geometry becomes too large, it may be necessary to model the architectural material on a mesoscopic scale. Thus, a representative volume is identified for which the properties of the material are homogeneous. The results of FEM analysis performed at the mesoscopic scale are used to determine equivalent material properties which can subsequently be transferred to the macroscopic model. When the flexural modulus is above 30, the members of a unit cell can be modeled as beams. The equivalent properties of a unit structure can thus be evaluated. The constitutive equations of beam elements can also be used to identify analytical equations to assess the mechanical properties of unit cells [51]. When the flexural modulus of the members is too low for them to be modeled by beam elements (below 30), solid elements are however necessary. Finally, a commonly used strategy to approximate the equivalent properties of porous materials at the mesoscopic scale is to use the scaling relationships. Indeed, the rigidity of porous materials can be approximated by the power law presented in equation I.1 in which  $E^*$  corresponds to the equivalent modulus,  $E_s$  to the modulus of the dense material,  $\rho$  to the relative density of the porous materials and  $C$  and  $n$  are specific coefficients to each material [51].

$$E^* = E_s C \rho^n \dots\dots\dots (I.1)$$

#### I.4.2.3 Microscopic scale modeling

##### a) Hexachiral lattice

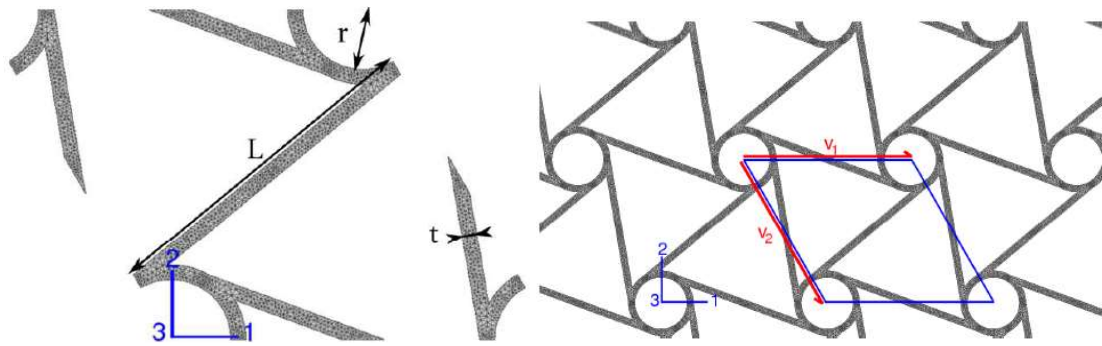
This chiral microscopic was first proposed as cell geometry, it can be described in this way: the circular nodes have radius  $r$ , the ligaments have length  $L$ , and both have in common wall thickness  $t$  (cf. Figure I.22. (a)) as well as depth  $d$ , which in our case is considered infinite due to periodicity conditions along direction 3. On Figure I.22. (b),  $a = 5$ ,  $\beta = 0.25$  and  $\gamma \rightarrow +\infty$ . These parameters correspond to a volume fraction of 15%. The microscopic cell is invariant by a rotation of order 6, which provides transverse hemitropy, which is equivalent to transverse isotropy in the case of linear elasticity [52].

$$a = L / r \dots\dots\dots (I.2)$$



$$\beta = t / r \dots\dots\dots (I.3)$$

$$\gamma = d / r \dots\dots\dots (I.4)$$



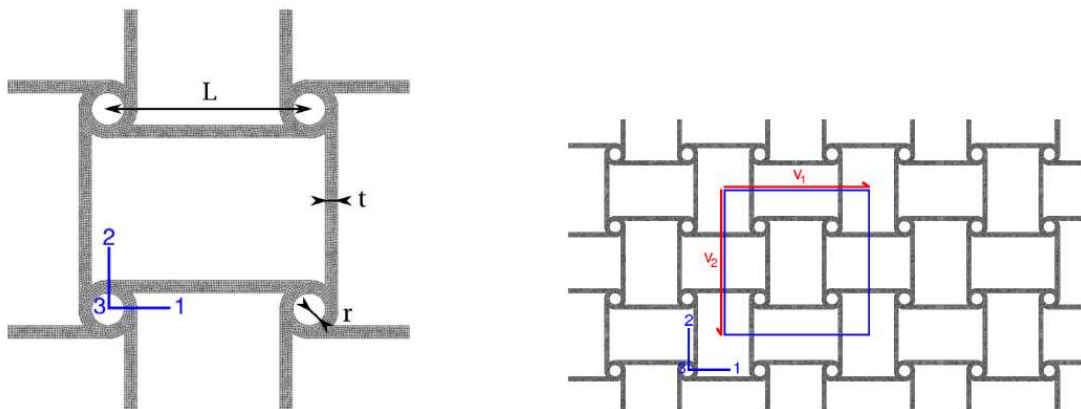
(a) Hexachiral unit-cell

(b) Hexachiral lattice

Figure I.22 (a) Periodic cell with geometric parameters, (b) Hexachiral lattice with unit-cell (blue) and periodicity vectors  $v_1$  and  $v_2$  (red) [52]

b) *Anti-tetrachiral lattice*

This anti-tetrachiral microscopic proposed and studied for cell geometry can be described exactly as for the hexachiral lattice, cf. Figure I.23. (a).  $a = 11$ ,  $\beta = 0.06$  and  $\gamma \rightarrow +\infty$ , cf. Figure I.23. (b). Volume fraction is 15%. The cell is invariant by a rotation in-plane of order 4, thus giving rise to quadratic elasticity [53].



(a) Anti-tetrachiral unit-cell

(b) Anti-tetrachiral lattice

Figure I.23 (a) Periodic cell with geometric parameters, (b) Anti-tetrachiral lattice with unit-cell (blue) and periodicity vectors  $v_1$  and  $v_2$  (red) [53]

c) *Rotachiral lattice*

This chiral microscopic, leads to study the impact of ligaments geometry on auxeticity for chiral lattices. Cell geometry is similar to the hexachiral case, except for the straight ligaments that

have been replaced by circular ones with diameter  $D$ , cf. Figure I.24. (a) [54]. A new dimensionless parameter is defined by:

$$\delta = D / r \dots \dots \dots (I.5)$$

As shown on Figure 24. (b),  $\delta = 2.4$ ,  $\beta = 0.1$  and  $\gamma \rightarrow +\infty$ . Volume fraction is 15%. As for the hexachiral lattice, the 6-fold symmetry provides transverse isotropy [55].

d) *Honeycomb lattice*

For the purpose of this work, the classical honeycomb lattice is considered as a comparison medium. The 6-fold symmetry provides transverse isotropy. Geometry can be described using the same parameters as for the rotachiral lattice. For a regular hexagonal honeycomb cell,  $r$  and  $D$  are not independent and  $\delta = p^3$ , cf. Figure I.24. (a). Also,  $\beta = 0.15$  and  $\gamma \rightarrow +\infty$ , which corresponds to 15% of volume fraction as for the other microstructures considered [55].

Unit-cell for this microscopic has been chosen hexagonal but it could have been square or rhomboid shaped as for the previous lattices, cf. Figure I.25. (b).

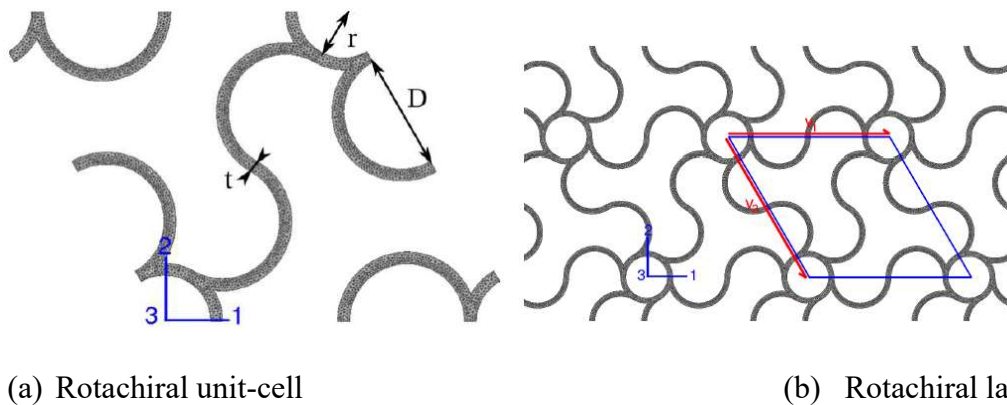


Figure I.24 (a) Periodic cell with geometric parameters, (b) Rotachiral lattice with unit-cell (blue) and periodicity vectors  $v_1$  and  $v_2$  (red) [55]

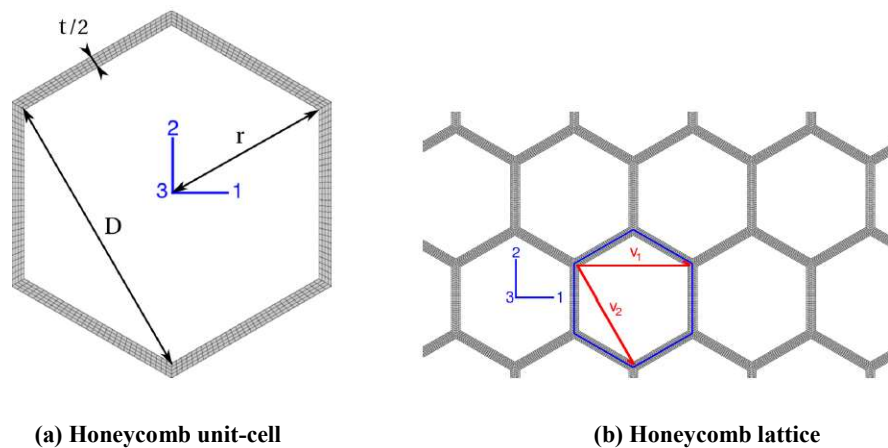


Figure I.25 (a) Periodic cell with geometric parameters. (b) Honeycomb lattice with unit-cell (blue) and periodicity vectors  $v_1$  and  $v_2$  (red) [55]

## **I.5 Conclusion**

In this chapter, a literary study is made on heterogeneous materials such as composite, porous and architectural materials. Great emphasis has been placed on porous and architectural materials imitating nature due to it is a combination of a monolithic material with space to generate a new structure which has the equivalent of a new monolithic material. The microstructure with lattice structures for architectural materials as a periodic material which have three-dimensional periodicity, which means that its unit cells are translated in three axes. These structures are frequently referred to as lattice or micro-truss materials. Also, types, properties and models are explained of lattice structures. In addition to clarifying the multi-scale structure of heterogeneous materials in three different measurements: macroscopic scale, mesoscopic scale, and microscopic scale.

In the second chapter, we will study in detail the three methods of optimization and focus on topological optimization and its application in this study depending on the network structures.

## Chapter II.

# Topology optimization



## II.1 Context of the problem

In a wide variety of engineering fields, identifying the best structure based on various mechanical criteria is paramount when designing bridges, buildings, vehicles or even airplanes. From a mathematical point of view, this leads to solving optimization problems. In this chapter, after having defined the general notions of an optimization problem, we present the classical process of structure optimization. Subsequently, we highlight the category of structures, and we detail the different types of optimization (dimensional, shape and topological). Finally, after having raised the scientific obstacles linked to the mechanical constraints considered, we present the various contributions in the topology optimization in this work.

## II.2 Introduction

Engineers are faced with structures of increasing complexity. These structures are getting smaller, lighter and more detailed. This tendency should not conflict the objective of the structure. A Planes, for example, would benefit from less weight for fuel cost reduction. The chassis however, should remain stiff enough to counteract deformations and provide safety. In the high-tech industry, and the equipment used there, the design space is getting smaller, especially in the Aviation and space industry. The structure should, however, be stiff enough to not conflict its reliability [56]. A very promising approach for this type of problems is the use of topology optimization. Topology optimization is a strong approach for generating optimal designs which cannot be obtained using conventional optimization methods. Improving structural characteristics by changing the internal topology of a design domain has been fascinating scientists and engineers for years. Topology optimization can be described as a distribution of a given amount of material in a specified design domain, which is subjected to certain loading and boundary conditions. This domain can then be optimized to minimize specified objectives, for example compliance. For static problems, topology optimization is extensively used [57]. However, the practical domain of TO has increased beyond a little linear structural response to include number of structures, acoustics, heat transfer, materials design, aeroelasticity, fluid flow, and other Multiphysics disciplines [58].

## II.3 Significance and History

The term Topology is the most mainstream in material science and field of science. Topology itself could be a generation of current science. Topology is the logical show for changes in mixed dimensional geometric modeling, resiliencies, and illustrating physical conduct. Thus, topology can fill in as the official together framework for hypotheses, techniques and

---

disobedient recognized with the depiction of geometry, assortments from apparent geometry, and conduct [59]. Leonhard Euler laid the foundation of topology; his 1736 paper on the Seven Bridges of Königsberg is seen as one of the vital valuable utilizations of topology. This incited his "polyhedron condition" (for the foremost portion called as Euler Polyhedral equation). Many pros see this examination as the most speculation, hailing the presentation of topology [60]. Headway in the midst of final period drove advancement of unused optimization strategy called Structure Optimization. By this various restricted components-based calculation have been executed in programming bundles associated for standard diagram issues. Until 1990s, the utilization of auxiliary optimization has been confined to measuring and shape enhancement. It has been illustrated the probability of advance advancement can be fulfilled by altering the basic arrange thought of course of activity of pit scattering interior a structure [61].

In afterward periods, by and large unused field in auxiliary mechanics named Topology optimization had created, which can bring approximately considerably more noticeable save reserves than unimportant cross-segment or shape improvements. This modern field had rapidly amplified and broadly utilized as a portion of various fabricating methods to form things with less material utilization, infers less weight and less fetched than typical. Topology optimization concerns not fair the measuring and the shape or geometry of a basic system however in expansion its topology, i.e. spatial gathering of its joints and components or components. An appealing portion of continuum auxiliary topology optimization is that it can be associated to the diagram of the both materials and basic systems or components [33].

## II.4 Optimization of structures

An optimization problem (II.1) generally consists in minimizing a function  $f$ , defined on a set  $C \subseteq \mathbb{R}^n$  and with a value in  $\mathbb{R}$ , under constraints defined by functions  $(g_j)_{1 \leq j \leq p}$  and  $(h_k)_{1 \leq k \leq q}$  with  $n, p$  and  $q \in \mathbb{N} \setminus 2\mathbb{N}$ . It can be formulated as follows:

$$\begin{aligned} & \underset{x \in C}{\text{minimize}} && f(x) \\ \text{s. l. c} & && g_j(x) \leq 0; \forall j = 1, \dots, p \\ & && h_k(x) = 0; \forall k = 1, \dots, q \end{aligned} \tag{II.1}$$

or:

- The vector  $x = (x_1, \dots, x_n)$  represents the unknowns of the problem. Each component  $(x_i)_{1 \leq i \leq n}$  is called a decision variable. In the case of the optimization of structures, they are also called

design or design variables, and they can characterize the dimensions, the presence or absence of material, etc ...

- The function  $f$  corresponds to the optimization criterion and is called the *objective function* or *the cost function*. As part of the optimization of structures, it can characterize the mass or the resistance to the forces of a structure.

- The functions  $(g_j)_{1 \leq j \leq p}$  and  $(h_k)_{1 \leq k \leq q}$  are respectively the constraints of inequalities and of equalities. Defining the admissible set  $E = \{x \in C: g_j(x) \leq 0, j = 1, \dots, p; h_k(x) = 0, k = 1, \dots, q\}$ . Within the framework of the optimization of structures, this one characterizes the accepted limits of behavior of the structure: maximum displacement, limit of resistance to the efforts or to buckling, etc ... For a vector  $x^* \in E$ , one says that a constraint  $g_j$  is active at  $x^*$  if  $g_j(x^*) = 0$  and inactive if  $g_j(x^*) < 0$ .

Depending on the nature of the design variables  $x_i$  and the functions  $f$ ,  $g_j$ , and  $h_k$ , an optimization problem can belong to different classes of optimization problems. We speak of a discrete (or combinatorial) optimization problem when the design variables correspond to integers. In the case where no restriction imposes an integer value on an unknown, then the space  $C$  corresponds to a bounded set of  $\mathbb{R}^n$  and the problem is said to be of continuous optimization. Certain formulations lead to simultaneously considering continuous and integer variables, one then speaks of an optimization problem in mixed variables.

When the functions  $f$ ,  $g_j$  and  $h_k$  are linear (respectively convex), then the problem is said to be of linear optimization (respectively convex). If the expression of any of these functions is nonlinear, then a nonlinear optimization problem is defined [62].

In the field of the optimization of structures, the resolution of the optimization problem generally follows an iterative process alternating two stages: the analysis of the behavior of the structure and the application of an optimization method see Figure II.1. The first phase consists of solving equations of states making it possible to determine the various deformations of the structure: calculation of displacements, resistance to forces, vibratory analysis, or even heat transfer [63]. As for optimization methods, they aim to determine an optimal value of the design variables [62].

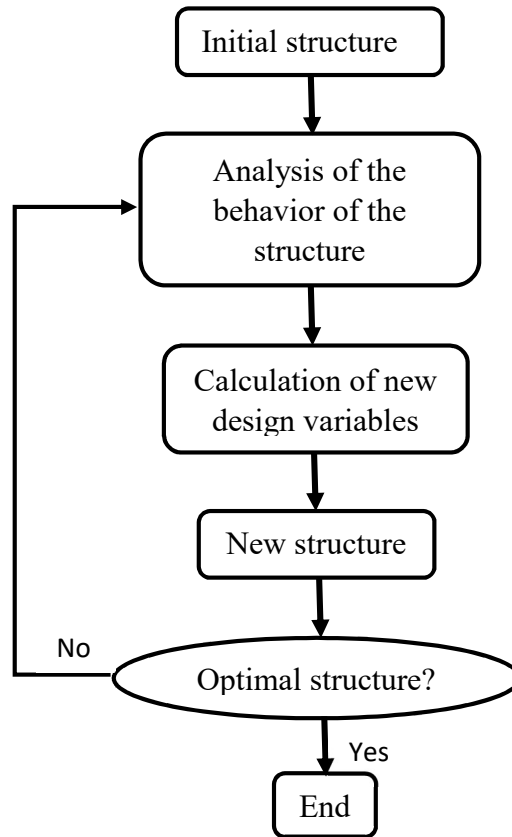
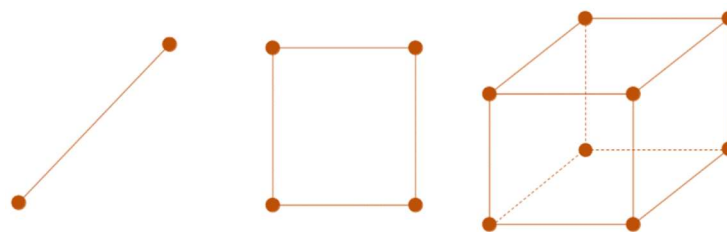


Figure II.1 the optimization of structures [63]

#### II.4.1 Types of discretization of a structure

During the optimization as shown in Figure II.2, the analysis of the behavior of the structure can be performed through numerical simulation. One of the main techniques is based on the finite element method, consisting in discretizing the structure according to a type of element which can be one, two or three-dimensional as shown in Figure II.2, each end of which is defined as a node of the structure. The result of this discretization is called a mesh. Depending on the type of finite elements used, there are two categories of structures: on the one hand the so-called lattice structures, made up of one-dimensional elements, and on the other hand the so-called continuous structures, discretized using two- and three-dimensional elements [62].



(a) One-dimensional

(b) Two-dimensional

(c) Three-dimensional

Figure II.2 Different types of finite elements [62]



### II.4.1.1 Lattice structures

Lattice structures correspond to a set of one-dimensional elements subjected to forces and fixings as shown in Figure II.3. With each element of the structure, we associate a cross section (for example, hollow square type) and a local coordinate system  $(x, y, z)$ , where  $x$  represents the main axis as shown in Figure II.3b. There are two types of uni-dimensional elements: beams and bars. Bars can only transmit axial forces (along the main axis of the element). As for the beam elements, axial and transverse forces (according to a plane of the section) as well as deformations related to rotations according to the three local axes are considered. A rotation along the  $x$  axis of the beam translates a force called torsional moment, while the rotations around the  $y$  and  $z$  axes define deformations called bending moments. Each cross-sectional geometry can be characterized by an area but also by moments of inertia and a polar moment. The moments of inertia, defined according to the  $y$  and  $z$  axes of the element, make it possible to analyze the resistance to bending moments, and the polar moment, defined at a point of the cross section, is related to the resistance at the moment twist. As for the area, this is directly related to the mass of the element [62].

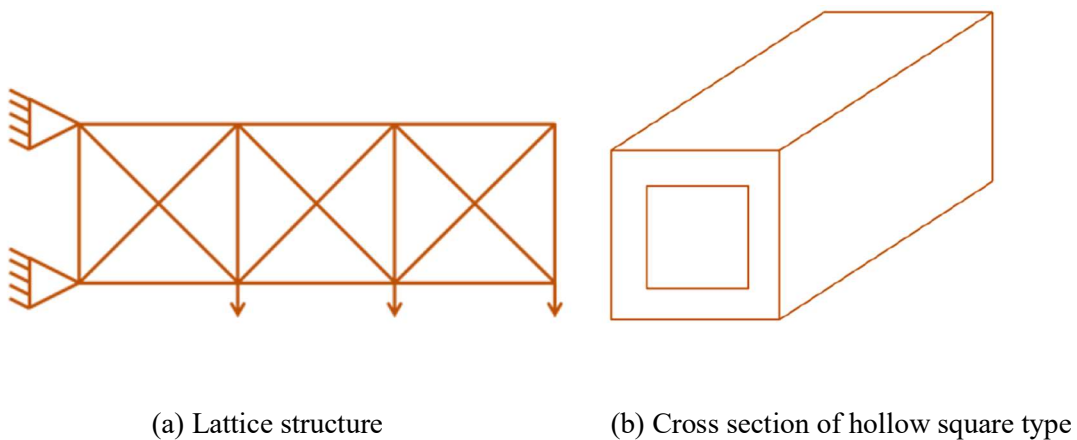
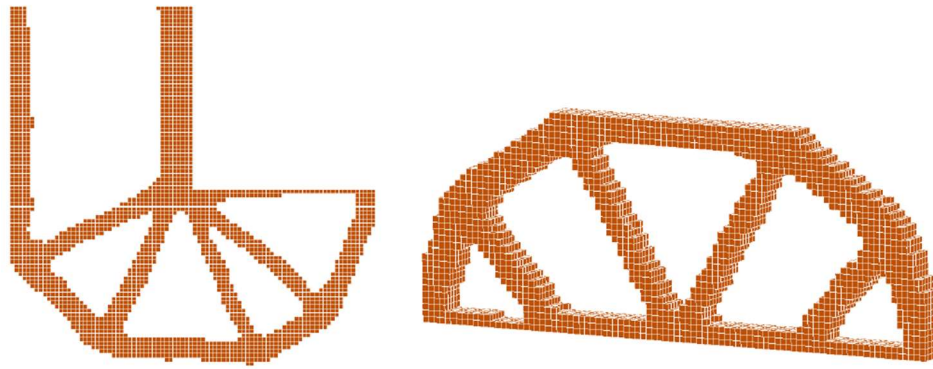


Figure II.3 Example of a truss structure and a cross section [62]

### II.4.1.2 Continuous structures

Two-dimensional (triangle or quadrangle) or three-dimensional (tetrahedron or hexahedron) elements can be used to represent continuous structures as shown in Figure II.4. With each node of these elements are associated three degrees of freedom, characterizing the movements in the three directions of space. Note that, in order to represent the third dimension, a thickness is associated with each two-dimensional element [62].



(a) 2D structure

(b) 3D structure

**Figure II.4** Different representations of continuous structures [62]**Remark.**

The modeling of a structure optimization problem depends directly on the choice of the discretization of the structure. Indeed, for a truss (bars) structure, the design variables can be associated with the areas of the cross sections. For discretized continuous structures with two-dimensional elements, the optimization can relate to the thickness of each element. In a representation based on three-dimensional elements, optimization can consist of determining which elements of the initial design domain must be present.

According to the structural design problem studied, the choice of the type of discretization (lattice or continuous) is more or less suitable. For hollow structures (ex an electricity pylon), a description based on a truss seems most appropriate because of its ability to represent large design areas in a simple manner. For smaller structures (for example part of an aircraft's landing gear), requiring good precision, the discretization tends towards continuous structures.

### II.4.2 Types of optimization of structures

There are three types of structural optimization: dimensional optimization, shape optimization and topological optimization.

#### II.4.2.1 Dimensional optimization

Dimensional optimization, also called parametric optimization, consists of solving continuous optimization problems where the design variables represent, for example, the dimensions of the cross sections of beams (diameter or thickness of a hollow cylinder - Figure II.5) or the thicknesses of a plate. In this type of optimization, the shape and topology of the structure

cannot be changed. For example, in a parametric optimization of a truss, the number of elements and the shape of each cross section are fixed.

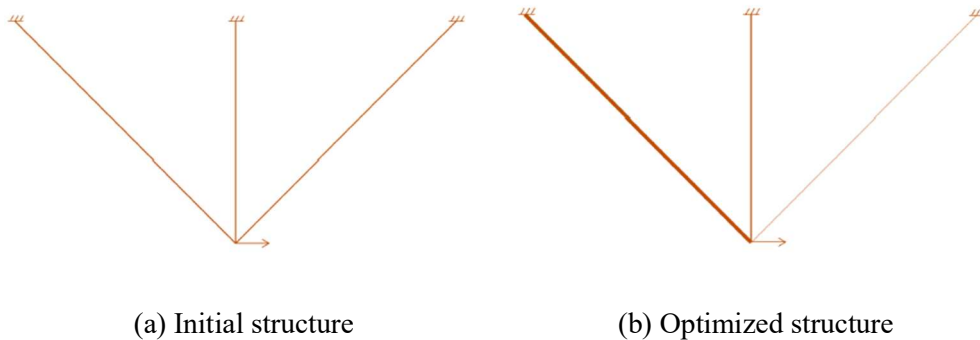


Figure II.5 Parametric optimization of a lattice[62]

#### II.4.2.2 Shape optimization

In shape optimization, also called geometric optimization, design variables parameterize the boundaries of the structure. The design domain is represented using so-called homeomorphic functions, in order to follow the evolution of the boundaries during the optimization and to keep a topology equivalent to the starting structure as shown in Figure II.6. Although this type of optimization allows the geometry of the structure to be modified, the result is extremely dependent on the initial topology, since the number of boundaries does not change during the optimization [62].

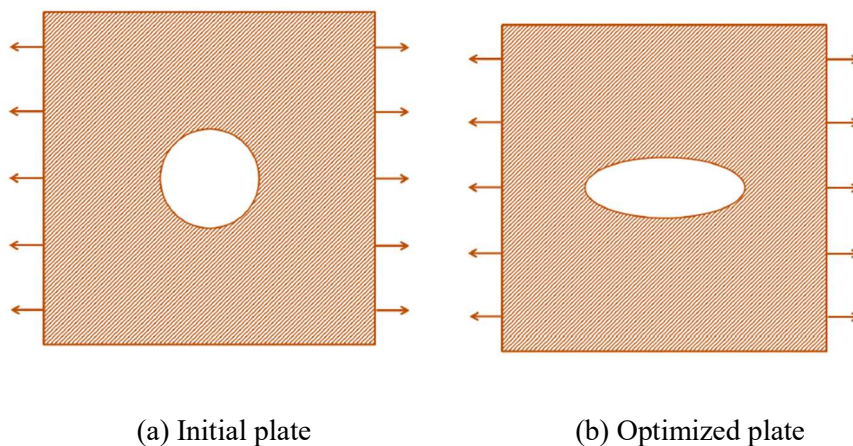


Figure II.6 Shape optimization of a plate [62]

#### II.4.2.3 Topological optimization

Topological optimization consists of finding, in a design space, the optimal distribution of material representing the structure. This optimization is much more flexible than the previous two, since only the size of the design area, and fixing and areas of structural loading design are known. No a priori is therefore considered on the boundaries of the structure as well as on the

shape and dimensions of the cross sections. This is why it is also given the name of generalized form optimization [64].

For lattice structures, topology optimization involves extracting an initial field as shown in Figure II.7.a an optimal subset of elements and the dimensions of the cross sections of each element as shown in Figure II.7.b. For this type of structures, a mixed variable optimization problem can be defined, where integer variables represent the presence of elements and continuous variables describe their cross sections. In the case of continuous structures, the goal is to determine which elements of the design area must be made of material or not as shown in Figure II.8, which can be formulated as a discrete optimization problem.

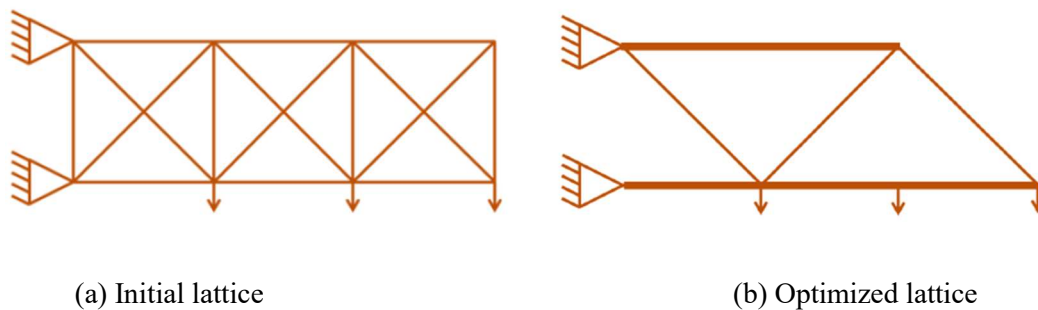


Figure II.7 Topological optimization of a truss [64]

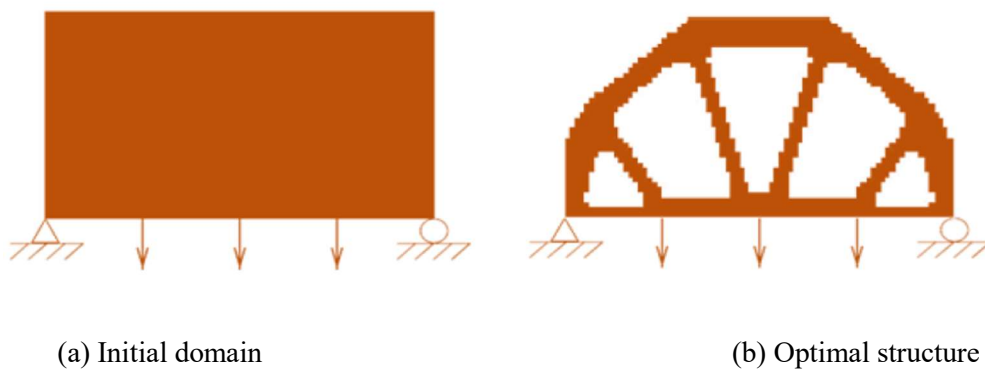


Figure II.8 Topological optimization of a continuous structure [64]

It is estimated that for common design problems, optimizing a performance criterion may lead to gains ranging from 40 to 100% with the topology optimization.

While, in the case of dimensional optimization, the gains range between 5 and 10% and between 10 and 30% for geometric optimization [65]. Thus, topological optimization takes a prominent place in the design of structures, including its ability to offer innovative optimal designs [62].

## II.5 Method of Topology optimization (TO).

Topology optimization is the method, which determines the optimal material placement within a certain design domain, for helps engineers to optimize the material under different constraints such as loads and boundaries, design space in order to obtain the best possible structural performance such as maximizing the abilities for the design. Since used of a homogenization method in topology optimization, used it within the engineering designs [66]. TO of elements can be described as a distribution of solid and void space within the design domain and gives the connectivity, shape and topology of elements. TO is the newest technique in the domain of structural optimization [57].

The optimization is mainly based on the design variables, structural optimization can be used in continuum and discrete structures, based on domain and the design properties. Structural optimization is divided in three essential categories a) Sizing b) Shape and c) Topology. The first one described to Sizing optimization of a truss structure, the second to shape optimization and the finally to Topology optimization shown in Figure II.9.[57].

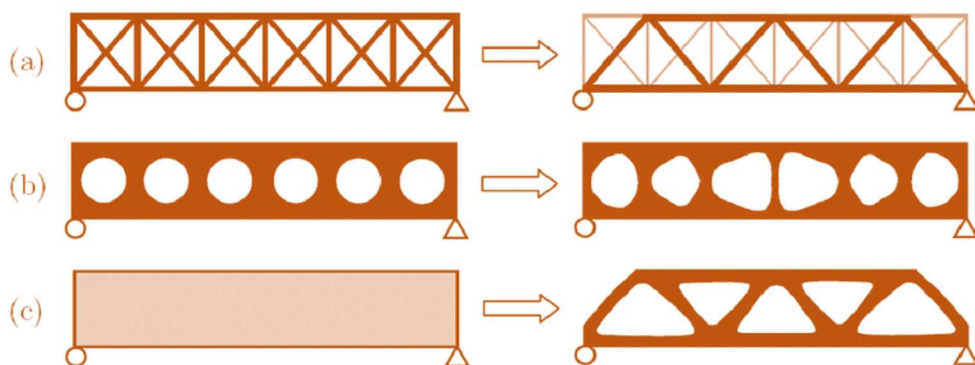


Figure II.9 Categories of optimization a) Sizing b) Shape c) Topology [57]

The first one describes to Sizing optimization of a truss structure is used to maximize the vertical stiffness by variable the cross-sectional space of each truss element. This cross-sectional space can consequently be considered as a design variable, the second to shape optimization is a variable the geometry of the pore can provide a higher stiffness. The space and number of pores remains fixed and is named a constraint. So, the shapes of the pores which are the design variables can be changed. However, in a lot of cases, structural optimization problems are not fixed at only sizing or only shape problems. A hodgepodge of the categories is needed, in order to obtained the optimal design to achieve maximum stiffness for a given amount of material. Used the typical topology optimization. The term topology is derived from the Greek word *topos* (τοπος), which is place or landscape [67]. TO applies FEA for verifying the

performance of the designing part. The performance is optimized based on different genetic algorithms [68]. TO operates on a fixed FE mesh of each discrete or continuum elements to optimally distribute material in the material layout. In the discrete element-based TO, the problem is solved by determining position, the optimum number, and mutual connectivity of structural member elements [56]. In the continuum element-based TO, the shape of the internal and external boundaries and the density of every continuum element in the structure are optimized using a homogenization method [69]. A TO problem requests to minimize compliance while satisfying several constraints like a given amount of weight, material, cost, manufacturing requirement, etc [70]. The comprehensive objective in TO is to minimize compliance Eq. (II.2).

$$\min_x : c(\rho) = U^T K U = \sum_{e=1}^N (\rho^e)^p u_e^T k^e u_e$$

$$\text{Subject to} \quad \begin{aligned} &: \frac{V(\rho)}{V_0} = f \\ &: K U = F \\ &: 0 < \rho_{min} \leq x \leq 1 \end{aligned} \quad (\text{II.2})$$

And the stiffness matrix for every element can be found from Eq. (II.3).

$$k^e = \int_{\Omega} H^T D H d\Omega = \sum_{i=1}^2 \sum_{j=1}^2 w_i w_j / J(\xi, \eta) / H(\xi, \eta)^T D H(\xi, \eta) \quad (\text{II.3})$$

The Young's modulus parameter does not affect the optimal results of TO. The create solution of the TO is constructed to minimize compliance using a Lagrange multiplier method Eq. (II.4).

$$L(\rho, \lambda) = f^T d(\rho) + \lambda^T (f - K(\rho)d(\rho)) \quad (\text{II.4})$$

By setting  $\lambda = d$  and  $k^e = \int_{\Omega} H^T (E_0 + (\rho^e)^p E_1 D^* H d\Omega$ , the derivative of the lagrangian equation with respect to the design variables can be determined as Eq. (II.5) [71].

$$\frac{\partial L(\rho, \lambda)}{\partial \rho^e} = -P(\rho^e)^{p-1} d^{eT} K_f^e d^e \quad (\text{II.5})$$

Using the bi-section algorithm, densities of elements in every iteration can be updated by a scheme. because to efficiency and numerical stability, an algorithm is proposed based on the Optimality Criteria (OC) method [72]. Eq. (II.6). A numerical constraint has been considered to limit the update for densities, m.

$$\rho_{new}^e = \left\{ \begin{array}{l} \text{if } \rho^e B_e^\eta \leq \max(\rho_{min}, \rho^e - m) \\ \quad \mathbf{max}(\rho_{min}, \rho^e - m) \\ \text{if } \max(\rho_{min}, \rho^e - m) < \rho^e B_e^\eta < \min(1, \rho^e + m) \\ \quad \rho^e B_e^\eta \\ \text{if } \min(1, \rho^e + m) \leq \rho^e B_e^\eta \\ \quad \mathbf{min}(1, \rho^e + m) \end{array} \right\} \quad (II.6)$$

Where  $B_e^\eta = -\frac{1}{\lambda} \frac{\partial c}{\partial \rho^e}$  and  $\eta = \left(\frac{1}{2}\right)$  is a numerical damping coefficient [73].

### II.5.1 Application of the topological optimization method

*The procedure for TO depend of the following fundamental steps:*

**a) Define and describe the problem**

Describe material properties (Young's modulus and Poisson's ratio), select the best possible elements types for TO, create a finite element model, and apply load and boundary conditions for different load cases or for a solitary load case investigation.

**b) Select the element types.**

Topological optimization bolsters 2-D planar, 3-D strong, and shell components. To utilize this procedure, your model must contain just the accompanying element types: 2-D Solids, 3-D Solids, Shells.

**c) Specify optimized and non-optimized regions.**

Elements recognized as type1 will be subjected to topological optimization. Utilize this to control which regions of your model to optimize or not. For instance, if you need to keep material near a hole or a support, you ought to distinguish those elements as type 2 or higher. You can utilize any suitable ANSYS select and modification command to control the type definitions for different elements.

**d) Define and control the load cases.**

You can perform topological optimization for a single load case or collectively for several load cases.

**e) Define and control the optimization process.**

The topological optimization process consists of two parts: defining optimization parameters and executing topological optimization. You can run the second part, executing topological optimization, in two ways. You can carefully control and execute each iteration, or you can automatically perform many iterations.

⇒

***Defining Optimization Parameters***



You first define your optimization parameters. Here you define the percentage of the original volume to be removed, the number of load cases to be treated collectively, and termination/convergence accuracy.

⇒ ***Executing a Single Iteration***

After defining your optimization parameters, you can launch a single iteration. After execution, you can check convergence and display and/or list your current topological results. You may continue to solve and execute additional iterations until you achieve the desired result. If working interactively, choose one iteration in the Topological Optimization dialog box (ITER field).

⇒ ***Executing Several Iterations Automatically***

After defining your optimization parameters, you can launch several iterations to be executed automatically. After all the iterations have run, you can check convergence and display and/or list your current topology. You may continue to solve and execute additional iterations if you want.

f) *Review results.*

Once your topological optimization solutions are complete, pertinent results are stored on the ANSYS results file and are available for additional processing [33].

## **II.5.2 The topology optimization methods developed in additive manufacturing applications**

### ***II.5.2.1 Homogenization optimization (Solid Isotropic Microstructure with Penalization (SIMP)) method***

In the optimum shape of components that are topologically equivalent to the premier design, computational schemes involve several kinds of remeshing of the FE approximation of the problem analysis. As mentioned already TO is a perfect solution between solid (1) and void (0) regions, this represents either hollow or full material. But there are several spaces that range between 0-1 and are defined as a part of an undesirable space. This method has to do with modern techniques and consisted of calculating the best spatial distribution of (SIMP) or an anisotropic material [74].

This method introduces a prosaic area of periodically distributed small pores in a given homogeneous “isotropic material” with the constrains and the loads and satisfy else design constraints [75]. Moreover, the area presents small pores inner the structure, and the problem of TO, is to find out the perfect way to improve this design, according to the con-strains.



Consequently, the problem is changed into a problem of improving the pores inside the construction “sizing problem”. To obtain there are new pores in the structure, without knowing if they have preceded the construction in the structure. So, it seems that the form and the topology of the model are optimized [76].

However, produces solutions which show that the internal part of the object has insignificant pores of resources that make the object optimally indefinite. In some cases, the volatility created by the algorithm in calculating the microprocessor does not produce real items, which are included into the structure and transform structure under different loads and stress into more sensitive. For solve these types of problems, a large number of variants of homogenization methods get participatory with the goal of ease the broker density that to created [77]. In addition to, the properties of the object are considered to be contiguous (isotropic materials), so the conversion of the object can variation the density of the elements (SIMP). While, the large of volatility and the computational complexity happen as the result of difficulties in realistic requirement of the structures [67].

### II.5.2.2 Evolutionary Structural optimization ESO-BESO method

The evolutionary structural optimization (ESO) method, this method is based on an empirical and simple concept of a structure with the lowest stresses, evolving into an optimal condition by slowly removing (hard-killing) elements [78]. For maximize the structure's stiffness, the stress criterion was replaced by the elementary stress energy condition [79]. This method achieved remarkable improvement in structure and in shape which means a total TO. In addition to, there have been resolve several types of structural problems with the use (ESO) model and the results agree with solutions of traditional models of optimization with the method of homogenization [80].

To achieve the removal of the material values are given 1/106 to the density of the items to be of their initial values. The removed element is continues based on the method of rotation energy of Von Mises to run repeatedly until all the values of the elements are calculated. The removal of 1-2% of elements of ESO model can achieve good results, but a higher percentage of removal elements  $2% > 0$ , will obtained different results though it has a small cost [76]. The ESO method is easy to program in a software package.

In addition to, the topographies have been generated have been accumulating presented as a promising method with empirical results. Have been developed several kinds of methods trying to ameliorate the algorithm in TO [81]. However, if that material is being removed from the algorithm, the ESO cannot of recovering elements that have been deleted [82].

Bi-directional evolutionary model optimization (BESO) method is a developed of the (ESO) method that permits the addition of new elements in the areas next to those elements with the highest stress. The stress energy criterion has been used of void elements was predestined by linear extrapolation of the displacement field for stiffness optimization problems [83]. So, ESO / BESO has been used which has greatly improved the potential of the process of solving a problem of optimization in a wide variety of applications [67].

### II.5.2.3 Level set method (LSM)

Level sets for moving interface problems in physics were first developed with the fundamental goal of tracking the motion of curves, surfaces and applied to topology optimization. In the early 2000s, where it was used to capture the free boundary of a structure in linear elasticity after that level sets with a shape sensitivity analysis framework for optimization of structural frequencies. That present a new method for the introduction of holes without the topological derivative using a secondary level set function. This enables a true topological design capability [58].

A limitation of these direct methods away from free boundaries are that algorithms cannot create new holes in the level set function and resulting solutions are heavily dependent on the initial state of the design problem. Topological derivatives represent the change of objective functional in the design domain with the introduction of infinitesimally small holes and permit for the nucleation of new holes. So, proposed an extension of the conventional level set method for use with a body-fitted finite element mesh, which is good when the design domain is irregularly shaped or nonrectangular. In the conventional level set methods, controlling the structural boundary is explicitly, often requires the reinitialization of level set functions when they become too flat or steep, both of which decrease the computational efficiency of the schemes for this place time step size restrictions for convergence stability. Boundaries are represented as the zero-level curve (or contour) of a scalar function (the level set function). Boundary modified, motion and merging, as well as the necessary introduction of new holes, are performed on this scalar function by controlling the motion of the level set according to the physical problem and optimization conditions. while a smooth boundary representation is realized in the design domain, most level-set formulations rely on finite elements [84]. consequently, boundaries are represented discretized, probable unsmooth, mesh in the analysis domain unless alternative techniques are utilized to map the geometry to the analysis model [58].

#### II.5.2.4 *Lattice structure topology optimization (LSTO) method*

Lattice is a new design structure that presents the compatibility between efficiency increase and weight reduction. It is created by repeating the unit cell of lightweight with superior characteristics and minimum material. Many of these structures are inspired by nature. Due to the presence a complex of cells, nodes, and beams the Lattice can be classified into 2D and 3D structures [85]. There are also thousands of types of lattice with different aesthetics and characteristics. Because of the difficulties in manufactured it, impossible to manufactured through traditional manufacturing. Wherefore, AM is the process that helps engineers to manufactured lattice structures to improve the performance of their design [67].

LSTO is an optimal lattice infill design tool that is widely used to infill component with graded lattice structure using homogenized model to gain efficiency [11]. It has been applied for determining the optimal density distribution of graded lattice structures in the designed space under specific stress constraints by filling the inner solid part of the blade with graded lattice structures. So far, lattice structures are mainly used in the biomechanics domain, but in fact, lattice structure shows great efficiency in thermal applications as well.

Lattice combination permit designers to try more shapes due to it can reduce the mass by 90% or more on the designing part only. The weight is reduced relative to the strength ratio and it does not reduce the strength of the structure by remove material in some critical areas of the component with a lattice structure and be operative at absorption of vibrations due to ability to endure enormous strains and their low stiffness. The design of lattice helps designers and engineers to confirm the design with some important features include cell structure, cell size and cell orientation and density of materials, as shown in Figure II.10. [86].

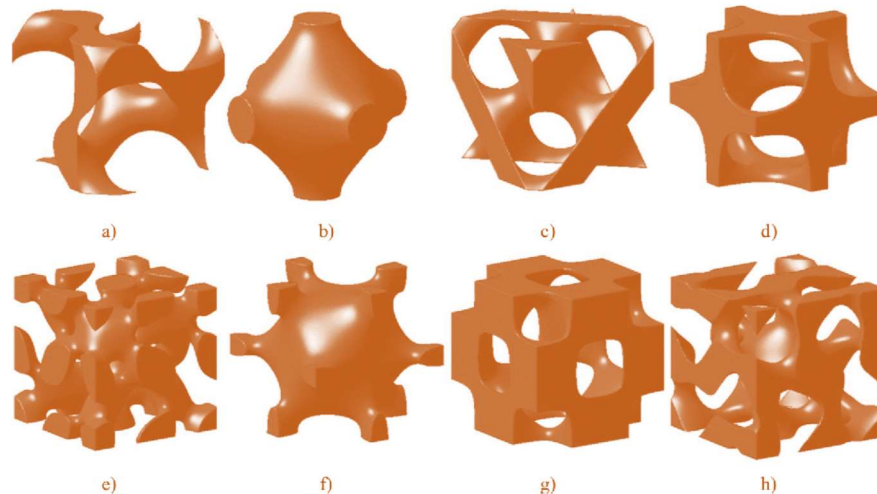


Figure II.10 a)Gyroid b)Primitive c)Diamond d)iWP e)Lidinoid f)Neovius g)Octo h)Spilt [86]

#### a) Cell structure

The most interesting and common in complex of the cell structure of lattice include star, diamond, hexagonal, octet, cubic, and tetrahedron. Because of their greater efficiency, with more pleasant aesthetic, and reduce energy better [67].

#### b) Cell size and density

This type of structure refers to the length and to the thickness of an individual unit explain the number of cells in a specific area. Large cells are stiffer and are easier to print as that a small cell permit a homogeneous response[67].

#### c) Cell orientation

Overall lattice makes complicated designing parts easier to create with the help of AM. So, no need for any extra supports because a structure is self-supported also the angle and the cell orientation from which is printed it is important because it is related to the support that is required [67].

#### d) Material selection

In general, be good to have a good material with perfect properties for the structure of lattice with smaller and denser structure so it can reduce the sag during the manufacturing [67].

### II.5.3 Modeling techniques for porosity gradients

For optimization replacement applications, it may be beneficial to adjust the porosity to vary the mechanical properties and optimize the biological behavior of architectural materials [87]. In addition to adjusting the overall properties of an architectural material, it may be advantageous to adjust its local properties to better represent the structure [88]. One way to perform this control without creating a discontinuity within the material is to apply a porosity gradient.

### II.5.3.1 Library of cells of uniform size

A cell library is sometimes used to model materials with variable porosity [89]. This technique consists of dividing a body into a finite number of voxels and filling each of them with a cell from the library. Discretized equations can be used to specify the distribution of cells in the body. Figure II.11 shows an example of an architectural material generated using an interpolation function and a cell library.

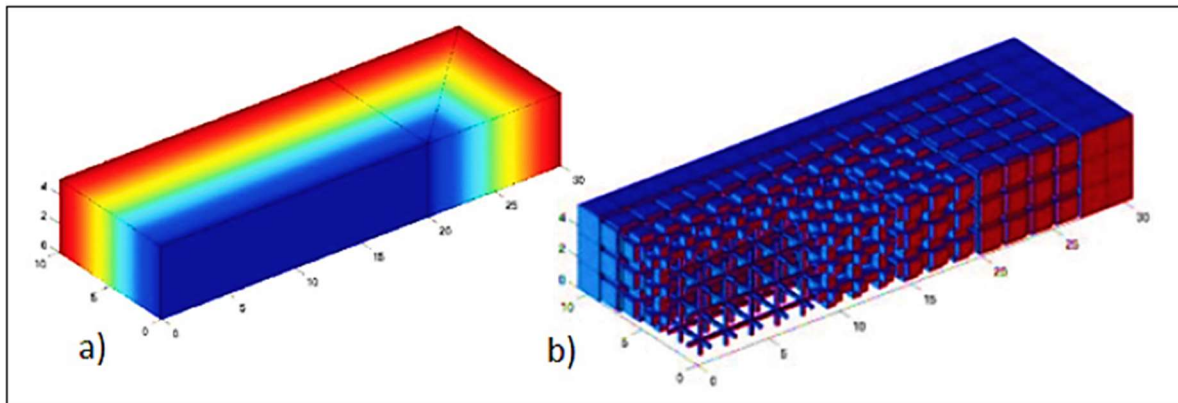


Figure II.11 Interpolation functions and cell library for the generation of architectural materials a) Visualization of linear interpolation b) Library cells added to the discrete body

The technique is easy to apply and offers a variety of methods for evaluating the mechanical properties of cells. The rule of mixtures, homogenization and numerical methods can among others be used to evaluate these properties [89]. The main disadvantage of the technique is that a large amount of memory may be required to store information about the distribution of cells.

### II.5.3.2 Parameterized cells of uniform size

Modeling with parameterized cells is similar to modeling with a cell library. The cells were however modeled by a single cell of variable geometry. The geometry is set and adjusted based on the composition information that is recorded in each volume. This modeling technique allows great control over the mechanical properties of each cell, particularly when used with CAD-based modeling approaches. It is therefore widely used for topological optimization [90]. Figure II.12 shows an example of an architected material, optimized and generated using parameterized cells.

For complex models, it can be difficult to assess the mechanical properties of individual cells. Homogenization is particularly well suited to approximate the properties of variable cells and generally reduces the computations associated with numerical simulations [91].

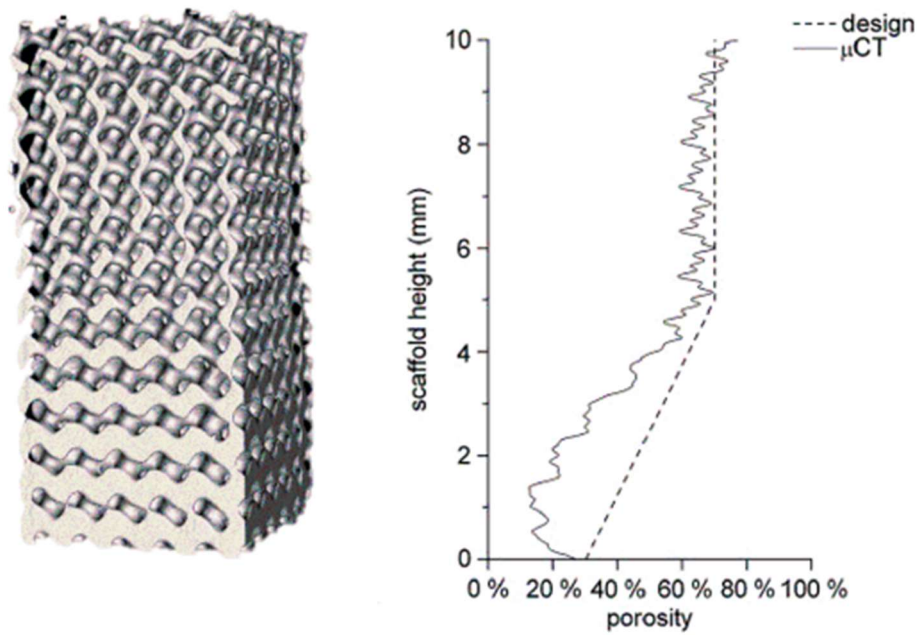


Figure II.12 Modeling of a linear gradient with representation by functions [91]

### II.5.3.3 Gradients for implicit surfaces

For the modeling approach based on implicit surfaces, a porosity gradient can be generated by adding a function to the base equation [92]. The structure shown in Figure II.13. shows an example where the addition of a linear function varies the porosity from 70% at the center of the structure to 30% at its lower end. This modeling technique is widely used for modeling architectural materials[93]. The disadvantage of the technique is the same as for modeling homogeneous materials using the implicit surface approach, i.e. the difficulty in defining the material boundary.

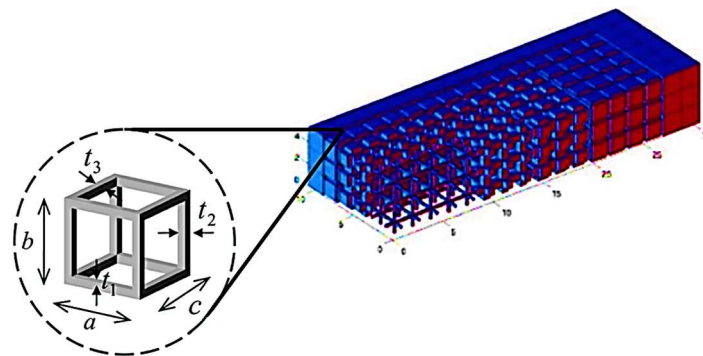


Figure II.13 Topological optimization produced with parameterized cells [93]

#### II.5.3.4 *Cells of variable sizes*

Used finite element (FE) mesh refinement principles to model architected materials having lattice structures with cells of varying sizes. Several techniques have also been developed to generate quasi-random gradients, well suited to model structures [40-41].

In this work, it is the technique of parameterized cells of uniform size that has been chosen to model the porosity gradient within the material. The ability to parameterize a cell and the ease with which the technique can be implemented with the CAD-based representation were the main reasons for this choice.

### II.6 Conclusion

In this chapter, state of the art Optimization approaches, multiscale modeling and homogenization approach, verification and validation techniques, and design optimization approaches are examined. Topology optimization operates on a fixed FE mesh of either continuum or discrete elements to optimally distribute material in the material layout. In the continuum element-based topology optimization, the shape of the external and internal boundaries and the density of each continuum element in the structure are optimized using a homogenization method. In discrete element-based topology optimization, the problem is solved by determining the optimum number, position, and mutual connectivity of structural member elements. In the third chapter, we will study in detail the Additive Manufacturing process, the different types of technologies, the properties of parts, materials and the building of the structure.

## Chapter III.

# **Additive Manufacturing**





### III.1 Introduction

In industrial mechanics, the manufacture of a part from a quantity of material delivered in the form of semi-finished products (sheets, bars, etc.) requires the implementation of a set of techniques. One of them is machining, that is to say removal of material by a cutting tool. The machining of a part is broken down into a succession of operations, defined by the machining range established by the methods office from the definition drawing from the design office [95].

Traditional machining is carried out, respecting the rules of metal cutting, on conventional or automated machine tools (numerically controlled machine tools interfaced with computer-aided design software). For the machining of refractory or very hard materials or in certain cases, to lower production costs, other processes are used which implement new techniques (Machining by Addition of Material) [67].

Thanks to the recent advancements in Additive Manufacturing technologies make it capable to fabricate strong, lightweight and complex based engineering structures. Additive Manufacturing (AM) is a method of transforming the 3D model, usually layer by layer in contrast to the conventional subtractive manufacturing process that requires de-tailed CAM analysis and Gcode to define the geometry in order to organize which feature should be produced [96].

In addition to these mechanical processes, material removal can also be obtained by chemical means: chemical machining, electrolytic machining, and electrician or by physical means: machining by water jet, by laser, or by PLASMA jet. TO offers to the various complex structures, the warranty that is required for AM to move on in the process [97]. Selecting the most appropriate additive manufacturing (AM) process for a particular application can be difficult. The very wide range of 3D printing technologies and materials available often means that several of them may be viable, but each offers variations in dimensional accuracy, surface finish and post-processing requirements [98].

This chapter is interested relates "additive manufacturing", the technologies of this process, its machines, its common manufacturers and the materials used and the applications and fields of use of each process and in particular the process PBF and its relationship to Topology optimization.

### III.2 Additive Manufacturing Materials

Additive Manufacturing process is a technology that we can use different kinds of materials, but the most important for industries and for AM technology is metal and plastic. We can also use ceramics, waxes, for many 3D models of these materials. Material property is definitely part of the AM area [99]. While selecting AM and computers, it is very important to be able to understand the intended usage. The material alone does not guarantee good quality, particularly when compared to conventional production.

A wide range of plastic printed in 3D is available. Even in the same part, the properties of each plastic can vary from different machine printing, it is very important that plastics have different temperatures of resistance [100]. Plastic material's properties may not tend to be reported as properties as they may differ outside the given range. For these types of materials, heat distortion temperature (HDT) is good to report. Many materials decrease rapidly when the temperature is increased and some gradually decrease over a longer range of temperature, thereby increasing the material's usefulness [101].

Some well-known plastics, such as acrylonitrile butadiene styrene (ABS), polyvinyl alcohol (PVA), polylactic acid (PLA), and polycarbonate (PC), are used in AM. ABS is the polymer's most popular type and can be found in many products. The advantages of ABS are good resistance to impact, strength, rigidity, and surface finish. The disadvantages of ABS are low incessant service temperature, very low dielectric strength and some diluent tolerance [102].

PLA is a thermoplastic biodegradable made from renewable resources such as maize starch or sugar cane. PLA is very sturdy and lightweight, but can be breakable and has a weak HDT. It is necessary to add fibers or filler materials to improve the mechanical properties of PLA. PLA parts are traditionally used primarily in biomedical and packaging applications. For example, in the automotive industry, reinforced material is used [103].

As it is dissolvable in liquid, PVA is used as a form of support material in AM. As PVA absorbs water, for better results, the environment must be controlled for moisture. Higher than usual moisture makes the material softer and more durable than hard and brittle [101].

When extruded, polycarbonate (PC) requires a high-temperature nozzle that can be difficult for 3D printers. PC as a material has many advantages such as high impact strength, strong dimensional stability, wear resistance, and all thermoplastic methods can handle it. PC is constrained by relatively soft substrate, only good resistance to solvents and poor sensitivity to

cracking pressure. For example, sports helmets and vehicle tail and headlights are common applications for polycarbonate [101].

In all cases of a metal structure, the powder material is used as input. Overall, based on Table III.1. Commercial materials used in the manufacturing of AM, any metal that can be welded under normal conditions can also be printed as 3D. Some commercial alloys are also available that can be used in the AM process [104].

**Table III.1 Commercial materials used in the manufacturing of AM**

Titanium	Aluminium	Tool steels	Superalloys	Stainless steel	Refractory
CP Ti	6061	Cermets	IN718	420	Alumina
ELI Ti	Al-Si-Mg	H13	IN625	347	CoCr
$\gamma$ -TiAl			Stellite	316 & 316L M	Ta-W

Metallic parts of AM go through continuous melting, heating removal, and crystallization during the process, and sometimes even through transformations in the state process. Compared to traditional manufacturing methods in Table III.1. Commercial materials used in the manufacturing of AM. The mechanical properties of metallic AM components are comparable with those of traditional manufacturing parts, certain defects such as micro porosity, increases the fatigue of AM properties but can be enhanced with methods such as TO or post-processing behavior such as hot isostatic processing or machining [104][105].

### III.3 Additive Manufacturing Technologies

There are different types of technologies in AM the difference between these categories is the manufacturing of layers and this affects the properties of parts, materials and the building speed of the structure. We can arrange categories of the AM process categories are seven based on the American Society for Testing and Materials as shown in Figure III.1 [104].

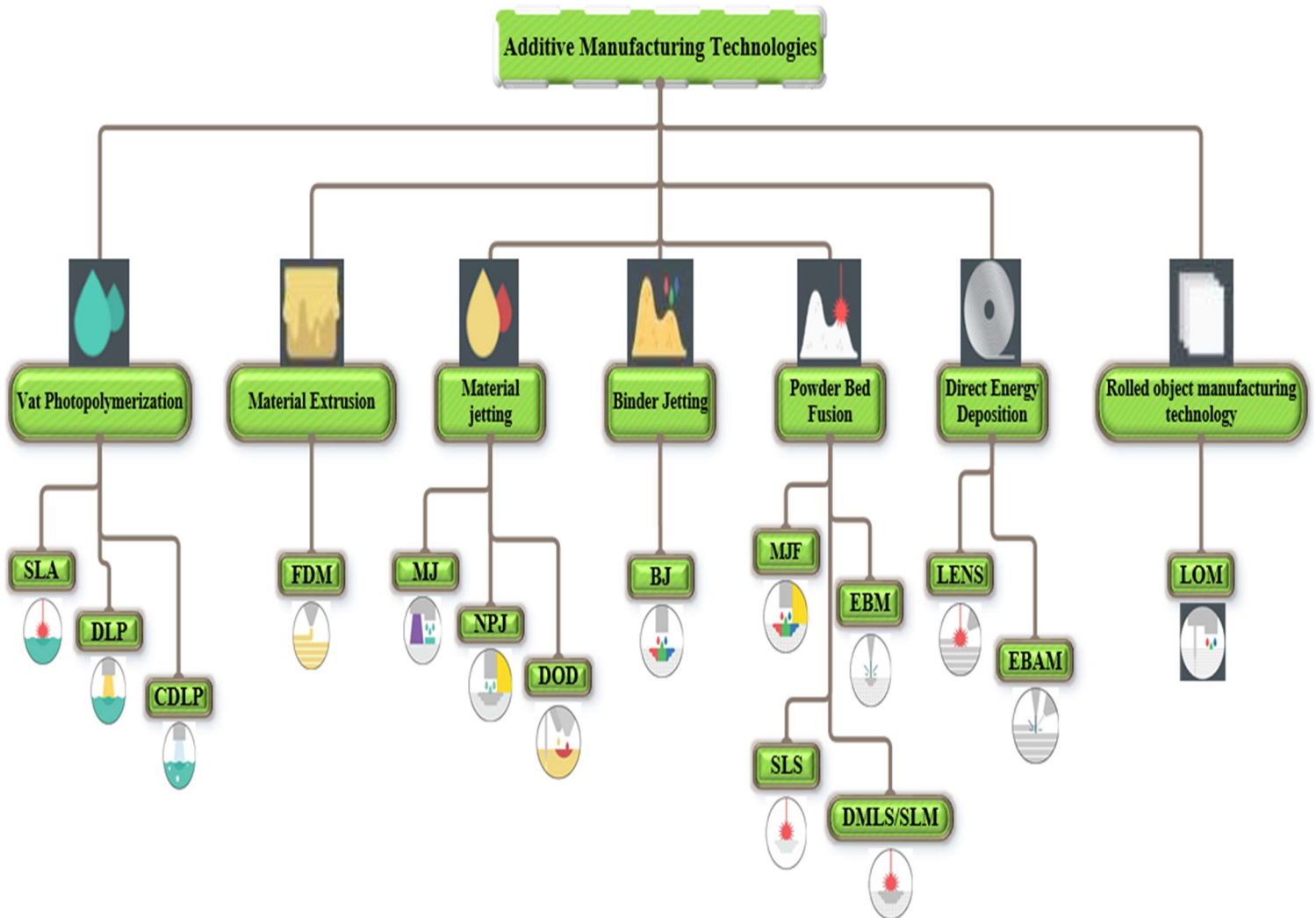


Figure III.1 Additive Manufacturing Technologies [104]

### III.3.1 Vat Photopolymerization

Vat Photopolymerization (SL) is a liquid photopolymer resin that is radiation-dried. Many machines use photopolymers that react to wave light's ultraviolet (UV) spectrum and some other machines use visible light to dry materials. The liquid material is solid when the radiation happens [95]. Many industrial devices use photopolymers that respond to wavelengths of the ultraviolet (UV) spectrum, but some systems also use visible light-curable materials. The liquid content is solid when is radiated [101].

Photopolymerization process, presents as the build platform moves down as the height of one build layer and the sweeper spreads the resin equally over the previous layer. Then the UV laser dried up the desired regions [106]. This process is continuously repeated until the part is complete as shown in Figure III.2. As the produced component is connected to the construction framework and can be lifted from the liquid photopolymer, the system can change direction and

operate upside-down. The light source is under the resin. This approach requires the liquid to have a shallow vat and is not limited in the process by the container depth [101].



**Figure III.2** Some SLA methods print parts upside down as they are pulled from the resin [101]

In contrast to other AM technologies, the main advantages of the vat photopolymerization process are the precision of the part as well as the surface polishing. This is a combination of mechanical transmission properties making photopolymerization an effective choice for structure and functional prototypes (Standard terms for AM-coordinate systems and test methodologies) [107]. Vessel curing processes are excellent for producing parts with fine detail and give a smooth surface finish. This makes them ideal for jewelry, low flow injection molding and many dental and medical applications as in Table III.2. The main limitations of tank polymerization are the fragility of the parts produced.

**Table III.2** Cell photopolymerization technologies, its manufacturers, and the materials used

Technology	Common manufacturers	Materials
SLA	Formlabs, 3D Systems, DWS	Standard resins, resistant, flexible, transparent and moldable
DLP	B9 Creator, MoonRay	Standard and moldable resins
CDLP	Carbon3D, EnvisionTEC	Standard resins, resistant, flexible, transparent and moldable

### III.3.1.1 Stereolithography (SLA) :

SLA uses a construction platform submerged in a translucent tank filled with liquid photopolymer resin. Once the build platform is submerged, a single point laser inside the machine maps a cross-sectional area (layer) of a design across the bottom of the tank solidifying the material. After the layer has been mapped and solidified by the laser, the platform lifts up and lets a new layer of resin flow under the part. This process is repeated layer by layer to produce a solid part. Parts are generally post-vulcanized by UV light to improve their mechanical properties as shown in Figure 3 [108].



Figure III.3 Form Labs machine from STL[109]

### III.3.1.2 Digital Light Processing (DLP):

DLP follows an almost identical method of producing parts as compared to SLA. The main difference is that DLP uses a digital light projector screen to flash a single image of each layer at one time. Because the projector is a digital screen, the image in each layer is made up of square pixels, resulting in a layer made up of small rectangular bricks called voxels. DLP can achieve shorter print times than SLA for some parts, as each entire layer is exposed at the same time, rather than tracing the cross area with a laser as shown in Figure III.4 [110].

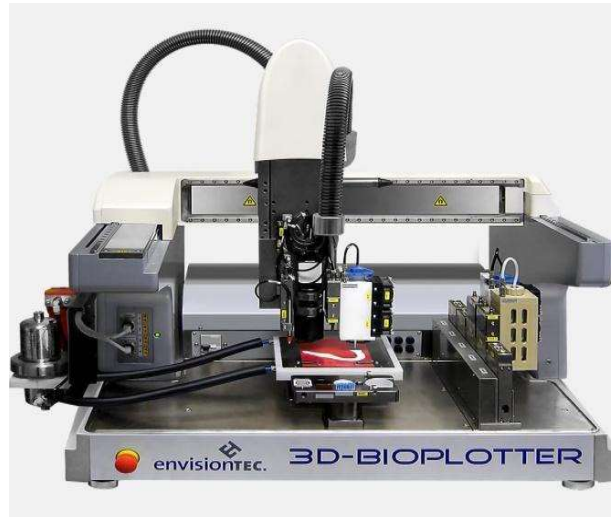
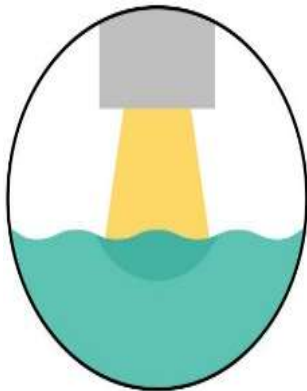


Figure III.4 DLP Envision TEC machine [110]

### III.3.1.3 Continuous Digital Light Processing (CDLP):

Continuous Digital Light Processing (CDLP) (also known as Continuous Liquid Interface Production or CLIP) produces parts in exactly the same way as DLP. However, it relies on a continuous movement of the build plate in the Z (upward) direction. This allows for faster build times as the printer does not need to stop and separate the part from the build plate after each layer has been produced as shown in Figure III.5 [111].

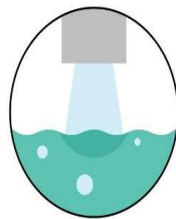


Figure III.5 CDLP Carbon 3D machine [111]

## III.3.2 Material Extrusion

Material Extrusion is the most common 3D printer trade procedure [112]. In this process, the material is melted and extruded from a nozzle to the construction base or on the surface of the previous layer. The material is either in a continuous filament or in a pellet or powder form in most systems as shown in Figure III.6 [113].



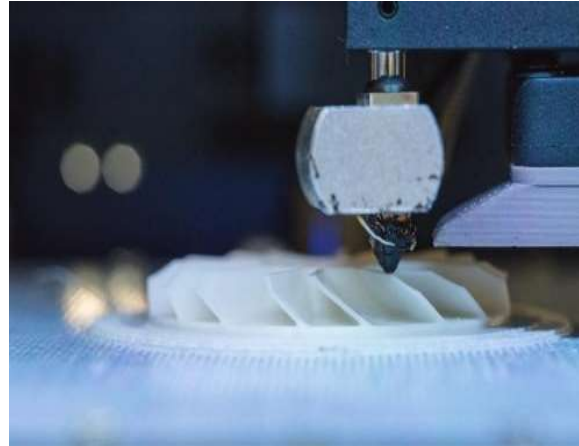


Figure III.6 FDM extrudes thermoplastic from a heated nozzle along a predetermined path to accumulate parts [113]

Fused Deposition Modeling is the most widely used extrusion technology that Stratasys produces and develops. We may conclude that FDM machines are more advanced worldwide than any other AM form machine as shown in Figure III.7 [95]. FDM can generate plastic of any kind, but ABS plus becomes the most sealing material, which is a little more creative of ABS. FDM can process valuable property parts and is relatively cheap. One of the disadvantages is the low construction speed and the accuracy depending on the use of the extrusion [114]. The nozzle presents inertia that, for example, limits movement speeds to a laser-based system. The radius of the nozzle defines both the final quality and the accuracy of the part [101]. Similar to the way toothpaste is squeezed out of a tube, material extrusion technologies extrude material through a nozzle and onto a build plate. The nozzle follows a predetermined path construction, layer by layer [115].

FDM (sometimes called Fused Filament Fabrication or FFF) is the most popular 3D printing technology. FDM builds parts using ropes of strong thermoplastic material, which comes in the form of a filament. The filament is pushed through a heated nozzle where it is melted. The printer continually moves the nozzle, securing the molten material in specific locations along a predetermined path. When the material cools, it solidifies building the part layer by layer [115].

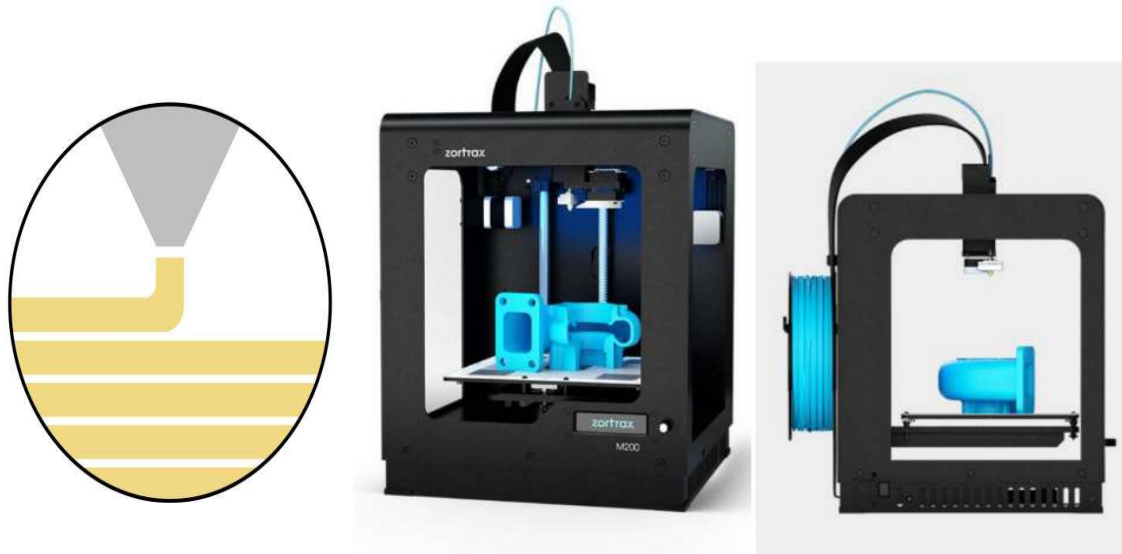


Figure III.7 Zortrax machine from FDM [115]

Material extrusion is a fast and cost effective way to produce plastic prototypes. Industrial FDM systems can also produce functional prototypes from engineered materials as shown in Table III.3. FDM has some dimensional accuracy limitations and is very anisotropic.

Table III.3 Material Extrusion technologies, manufacturers, and materials used

Technology	Common manufacturers	Materials
FDM	Stratasys, Ultimaker, MakerBot, Markforged	ABS, PLA, Nylon, PC, Fiber reinforced nylon, ULTEM, exotic filaments (wood-filled, metal-filled, etc.)

### III.3.3 Material jetting (MJ)

Jetting material is very similar to two-dimensional printing because on the construction platform, the build material is thrown into droplets. The material jetting on the platform is either hardened by using UV light or by allowing it to cool down and harden. We manage to limit the available materials when we deposit the material. The material jet is often compared to the process of 2D ink projection. Photopolymers, metals or wax that harden or harden when exposed to UV light or high temperatures can be used to fabricate parts one layer at a time. The nature of the material projection process allows for multi-material printing as shown in Table III.4. Most of the time, owing to their skill and ability to form drops, we use substances such as polymers and waxes. However, the latest research types have shown that metals and ceramics also have potential. Jetting material is a process that includes high precision and makes it

possible to use multiple colored materials under the same process as shown in Figure III.8. [101] [116].

**Table III.4 Jet technologies of materials, manufacturers, and its materials used**

Technology	Common manufacturers	Materials
Jets of matter	Stratasys (Polyjet), 3D Systems (MultiJet)	Rigid, transparent, multicolored, rubber-like, ABS-like. Multi-material and multi-color printing available
NPJ	Xjet	Stainless steel, ceramic
DOD	SolidScape	Wax

The material jet is ideal for realistic prototypes, providing excellent detail, high precision and a smooth surface finish. Material projection allows a designer to print in multiple colors and multiple materials in one print. The main drawbacks of material spraying technologies are the high cost and fragile mechanical properties of UV-activated photopolymers.



**Figure III.8 An inkjet printer illustrating the size of the machines [101] [116]**

### **III.3.3.1 Single Material jetting (SMJ) :**

The Materials Jet dispenses a photopolymer from hundreds of tiny nozzles into a print head to build layer by layer. This allows material blasting operations to deposit building material in a quick and linear fashion compared to other point deposition technologies that follow a path to complete the cross section of a layer. When the droplets are deposited on the build platform, they are hardened and solidified using UV light. Material blasting processes require support

and this is often printed simultaneously during construction from a dissolvable material which is easily removed during post processing as shown in Figure III.9 [116].



Figure III.9 MJ's Stratasy machine [116]

### III.3.3.2 Nanoparticle Jetting (NPJ) :

Nanoparticle Jetting (NPJ) uses a liquid, which contains metallic nanoparticles or carrier nanoparticles, loaded into the printer as a cartridge and projected onto the build plate in extremely fine layers of droplets. High temperatures inside the building envelope cause the liquid to evaporate and leave behind metal parts as shown in Figure 10 [117].

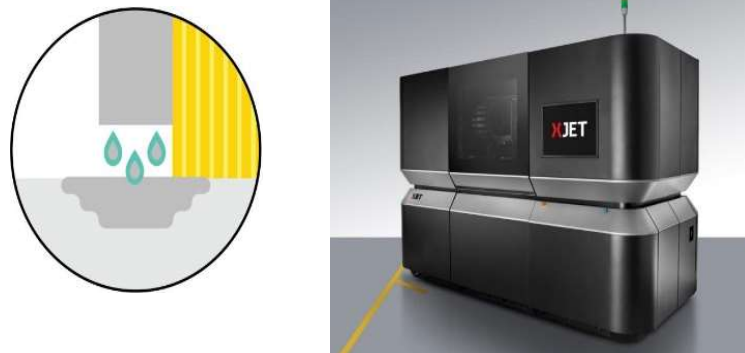


Figure III.10 : NPJ Xjet machine [117]

### III.3.3.3 Drop-On-Demand (DOD) :

DOD material jet printers have two printing jets: one for depositing building materials (typically a wax-like liquid) and another for soluble support material. Similar to traditional AM techniques, DOD printers follow a predetermined path and drop material in a point-wise fashion to build the cross section of a component as shown in Figure III.11. These machines also use a fly cutter that skims the build area after each coat to ensure a perfectly flat surface before printing the next coat. DOD technology is typically used to produce "wax-like" patterns for lost wax casting / investment casting and mold making applications [118].

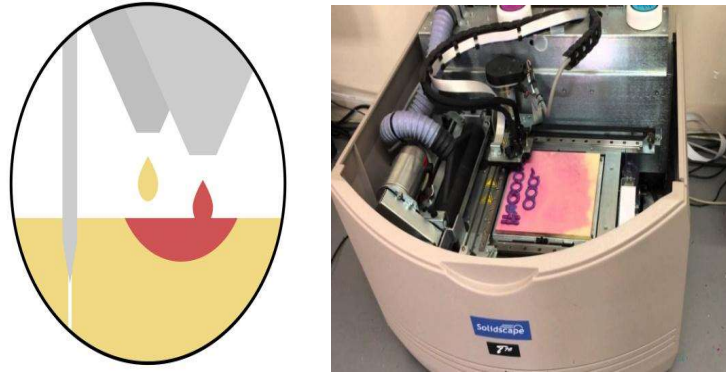


Figure III.11 DOD SolidScape machine [118]

### III.3.4 Binder Jetting (BJ)

Binder jetting process is a method that distributes a layer of powder as a powder bed fusion machine does in a build frame. To create a layer for the part, a liquid connecting agent is selectively applied to this powder layer. The base then decreases and a new powder layer cover the surface and the process is repeated until the part is finished. The advantages of this method is that due to the powder bed and the way the part is in the powder, the process does not require any support structures. This also enables parts to fill the entire construction volume [95]. Jetting binder is a fast and cheap technology that works with many different materials, including metals, polymers, and ceramics. Unless further processed, the parts that are made with this process have some kind of minimal mechanical properties as shown in Figure III.12.



Figure III.12 A binder projection part after removing the printing powder [95]

Ceramic-based Binder Jetting is ideal for applications that enhance aesthetics and form: architectural models, packaging, ergonomic verification, etc. It is not suitable for working prototypes, as the parts are very fragile. Ceramic binder smoothing can also be used to create molds for sand casting as shown in Table III.5. Metal binder spray parts can be used as

functional components and are more cost effective than SLM or DMLS metal parts, but have poorer mechanical properties [119].

**Table III.5 Binding Jet Technologies, Its Manufacturers, and Materials Used**

Technology	Common manufacturers	Materials
Binding jet	3D systems, Voxeljet	Silica sand, PMMA particles, gypsum
	ExOne	Stainless steel, ceramic, cobalt-chromium, tungsten carbide

Binder Jetting deposits a bonding adhesive agent on the thin layers of powder material. Powdered materials are ceramic (eg glass or gypsum) or metal (eg stainless steel). The print head moves across the build platform depositing droplets of binder, printing each layer the same way 2D printers print ink on paper. When a layer is complete, the powder bed moves down and a new layer of powder is spread over the build area as shown in Figure III.13. The process repeats until all parts are complete. After printing, the parts are in a green state and require additional post-processing before they can be used. Often, an infiltrator is added to improve the mechanical properties of the parts. The infiltrator is usually a cyanoacrylate (in the case of ceramic) or bronze (in the case of metals) adhesive [119].



**Figure III.13 BJ's EXOne machine [119]**

### III.3.5 Powder Bed Fusion

Powder bed fusion (PBF) technologies produce a solid part by using a heat source that induces fusion (sintering or melting) between particles of a plastic or metal powder one layer at a time.



Most PBF technologies use mechanisms to spread and smooth thin layers of powder as a part is built, resulting in the encapsulation of the final component in the powder after the build is completed as shown in Figure III.14. The main variations of PBF technologies come from different energy sources (e.g. lasers or electron beams) and powders used in the process (plastics or metals) [120] [101].



**Figure III.14 Powder pin removal from the SLS process with the printed parts still enclosed in the unsintered powder**  
[120] [101]

In available materials there are many differences[105]. For this reason, there is a wide range of available materials, including metals, polymers, ceramics and composites, as a process can use all the materials that can be melted and recrystallize. Because of the material properties, these methods can be used for the processing of final products since the properties of the materials are comparable to those of traditional parts [101]. Polymer-based PBF technologies offer great freedom of design, as there is no need for support, allowing the fabrication of complex geometries. PBF metal and plastic parts typically have very high strength and rigidity and mechanical properties which are comparable (or sometimes even better) than bulk material as shown in Table III.6. There is a wide range of post-processing methods available which means that PBF parts can have a very smooth finish and for this reason they are often used to make finished products. The limitations of PBF are often related to surface roughness and internal porosity of parts, shrinkage or distortion during processing, and challenges associated with handling and disposing of the powder [1].

**Table III.6 Powder Bed Fusion Technologies, Its Manufacturers, and Materials Used**

Technology	Common manufacturers	Materials
MJF	HP	Nylon

SLS	EOS, Stratasys	Nylon, alumide, nylon filled with carbon fibers, PEEK, TPU
DMLS / SLM	EOS, 3D Systems, Sinterit	Aluminum, titanium, stainless steel, nickel alloys, cobalt-chromium
EBM	Arcam	Titanium, cobalt-chrome

### III.3.5.1 Multi Jet Fusion (MJF):

MJF is essentially a combination of SLS and Material Jetting technologies. A carriage with inkjet nozzles (similar to nozzles used in desktop 2D printers) passes over the print area, depositing the fuser onto the thin layer of plastic powder as shown in Figure III.15. At the same time, a detailing agent that inhibits sintering is printed near the edge of the part. A high-powered IR (InfraRed) energy source then passes over the build bed and breaks up the areas where the fuser has been distributed, while leaving the rest of the powder intact. The process repeats until all parts are complete [121].



Figure III.15 HP Jet Fusion 4200 machine from MJF [121]

### III.3.5.2 Selective Laser Sintering (SLS):

SLS produces solid plastic parts by using a laser to sinter thin layers of powdered material one layer at a time. The process begins by spreading an initial layer of powder on the build platform. The cross section of the part is scanned and sintered by the laser, solidifying it. The build platform then drops a layer thickness and a new layer of powder is applied. The process repeats until a solid part is produced. The result of this process is a component completely enclosed in



an unsintered powder. The part is removed from the powder, cleaned, then ready for use or after processing as shown in Figure III.16 [122].



Figure III.16 SINTERIT machine from SLS [122]

### III.3.5.3 Direct Metal Laser Sintering (DMLS/ SLM):

Selective laser melting (SLM) and direct metal laser sintering (DMLS) produce parts via the same method as SLS. The main difference is that SLM and DMLS are used in the production of metal parts. SLM achieves complete fusion of the powder, while DMLS heats the powder to temperatures close to fusion until it chemically fuses. DMLS only works with alloys (nickel alloys, Ti64 etc.) while SLM can use single component metals, such as aluminum. Unlike SLS, SLM and DMLS need support structures to compensate for the high residual stresses generated during the construction process. This helps to limit the likelihood of warping and distortion. DMLS is the best established AM metal process with the largest installed base as shown in Figure III.17 [123].

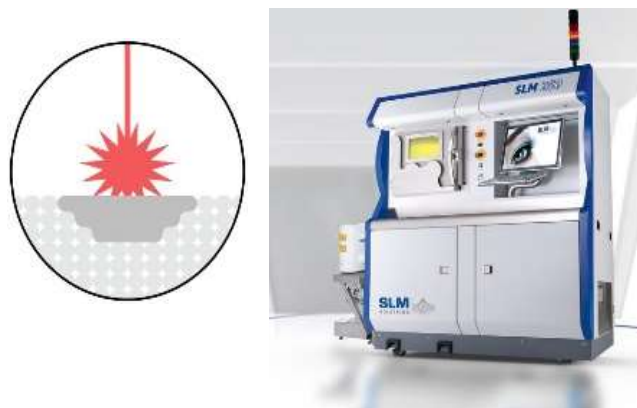


Figure III.17 SLM machine from SLM [123]

### III.3.5.4 Electron Beam Melting (EBM):

EBM uses a high-energy beam rather than a laser to induce the fusion between particles of a metal powder. A focused electron beam sweeps across a thin layer of powder, causing localized melting and solidification over a specific cross-area. Electron beam systems produce less residual stress in parts, resulting in less distortion and less need for anchors and support structures as shown in Figure III.18. In addition, EBM consumes less power and can produce layers faster than SLM and DMLS, but the minimum size, powder particle size, layer thickness and surface finish are generally inferior. EBM also requires that parts be produced under vacuum and that the process can only be used with conductive material [124].



Figure III.18 EBM Arcam Q10 plus machine [124]

### III.3.6 Direct Energy Deposition

Direct Energy Deposition (DED) is a last AM method process. The nozzle is moving in three directions in a DED system. Nevertheless, it is possible to mount the deposition nozzle on a multi-axis neck. This makes it easier to maintain and repair existing structures as the material can be deposited in the process from various angles. The material deposits from the nozzle in the form of powder or wire and is melted with a laser or electron beam. Generally, the DED process is used with metals but can also be used with polymers and ceramics as shown in Table III.7. This method may be used to make similar structures in functional parts, high quality or repair. DED processes with a full-dense part can produce highly controllable microstructural features. Limited resolution and surface finishing is the key drawback of DED processes, while speed can sometimes be sacrificed for better surface quality and higher precision. The time may be very significant as the construction time is already very long [101].

DED technologies are used exclusively in the manufacture of metal additives. The nature of the process means they are ideally suited for repairing or adding hardware to existing components

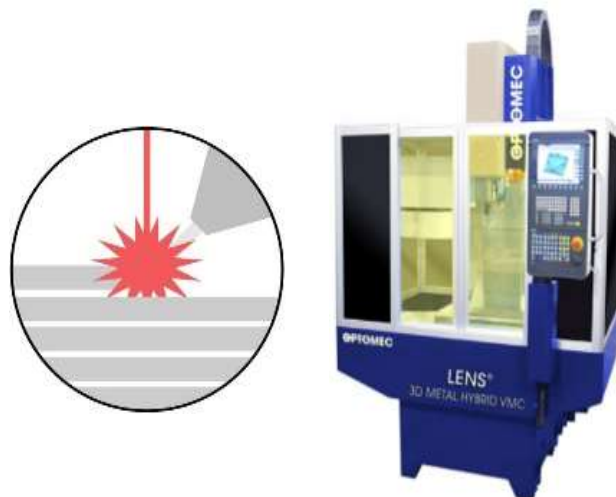
(such as turbine blades). The use of dense support structures makes DED not ideally suited for producing parts from scratch [125].

**Table III.7 Direct energy deposit technologies, their manufacturers, and the materials used**

Technology	Common manufacturers	Materials
LENS	Optomec	Titanium, stainless steel, aluminum, copper, tool steel
EBAM	Sciaky Inc	Titanium, stainless steel, aluminum, copper nickel, steel 4340

### III.3.6.1 Laser Engineering Net Shape (LENS):

LENS uses a deposition head consisting of a laser head, powder delivery nozzles, and inert gas tubing to melt the powder as it is ejected from the powder delivery nozzles to form a solid layer by layer. The laser creates a melt on the build area and powder is sprayed into the pool, where it is melted and then solidified as shown in Figure III.19. The substrate is typically a flat metal plate or an existing part to which material is added (e.g. for a repair) [126].



**Figure III.19 LENS OPTOMEc machine** [126]

### III.3.6.2 Electron Beam Additive Manufacturing (EBAM):

EBAM is used to create metal parts using metallic powder or wire, soldered together using an electron beam as a heat source as shown in Figure III.20. Producing parts in a manner similar to LENS, electron beams are more efficient than lasers and operate under vacuum with technology originally designed for use in space [127].

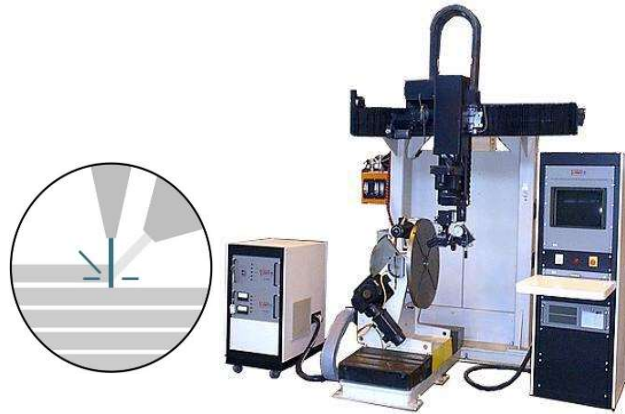


Figure III.20 EBAM SCIACY machine [127]

### III.3.7 Sheet lamination

Laminated object manufacturing is a lesser-known additive manufacturing process where an object is created by successively layering sheets of building material, gluing them through heat and pressure and then cutting them into the desired shape using a blade or a carbon laser. MCor Technologies offers a new form of the process known as selective deposition lamination. In this process, sheets of standard A4 or Letter paper are cut to shape using a tungsten carbide blade and then glued by selectively placed droplets of a water-based adhesive. The areas that will be the final part receive a high concentration of the adhesive, while the areas used for the backing receive less [1]. The machines are mainly used in the rapid production of plastic parts for prototyping as shown in Table III.8. Its low cost and speed make it useful in creating prototypes, even if the objects produced fall short of the quality of finish of the finished parts [128].

Table III.8 Laminated object manufacturing technologies, its manufacturers, and the materials used

Technology	Common manufacturers	Materials
Laminated Object Manufacturing LOM	MCor, EnvisionTec, IMPOSSIBLE OBJECTS	PVC thermoplastics; Paper (0.002-0.06 inch); Composites (Ferrous metals, Non-ferrous metals, Ceramics)

Mcor offers a special version of LOM which they named Selective Deposition Lamination (SDL). This paper-based technology adds color to the print. Sheets of paper are printed in color,

then selectively glued and cut with a blade. The glue is applied only to the surface of the object, so it is easy to remove the finished object as shown in Figure III.21. In addition, the addition of color allows this technology to compete with binder projection techniques in the production of multicolored objects, although the quality is not the same [128].

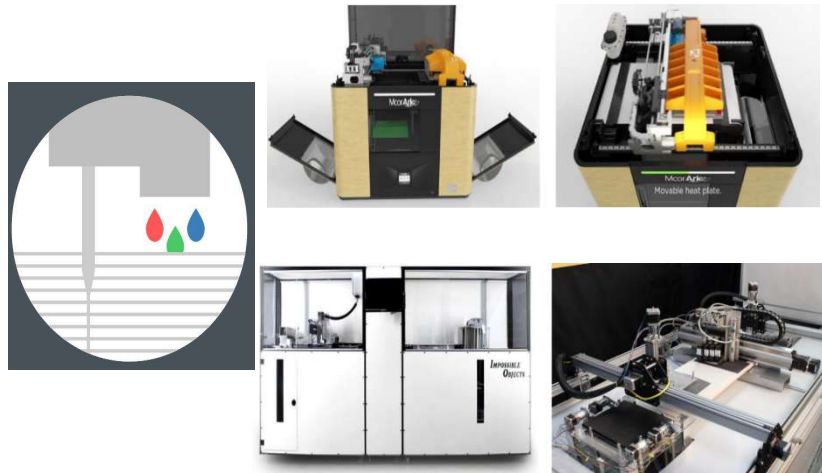


Figure III.21 LOM's MCOR machine (for paper) and IMPOSSIBLE OBJECTS machine from LOM (for composites) [128]

### III.4 Applications fields of additive manufacturing

3D printing technology has been applied in a wide variety of industries. Figure III.22 shows the different types of 3D printing usage that include research, artistic objects, visual aids, presentation models, device covers, custom parts, functional models and patterns as well as mass production as shows in Figure III.22.

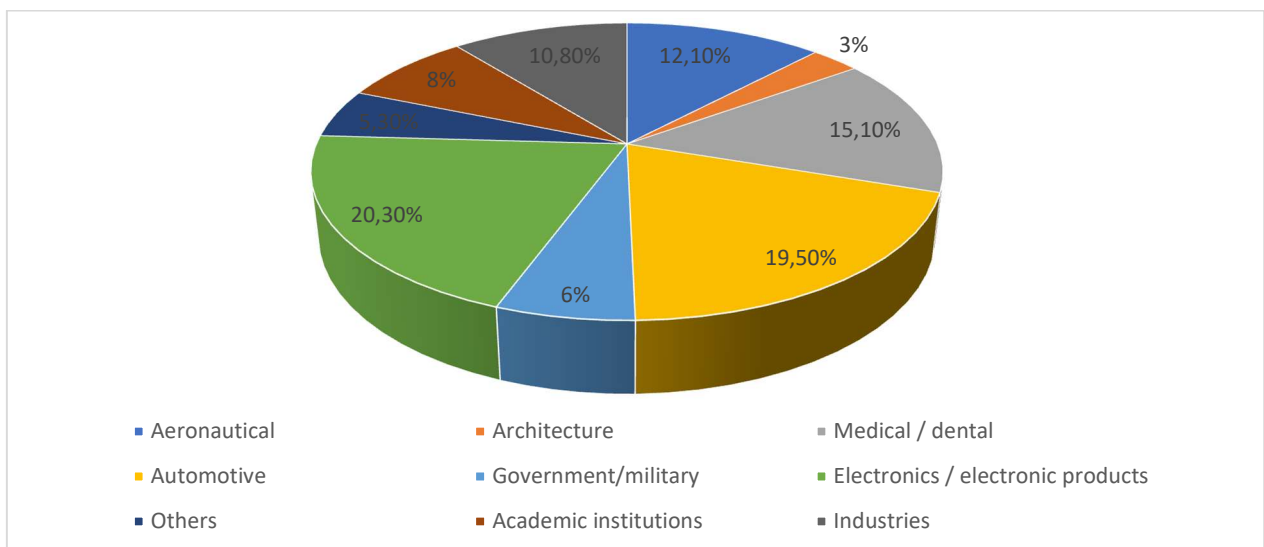


Figure III.22 3D printing applications

### III.4.1 Civil Engineering Construction

In China, they were able to build 10 one-story houses in a day, a process that normally takes weeks to months [129]. 3D printing thus offers a cheaper, faster and safer alternative to more traditional construction. Four giant 3D printers were used by Win Sun Decoration Design Engineering to build houses in Shanghai; using a mixture of cement and construction waste to build the walls layer by layer. Each of these houses is 10 meters wide and 6.6 meters high with each house costing less than \$ 5,000; it has been proven cost and time-efficient [130]. (Figure III.23)



Figure III.23 3D construction [129]

### III.4.2 Manufacturing

3D printing has ushered in an era of rapid manufacturing. The prototyping phase can now be skipped and go straight to the final product. Parts of cars and planes are printed using 3D printing technology. The printing of parts is done quickly and efficiently, thus contributing enormously to the value chain [131].

Custom products can be manufactured as customers can edit the digital design file and send it to the manufacturer for production. Nokia Company has taken the lead in manufacturing in this area by releasing 3D design files of its case to its end users so that they can customize it to their specifications and have the case 3D printed [130]. (Figure III.24).

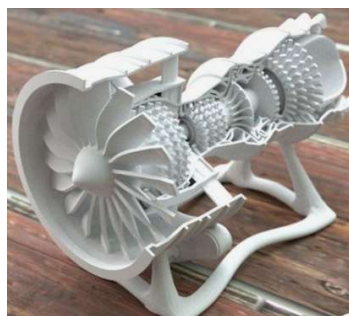


Figure III.24 3D model of turbine [131]



### III.4.2.1 Additive manufacturing in the aircraft industry

Additive manufacturing has been used in the aviation industry since the technology was adopted in the 1980s. It saves time and money during the period of product development. Its role is important in product design, direct manufacturing of parts, assembly, repair and maintenance. With its recent developments, it has become a revenue-generating technology along the entire supply chain. The examples of applications in the aeronautical sector are numerous, as we describe in our numerous case studies: various hinges and supports, components of the interior cabin, turbine blades with internal cooling channels, fuel injectors, compressors and integrated piping systems, etc. Exterior and structural applications continue to develop, but it is in the cockpit of airplanes that 3D printing has become an essential industry technology: it allows the design of lighter components with thinner walls than injection molding. It also offers the possibility of easily creating complex geometries, at a production cost that does not exceed that of the design of simple parts. Finally, it makes it possible to considerably reduce the weight of the vehicles, while offering the possibility of personalizing them. From airplanes to space vehicles, additive manufacturing contributes significantly to the development of the aviation industry [132]. (Figure III.25).

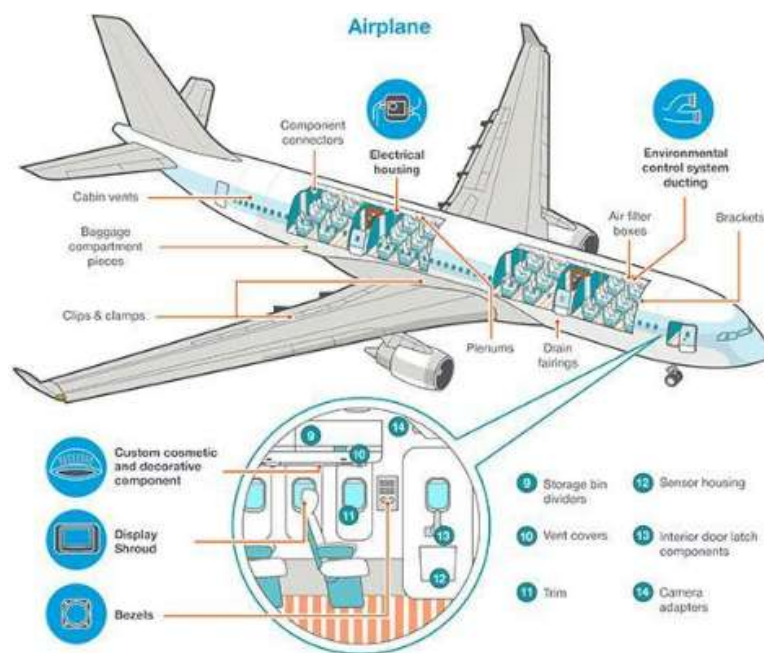


Figure III.25 Applications of additive manufacturing in the aeronautics sector - Source Stratays [132]

The attributes of additive manufacturing in the aircraft industry Additive manufacturing offers many advantages to the aviation and space industry:

- Shortened development cycles for faster time to market



- Flexibility in the design of complex parts
- Maximize performance
- Consolidate design and improve reliability
- Achieve lighter components to reduce fuel consumption
- On-demand and outsourced spare parts manufacturing
- Reduced material consumption for more savings
- The promises of quality assurance carried out in parallel with the manufacture of components [133].

### III.4.3 Medicine

#### III.4.3.1 Bio-printers

The impression of organs or parts of the body is being printed and some parts are being used as implants of real parts of the body. Body parts such as titanium pelvis, plastic tracheal splint, titanium jaws just to name a few have been printed [134]. (Figure III.26)

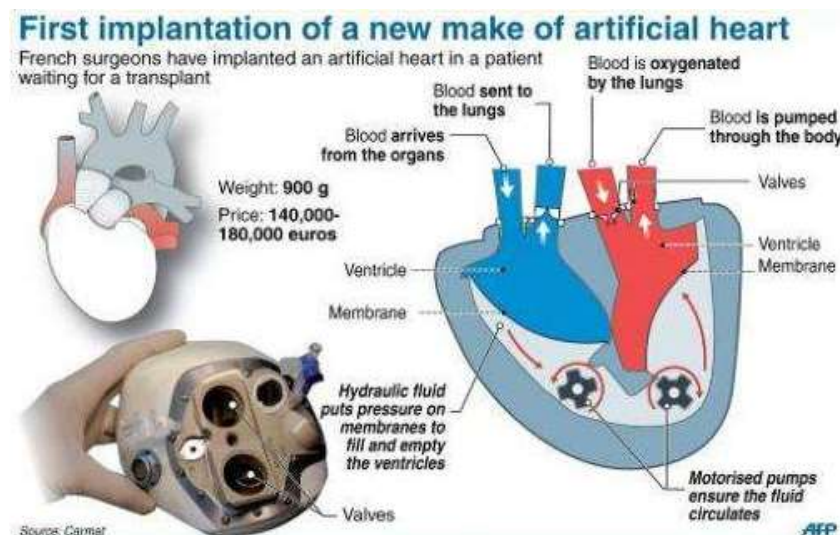


Figure III.26 First total and autonomous artificial heart [134]

#### III.4.3.2 Digital dentistry

People get personalized 3D printed teeth for the individual. Dental implants are manufactured on a commercial level and make the whole process faster and more efficient. Before, false teeth were one size, it all depends on age, now people of the same age can have [135]. Teeth of different sizes, which makes people uncomfortable with ill-fitting false teeth. Therefore,

personalized implants have truly brought a sigh of relief to consumers as they are now able to receive teeth that are suitable for them. (Figure III.27).



Figure III.27 3D printing and the dental world [135]

#### III.4.3.3 Prostheses

There are multitudes of people in need of replacement body parts, from people born without limbs to victims of accidents. The cost of obtaining substitute body parts was extremely expensive, but thanks to 3D printing; the cost has been drastically reduced. Prosthetics have really done wonders for people with disabilities, with Paralympic champion Oscar Pistorius being a world-famous example. As a child, Oscar Pistorius had his legs cut off, but that didn't stop him from running, much less at the Olympics [134]. (Figure III.28).



Figure III.28 Hand prostheses [134]

#### III.4.3.4 Artificial organs

Additive manufacturing of stem cells has also led to various possibilities for printing artificial organs, although most of the work is still in the experimental stage. For example, thanks to 3D printing, scientists at Heriot-Watt University were able to produce clusters of embryonic stem cells. An endless world of possibilities awaits this world with the prospect of imprinting real functional artificial organs [136]. (Figure III.29).



Figure III.29 Artificial organs for the study of medicine [136]

#### III.4.4 Domestic use

3D printers can be used at home to make small items such as ornamental items as necklaces and rings. Small plastic toys can also be printed in a home setting. In the future, people will be able to print their own products at home instead of buying in stores [136].

#### III.4.5 Clothes

The fashion industry has not been spared either. 3D printed garments are being manufactured. Fashion designers are experimenting with 3D printed bikinis, shoes and dresses. Nike manufactured the Vapor Laser Talon 2012 soccer shoe and New Balance custom shoes for athletes using a 3D prototype [137]. The production was done on a commercial scale.

#### III.4.6 Academic

3D printing is now integrated into the learning program. With applications ranging from printed molecular models to plastic gears. Students are now able to 3D print their prototype models and this helps in the learning process of students. Students are better able to understand concepts because they can be shown to them in a practical way [138].

### III.5 Conclusion

Additive Manufacturing (AM) is a manufacturing process that began to develop in the 1980s and is currently reaching a maturity that allows it to be used profitably and functionally by manufacturers. Additive manufacturing is defined as the process of shaping a part by adding material, as opposed to traditional shaping by removing material (machining). Additive manufacturing was originally reserved for prototyping and therefore for the pre-production part of a product's lifecycle. Currently it is also used in the production phase of a product. However, it has the limit of being much less productive than traditional machining and is therefore limited to the production of parts in small and medium series. Additive manufacturing is also part of

the post-production phase of a product's life cycle. Indeed, it can be used to repair damaged parts or to replace old parts whose serial production has ended and which are no longer in stock.

AM has many advantages, in particular it makes it possible to manufacture very complex shapes, some of which cannot be achieved with conventional processes, and with a wide variety of materials. This also makes it possible to produce monobloc parts, that is to say parts without assembly. Manufacturing times are also interesting for the production of parts in small series (no tools). Depending on the parts, additive manufacturing can allow a significant reduction in manufacturing costs and simplification of the overall process (elimination of certain heat treatments, no multiple turning + milling operations).

The fields of application of AM are already very varied today. It is widely used for rapid prototyping during the design of an object with the aim of reducing prototype manufacturing times and lowering their cost. Additive manufacturing also finds many applications in fields such as aeronautics (Safran manufactures parts for the Silvercrest engine), medicine (production of tailor-made bone substitutes, dental implants) or even the automotive industry.

AM is therefore a relatively new manufacturing process which, used correctly, has many advantages: that of producing differently but also, which represents a significant breakthrough potential in engineering, that of designing systems based on new geometries and new material combinations.

## Chapter IV.

### **Case Study**



## IV.1 Introduction

This chapter describes the method of our proposed approach and designing the lattice structures with a different architecture in two different fields: Aerospace and Biomechanical.

- ❖ In the field of aerospace, we consider the gas turbine blade as follow:

We introduce the design stage of the CAD model equivalent for the designed turbine blade, the properties of the materials used and the applied boundary conditions. Then presents the method of Topology Optimisation to find the optimal density distribution of lattice structures. After this method, the methodology for generating graded lattice structures was derived from the triply periodic minimal surface (TPMS) and selected the proposed technique for manufacturing the lattice structures.

- ❖ In the field of biomechanical, we consider the cancellous bone as follow:

Created a new design based on three lattice structures from triply periodic minimal surfaces (TPMS) with a different volume porosity to replace cancellous bone based on predicting the mechanical stiffness. To predict the mechanical stiffness, the relationship between the effective modulus of elasticity and different porosity ratios of the lattice structures was determined by using three methods: i) finite element modelling (FEM) simulation, ii) Gibson and Ashby method and iii) a uniaxial compression test after manufacturing the lattice structures by using Fused Filament Fabrication (FFF) technology.

## IV.2 The Field of Aerospace

### IV.2.1 Designing Lattice Structures

In this section, an introduction to the design stage of the lattice structures is presented through the proposed architecture as shown in Figure IV.1, CAD model equivalent for the designed turbine blade, the properties of the material used and the applied boundary conditions.

### IV.2.2 General Architecture of the Proposed Procedure

The proposed system architecture for lattice structures design is introduced, as illustrated in the flowchart Figure IV.1.

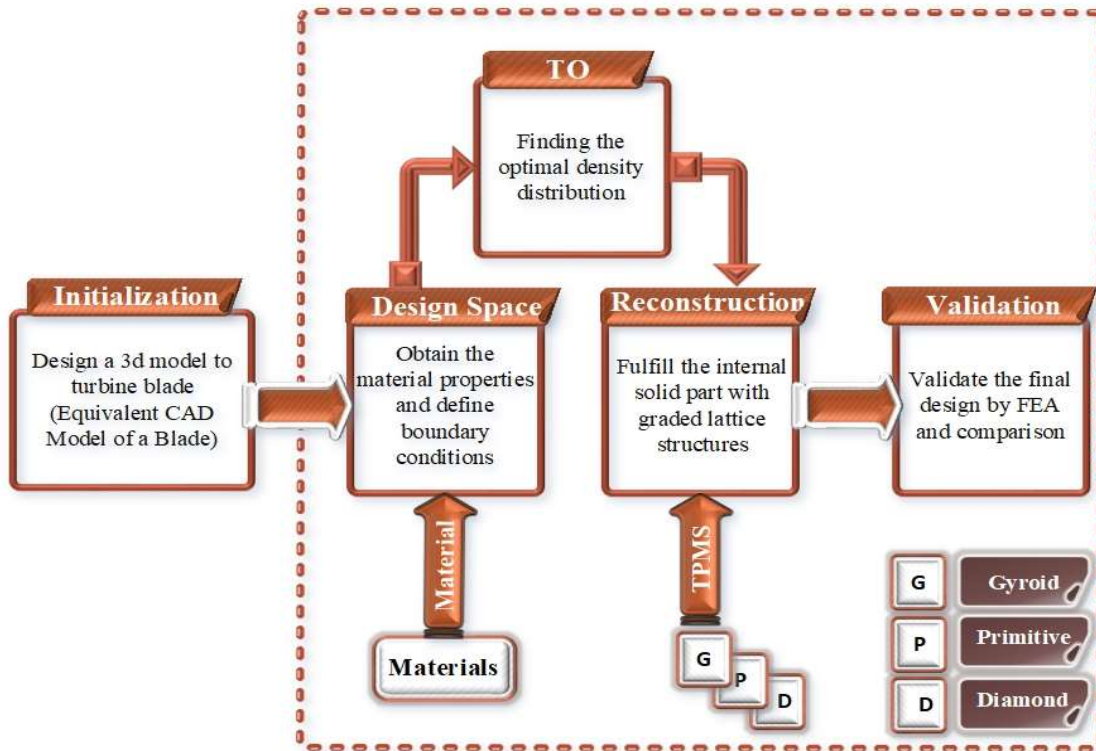


Figure IV.1 General architecture of the proposed procedure

### IV.2.3 Design of Equivalent CAD Model for Turbine Blade. (Initialization)

In this section, we work on designing a turbine blade using a coordinate of profile NACA (NACA 2412 (naca2412-il)) data to produce a similar simplified 3D model for turbine blade. The design and the numerical parts are conducted in SolidWorks 2019 and ANSYS 2020 R1 software respectively taking into account the engineering changes that occur in the design space during the TO routine. The proposed geometric pattern of the blade is illustrated in Figure IV.2.

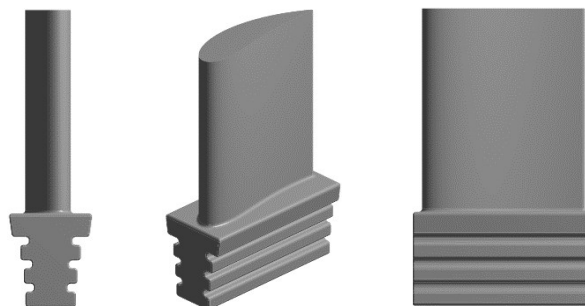


Figure IV.2 3D model to turbine blade

To simulate the mechanical behaviour of our turbine blade model, we need to determine material properties and boundary conditions as input parameters.



### IV.2.3.1 Properties of Material

Today's aviation field is based on modern jet engines. Thus, the components of turbines have to meet the requirements of high thermomechanical operations [139]. Various materials have been developed to suit the environment in which these turbines operate, especially nickel base superalloys for their immense ability to withstand both mechanical and thermal loads [140]. In the present study, we suggest producing a turbine blade by a graded lattice structure to replace the solid internal volume of the blade using Inconel 718 material. Inconel 718 material has a good mechanical resistance to high temperatures, good thermal conductivity, high electrical resistivity, high hardness, good wear resistance, chemical inertia [141]. These properties make it an ideal material for turbine blade in the gas engines. Table 1 shows the physical and mechanical properties of Inconel 718 [142].

**Table IV.1 Physical and Mechanical properties of Inconel 718**

Property	Unit	
Density	Kg/m <sup>3</sup>	8190
Young's Modulus	GPa	200
Ultimate Tensile Strength	MPa (min)	1375
Yield Tensile Strength	MPa	1100
Thermal Conductivity	w/m <sup>°K</sup>	11.4
Specific Heat Capacity	J/Kg <sup>°C</sup>	435
Melting Point	°C	120-1336
The Bulk Modulus	MPa	1.375e <sup>+05</sup>
Shear Modulus	MPa	63463
Poisson's Ratio		0.3

### IV.2.3.2 Boundary Conditions

Early gas turbines operated in temperatures around (820 °C), while the modern turbines face temperatures around (1370 °C) [143]. In the present study, the applied boundary conditions

were determined based on the realistic operating conditions of gas turbines in an environment with a thermo-mechanical behaviour and the type of the material used in the manufacturing of blades (Inconel 718 was used in this study due to its high resistance to temperatures around (1350 °C)) [144]. In addition, calculations were conducted using a numerical simulation based on the finite element method in the ANSYS 2020 R1 software. In the suggested model, the methodology is divided into two parts: geometric modelling and thermo-mechanical analysis. In geometric modelling, a tetrahedron mesh is generated (because the tetrahedrons shapes fit into the curvatures of the blade) by using patch independent method (i.e. can define the minimum element size and maximum element size) in order to facilitate the thermo-mechanical analysis applied to the turbine blades. In thermo-mechanical analysis, the thermo-mechanical behaviour of the initial design of the blade was analysed under the effect of the thermo-mechanical coupling. The thermo-mechanical behaviour of final designs of the blade whose internal volume consists of three different lattice structures (Diamond, Gyroid and Primitive) was also analysed. The same boundary conditions are applied to both cases in two stages: In the first stage, thermal loading of the blade is considered as the jet hot of thermal steam in leading edge of the blades. The thermal loads and convection are applied to the blade according to the boundary conditions as shown in table (2) and Figure IV.3 (a). In the second stage, the mechanical analysis (static- structural) is conducted under the coupled effect of thermo-mechanical load with the elimination of all degrees of freedom for the embedding part (fixe the root of the blade). The thermal load is taken from the first stage, while the applied pressure on the tip of the blade as shown the Table (2) and Figure IV.3 (b) causes the mechanical load. Finally, the finite element method has been used to analyse several process parameters such as: weight, stress and deformation to demonstrate the effectiveness of our proposed method [145].

Table IV.2 Steady-state Boundary Condition for the thermo-mechanical analysis

Parameters	Value
Pressure	10 MPa
heat transfer coefficient	0.000025 W/mm <sup>2</sup> ° C
ambient temperature	1350 ° C
initial temperature	350 ° C

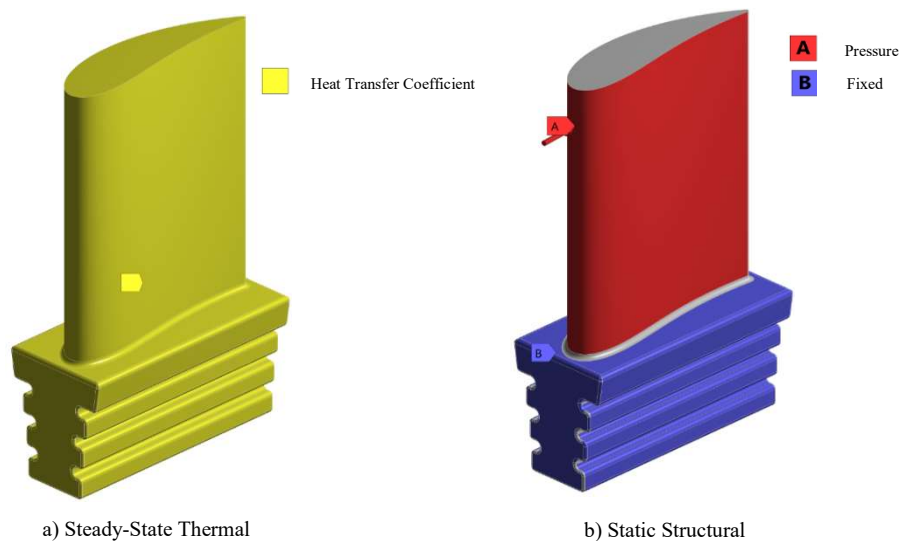


Figure IV.3 Boundary conditions of thermo-mechanical loads applied on blade

#### IV.2.4 Topology Optimization of Lattice Structures Design

Recently, the topology optimization (TO) technique is getting a considerable attention due to its ability to come up with novel cellular structures designs [146]. TO is a highly effective design tool. Its basic principle is to find the optimal density distribution of materials by repeatedly eliminating or redistributing them inside the design area under certain constraints to reduce the structural strain energy [1][6][127]. A number of topology optimization methods are developed in additive manufacturing applications such as: solid isotropic material with penalization (SIMP) method, evolutionary structural optimization (ESO) method, level set method (LSM) [6], [127], [147]. Although topology optimization is an efficient tool to generate structures with lightweight designs for AM [7], [148], it still has problems. For example, a number of overhanging ligaments produced by TO may require enormous amount of support material. Besides, the results of TO may convert a number of the intermediate densities to 0/1 (i.e. void/solid). This type of conversion leads to stress maldistribution between efficient design and its realization by AM [11], [149]. To overcome these drawbacks, we suggest using a homogenization-based lattice structure topology optimization method (LSTO) to fill the solid inner part of the turbine blade with graded lattice structure as illustrated in **Figure IV.4**. The use of the LSTO at TO has many advantages such as: finding the optimal density distribution of lattices, effectively dealing with the intermediate densities in conventional TO, preserving the original design and giving an accurate prediction of overall performance of the components [150].

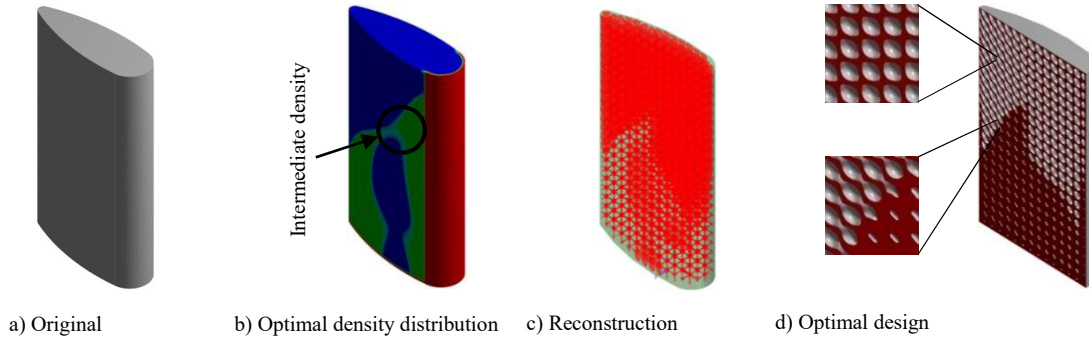


Figure IV.4 Standard topology optimization design for a part of blade

#### IV.2.4.1 Optimization

The homogenization-based topology optimization method is employed to design a graded density lattice structure. We conduct lattice optimization (LO) at ANSYS. LO at ANSYS is used as a mechanical analyser to reduce mass with stress constraints. The optimization is based on the homogenization method developed by Cheng et al. from the University of Pittsburgh [11], [150] which can be mathematically formulated as the follow:

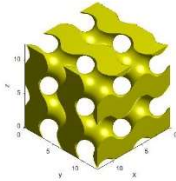
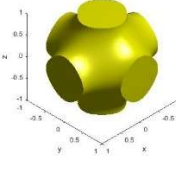
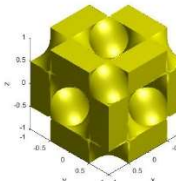
$$\begin{aligned}
 & \text{minimize } \mathbf{m}(\boldsymbol{\rho}) = \sum_{e=1}^N \boldsymbol{\rho}_e \mathbf{v}_e \\
 & \text{w. r. t } \boldsymbol{\rho}_e \\
 & \text{Such that } \left\{ \begin{array}{l} \mathbf{K}\mathbf{u} = \mathbf{f} \\ \mathbf{C} = \mathbf{C}(\boldsymbol{\rho}) \\ \bar{\boldsymbol{\sigma}}_{max}^H = \max_{e=1 \dots N}(\bar{\boldsymbol{\sigma}}_e^H) \leq 1 \\ \boldsymbol{\gamma} \bar{\boldsymbol{\sigma}}_{max}^H \leq \bar{\boldsymbol{\sigma}}^\gamma \\ \boldsymbol{\gamma} \geq 1 \\ \mathbf{0} < \boldsymbol{\rho} \leq \boldsymbol{\rho}_e \leq \bar{\boldsymbol{\rho}} \leq 1, \quad e = 1, \dots, N \end{array} \right. \quad (\text{IV.1})
 \end{aligned}$$

Where  $\mathbf{m}(\boldsymbol{\rho})$  is the objective function which represents the overall volume mass of the structure.  $\boldsymbol{\rho}_e$  represents relative density of element  $e$ , while  $\mathbf{v}_e$  is its volume of element  $e$ .  $\mathbf{K}$  is the global stiffness matrix,  $\mathbf{U}$  is the global displacement vector and  $\mathbf{F}$  represents the prescribed external loads.  $\bar{\boldsymbol{\sigma}}_{max}^H$  represents the maximum stress in the design domain, while  $\max_{e=1 \dots N}(\bar{\boldsymbol{\sigma}}_e^H) \leq 1$  represents the modified stress on element  $e$ .  $\boldsymbol{\gamma}$  is the factor of safety for a safe allowable stress.  $\bar{\boldsymbol{\sigma}}^\gamma$  represents the yield strength of bulk material.  $\boldsymbol{\rho}$  and  $\bar{\boldsymbol{\rho}}$  are the minimum and maximum allowable design variables for the optimization. The second constraint in Eq. (IV.1) is the elastic scaling law of lattice structure. The three independent elastic constants are calculated in terms of relative density by the homogeneity method, see Ref. [150].

### IV.2.5 Triply periodic minimal surface (TPMS) -based Lattice Structures Design

Lattice structures attract a considerable attention in a number of fields including: aerospace and biomedical industry. The need for lattice structures comes from their contribution in weight reduction and easing the control of the mechanical and physical properties of the component [151], [152]. In addition, lattice structures have the ability to absorb energy, control the heat transfer easily as it has an effective surfaces area, and allow freedom in designing without the need for wholly change the structural shape (i.e replacing the solid part of the component with lattice structures in the required areas) [2][153]. This is what leads to think of using lattice structures in the manufacture of the turbine blades. In this work, we replace the internal solid part of the blade with graded lattice structures taking into account achieving appropriate homogenization between the material, unit cell and AM technique in order to reach the best mechanical and physical properties for these lattice structures [6]. Understanding the topological relationship between lattices and its component materials is a key factor in allowing blades to be designed with improved end-use characteristics [154]. However, the main challenge remains in choosing the suitable lattice design. We suggest three different lattice structures with implicit surfaces derived from the TPMS namely: Diamond, Gyroid and Primitive. Due to their appealing topological characteristics, TPMS structures depend on mathematical formulas to create surfaces and connect them with high efficiency to produce a three-dimensional structure through curved surfaces and multiple voids [155]. TPMS lattices are mathematically defined using level-set approximation equations [154], [156]. The software MATLAB is used to model these equations consisting of trigonometric functions. Table 3 presents the unit cell of each TPMS. For each unit cell of TPMS obtained, we use the lattice structure topology optimization (LSTO) in ANSYS based on the homogenization method to form the graded lattice structure built from these cells which were replicated in 3D with optimal distribution to fulfil a given load case [157], [158]. In the other hand, the manufacturability of complex TPMS lattices depends highly on Additive Manufacturing technology because of its engineering flexibility and high ability to exploit and compile the complex results of optimizing topology [145].

Table IV.3 the unit cells of each TPMS

Lattices	Level-set approximation equation	Graphical representation
<b>Gyroid</b>	$\sin(\pi * x) * \cos(\pi * y) \\ + \sin(\pi * y) \\ * \cos(\pi * z) \\ + \sin(\pi \\ * z) \cos(\pi * x)$	
<b>Primitive</b>	$\cos(\pi * x) + \cos(\pi * y) + \cos(\pi * z)$	
<b>Diamond</b>	$\cos(\pi * x) * \cos(\pi * y) \\ * \cos(\pi * z) \\ - \sin(\pi \\ * x) \sin(\pi * y) \sin(\pi \\ * z)$	

Where: The constant (t) is used to control the volume fraction of the lattice.

#### IV.2.6 Manufacturability of Lattice Structures

The additive manufacturing technology is regarded as one of the most important technologies for producing lightweight structures with complex parts in engines; especially in the automotive and aviation industry field which aims mainly at reducing the manufacturing costs and increasing the performance [159][160]. Additive manufacture better suits the production of the lightweight lattice structures with a complex geometrical nature due to its ability to: offer the design freedom, grow the efficiency of material utilization and decrease manufacturing cost and time.

Thanks to the advancement in the technology AM that allows applying the obtained results of topology optimization technique, it became easy to design and manufacture lattice structures

built from repeatable unit cells using the implicit surfaces derived from TPMS [161], [36-152]. To generate complex TPMS lattices, we suggest using Selective Laser Melting technique (SLM) which is from the Powder Bed Fusion family (PBF) from AM technologies due to its efficient material utilization, high cooling rate, efficiency in saving time and manufacturing abilities for complicated structures [6][164].

SLM technique depends on producing the metallic parts Layer-by-layer by fusion of metallic powders using a laser energy source. Moreover, this technique allows improving the dimensional properties as well as the mechanical properties of lattice structures by selecting the ideal process parameters. For SLM technique, the most essential process parameters are : scanning speed, laser power and hatch spacing and layer thickness [159]. At this additive manufacturing by Selective Laser Melting (SLM) is highly promising as it allows the fabrication of fully functional metal machine and tool parts. SLM offers unique design possibilities at arbitrary lot sizes and is highly material efficient [165]. In SLM a workpiece is built up from a powder bed. A thin powder layer as well as a part of the subjacent layer is molten up by a laser controlled by a scanner system.

When the material solidifies again, a melt metallurgic connection between adjacent and subjacent lines is formed. The building platform is lowered, a new powder layer is delivered and the process starts from the beginning [166]. At this layer-wise 3D printing of massive, metal free form components can be realized. The principle of SLM is shown in Fig. IV.5 a. Fig. IV.5 b shows the SLM process during operation. Whereas SLM of materials like aluminum, steel, titanium, nickel and cobalt chromium alloys is already well established and already applied in industrial production, the processing of molybdenum by SLM is still a big technical challenge as the processing window is significantly narrower.

Nevertheless, for complex workpiece geometries, SLM is an attractive alternative to classical powder metallurgical fabrication routes and by a proper choice of processing parameters complex geometrical structures can be fabricated. Figs. IV.5 c and d show examples of thin walled, tapered grid structures as well as massive demonstrator parts that were fabricated at Plansee SE by SLM of molybdenum.

For a successful, stable and repeatable processing of molybdenum by SLM a fundamental process understanding is essential. For this aim multi-physical transient process simulations are a powerful tool in order to analyze the process on a mesoscopic level, study defect formation mechanisms and to learn about the influence of processing parameters and powder characteristics on process dynamics and processing result[167]. Consequently, we obtain a finer



microstructure with idealized mechanical properties [6]. Besides, the lattice structures help AM to save time and material, minimize material losing on supports and scale down power expenses during the manufacturing [168].

The topology optimization technique is also beneficial to AM, as it provides: plan light-weight and purposeful portions, limit the quantity of support structures wanted throughout the manufacturing stage and outline choices infill strategies for existing designs [168].

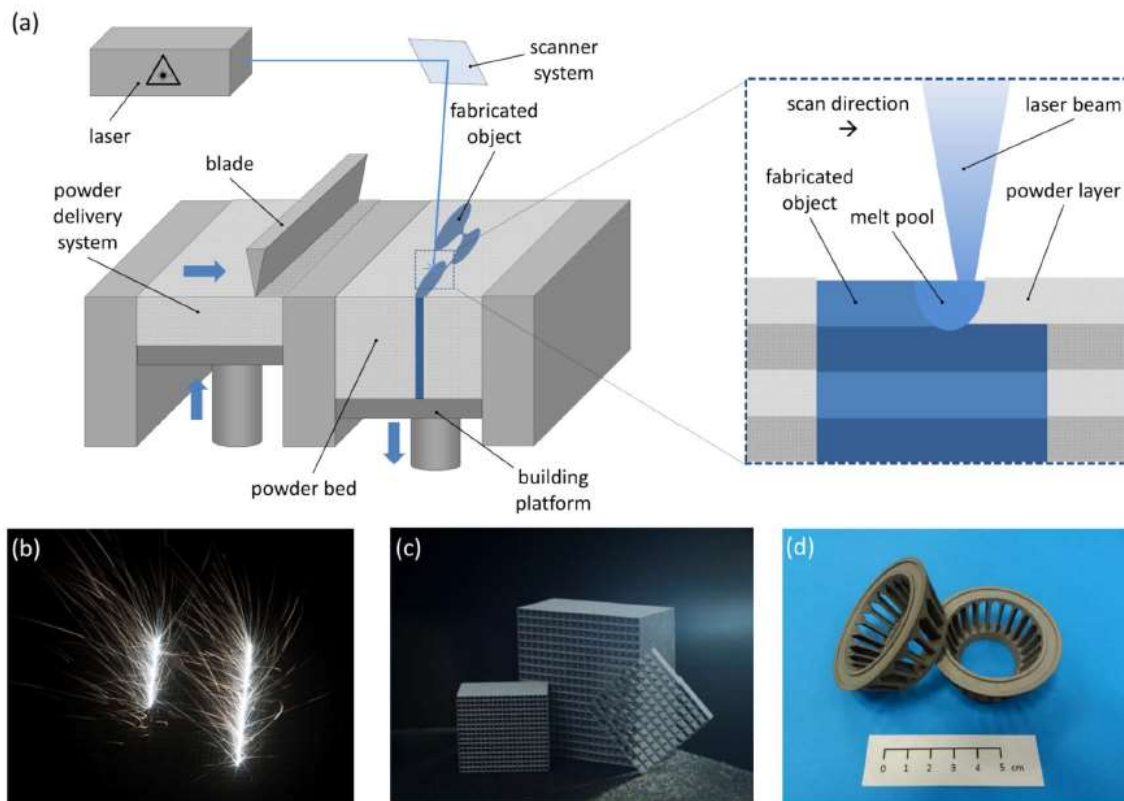


Figure IV.5 Selective Laser Melting (SLM): (a) technology principle, (b) process during operation and (c, d) molybdenum demonstrator parts fabricated by SLM at Plansee SE

#### IV.2.7 The effectiveness of the proposed method

Our approach is well-implemented using Topology Optimization and Lattice Structures in the gas turbine blade by the CAD model equivalent for the designed turbine blade, the properties of the materials used and the applied boundary conditions and selected the proposed technique for manufacturing the lattice structures.

### IV.3 The field of Biomechanical

#### IV.3.1 General Architecture of the Proposed Procedure for the cancellous bone.

The proposed system architecture for lattice structures design is introduced, as illustrated in the flowchart Figure IV.6.

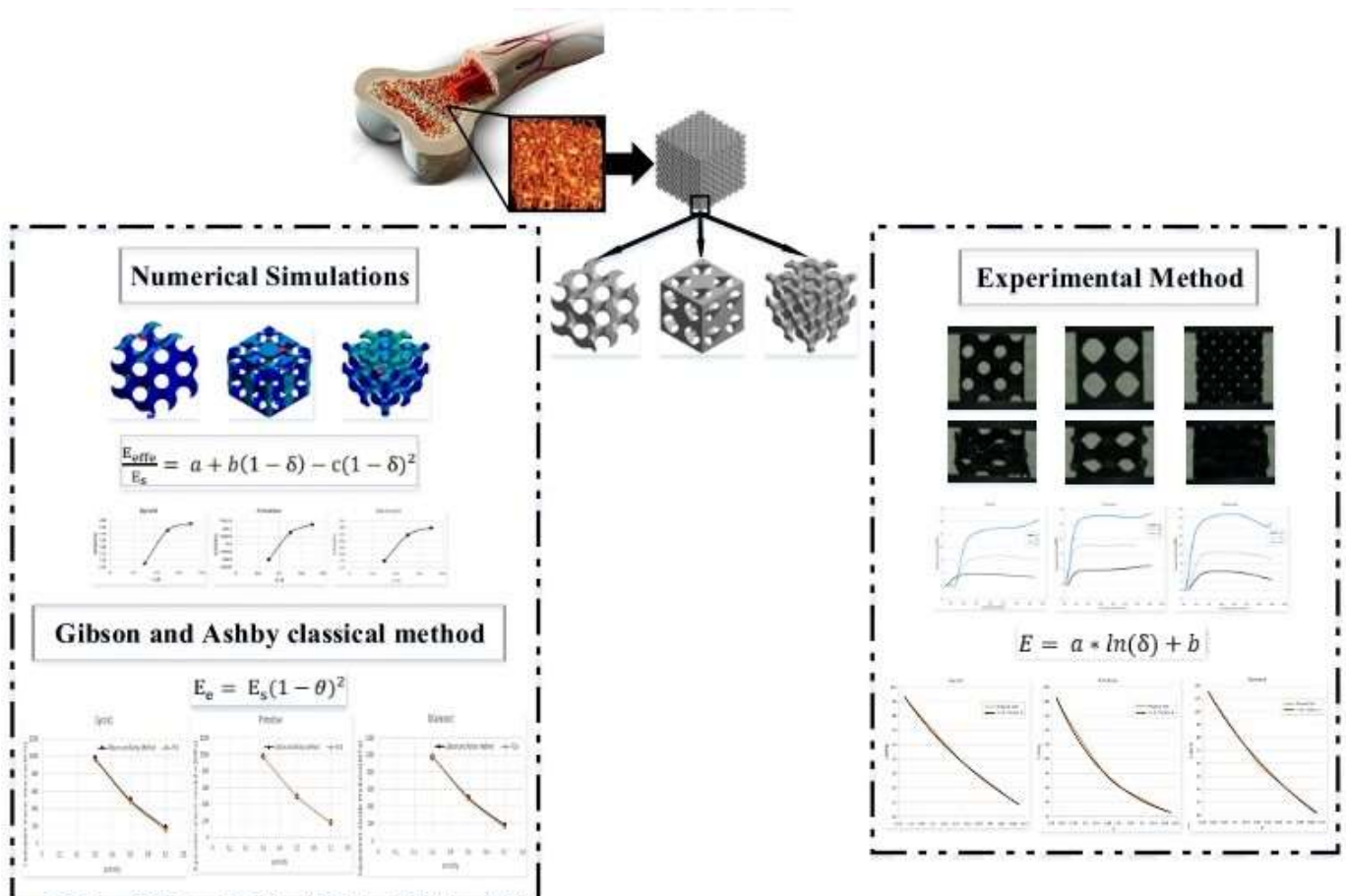


Figure IV.6 General architecture of the proposed procedure

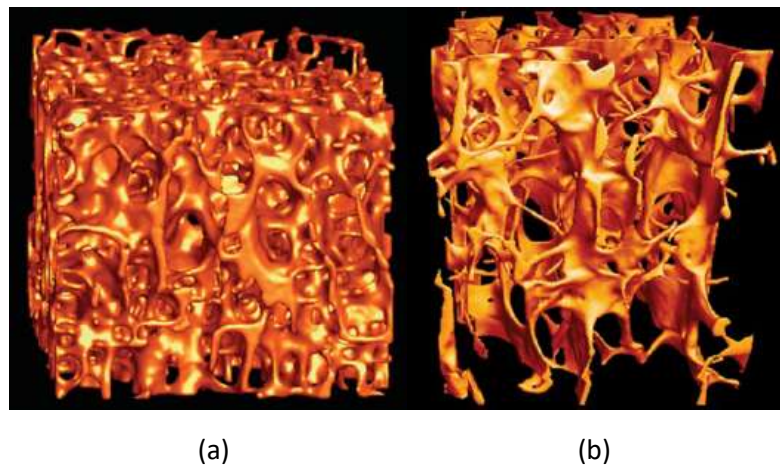
#### IV.3.2 Material

In this section, the lattice structures of different porosity are designed by using Triply-periodic minimal surfaces (TPMS).

##### IV.3.2.1 The Design of the human bone with Porous Lattice Structures

In the human bone, the cancellous bone contains a heterogeneous complex structure, porous and it varies according to age and gender. Figure IV.7 (a) A three-dimensional image of a 4-millimeter-cube of bones for a 30-years-old person with architecture and normal density. While Figure IV.7 (b) 3D cube image of bones shows for a 63 years old person with fragile architecture

and low normal density [3]. Therefore, the architecture of biomimetic cancellous bone should be meet that of natural cancellous bone in terms of the key parameters for the architecture cancellous bone of pore size, porosity, bearing capacity, pore connectivity and thickness of cancellous bone. Therefore, It was based on a model of porous cancellous bones similar to human bone in terms of the range of porosity is between 30%–70%, the range of pore size of cancellous bone from 500  $\mu\text{m}$  to 1000  $\mu\text{m}$  and the elastic modulus from 50 MPa to 500 MPa [13]. To obtain the bone is firm and lightweight can transport nutrients due to the compatibility of the architecture with the host bone.



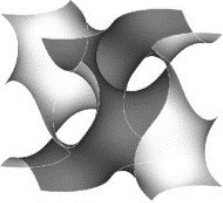
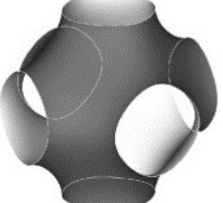
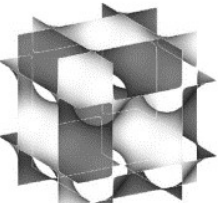
**Figure IV.7** A three-dimensional image of a 4-millimetre-cube of bones (a) a 30-years-old person with architecture and normal density (b) a 63 years old person with fragile architecture and low normal density

In this study, several structure models were established based on the architecture of cancellous human bone by means of CAD particularly: Gyroid, Primitive and Diamond.

#### *IV.3.2.2 Design 3D Lattice structures for Cancellous Bone TPMS-based*

Triply-periodic minimal surfaces (TPMS) are subsets of lattice structures that attract large attention in several fields including the biomedical industry and aerospace due to easy control of the physical and mechanical properties and their lightweight [145]. In addition, these surfaces have unparalleled advantages such as: providing flexibility, ease of representing complex topologies, freeform deformation operations compared to other surfaces and engineering representation by the mathematical aspects. The unit cell of each TPMS lattices is mathematically represented using the software MATLAB by level-set approximation equations as shown in Table IV.4 [169].

Table IV.4 The unit cells for each lattice structure of TPMS

Lattices	Level-set approximation equation	Graphical representation
<b>Gyroid</b>	$\sin(\pi * x) * \cos(\pi * y)$ $+ \sin(\pi * y)$ $* \cos(\pi * z)$ $+ \sin(\pi$ $* z) \cos(\pi * x)$	
<b>Primitive</b>	$\cos(\pi * x) + \cos(\pi * y)$ $+ \cos(\pi * z)$	
<b>Diamond</b>	$\cos(\pi * x) * \cos(\pi * y)$ $* \cos(\pi * z)$ $- \sin(\pi$ $* x) \sin(\pi * y) \sin(\pi$ $* z)$	

Consequently, the lattice structures were built in 3D by repeatable unit cells depending on using the implicit surfaces derived from (TPMS) namely, Gyroid, Primitive and Diamond with uniform porosity. To obtain lattice structures based on the repetitive cell unit with the same pore size and porosity cube-shaped, we created three cubes of Gyroid, Primitive and Diamond lattice structures with different porosity and all they are uniform geometric structures as shown in Figure IV.8.

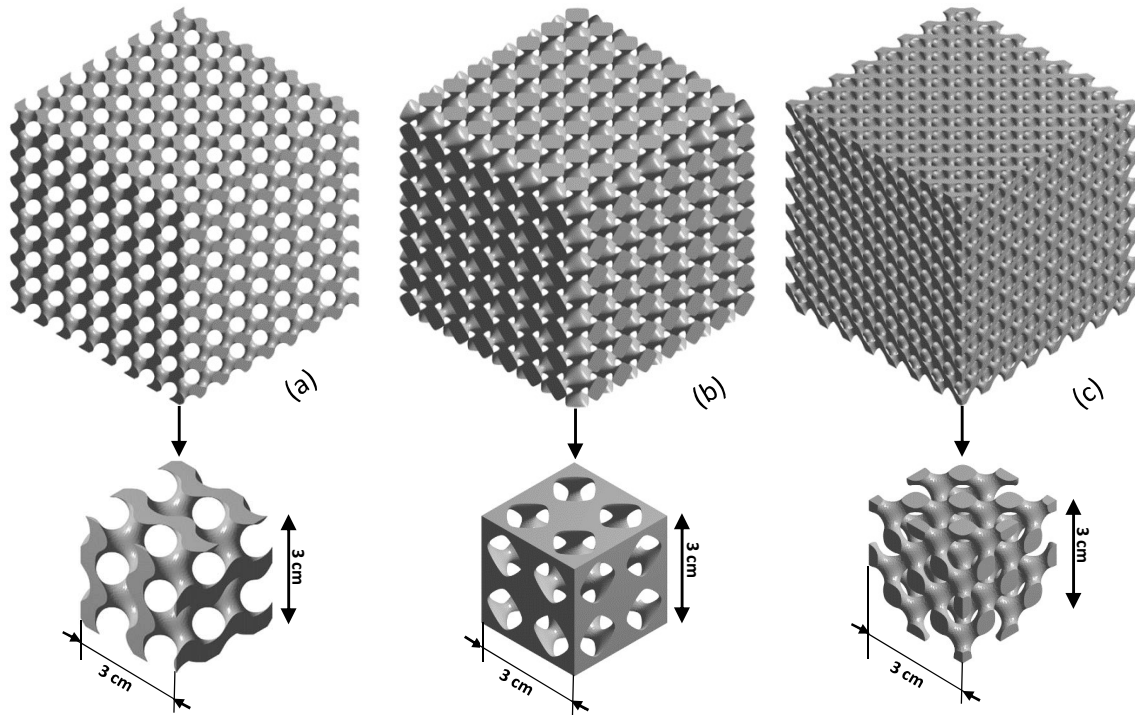


Figure IV.8 3D model to the cube of the lattice structure (a) Gyroid, (b) Primitive and (c) Diamond

In this part, the design information of all structures in terms of pore size and porosity was changed to obtain a porosity varying at 30%, 50% and 70% for each structure. In the first, a sample was taken from each cube with a unit length of 3 cm, a width of 3 cm and a height of 3 cm from the original designs. Secondly, change the design parameters of three lattice structures with different porosity based on relative density, once by 30%, again by 50%, and the last by 70% for all lattice structures. In addition, we used the lattice structures based on the homogenization method built from these cells to create the lattice structure 3D with the pore size distribution as shown in Figure IV.9.



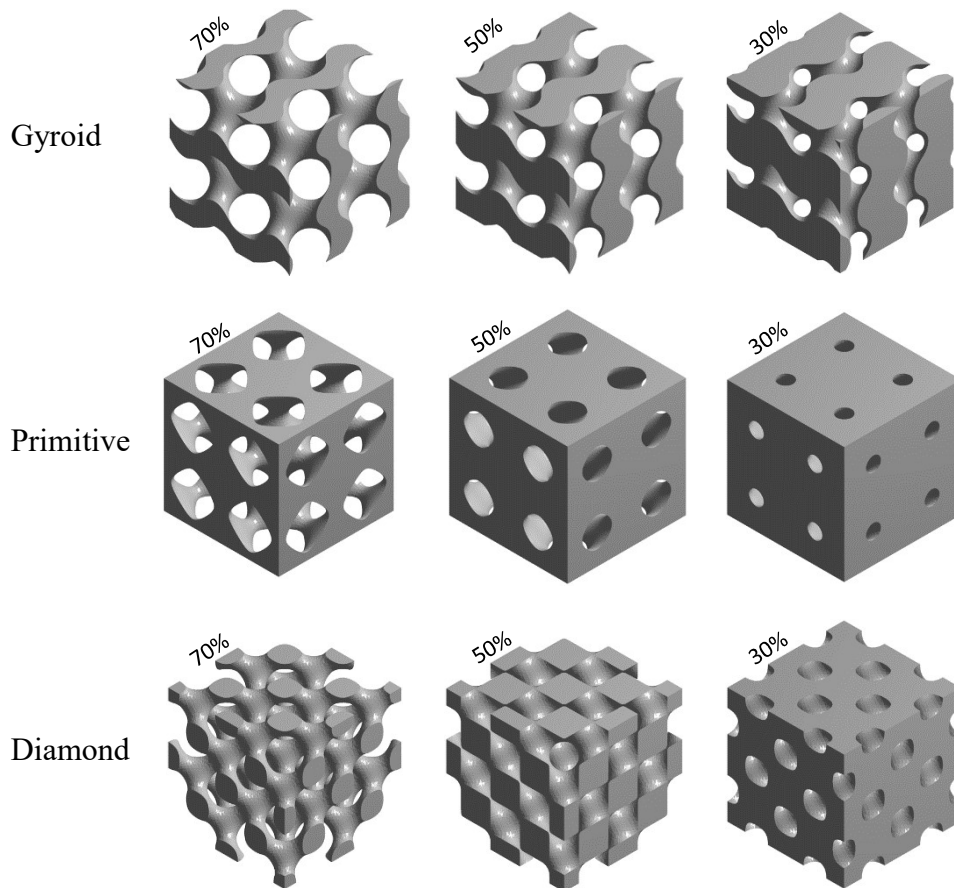


Figure IV.9 The unit cells of the lattice structures with the various regularly for the lattice structures

### IV.3.3 Method

In this section, the stiffness of lattice structures of different porosity is predicted by three main methods: 1) Numerical simulations by finite element analysis. 2) Calculation Gibson and Ashby classical method of the lattice structures. 3) Experimental Method by manufacturing the lattice structures and testing them by a uniaxial compression test.

#### IV.3.3.1 The study of numerical simulations of lattice structures

The compression performance of the lattice structures with uneven porosities was analyzed to determine the optimal model with the Prediction of safety factor and appropriate porosity by finite element analysis. The compression loads are applied on the lattice structures for obtaining the maximum stress and deformation depending on the loads applied on the human bone according to the boundary conditions. As two parallelepiped panels were added at the top and the bottom for each of the three models and the bottom plate in z-axis was fixed and applied the pressure on the upper plate as shown in Figure IV.10. The numerical simulations model was applied in the finite element analysis software ANSYS 2020 R1 software. In the first stage, the

analysis model was created with optimized mesh to validate the efficiency by using patch independent method (Tetrahedrons element method) with defining the maximum and minimum of element size for creating a mesh to suit the bends and angles that from built by repeatable unit cells as shown in Table IV.5. In the second stage, the loads are applied to the lattice structures with the elimination of all degrees of freedom for the bottom surface was subject to fixed constraints. As has been frictionless constraints were applied between the model of the structure and the cover slab and shown the contact surface in blue as illustrated in Figure IV.10.

Table IV.5 Elemental distribution of mesh

Model reference	Max element size (mm)	Min element size (mm)	Total nodes	Total elements
Gyroid 30%	0.2	0.01	747527	514621
Gyroid 50%	0.2	0.01	735220	512689
Gyroid 70%	0.2	0.01	703583	496971
Primitive 30%	0.2	0.01	754836	519535
Primitive 50%	0.2	0.01	753994	526462
Primitive 70%	0.2	0.01	702381	498182
Diamond 30%	0.2	0.01	733543	499067
Diamond 50%	0.2	0.01	737043	509240
Diamond 70%	0.2	0.01	716430	501197

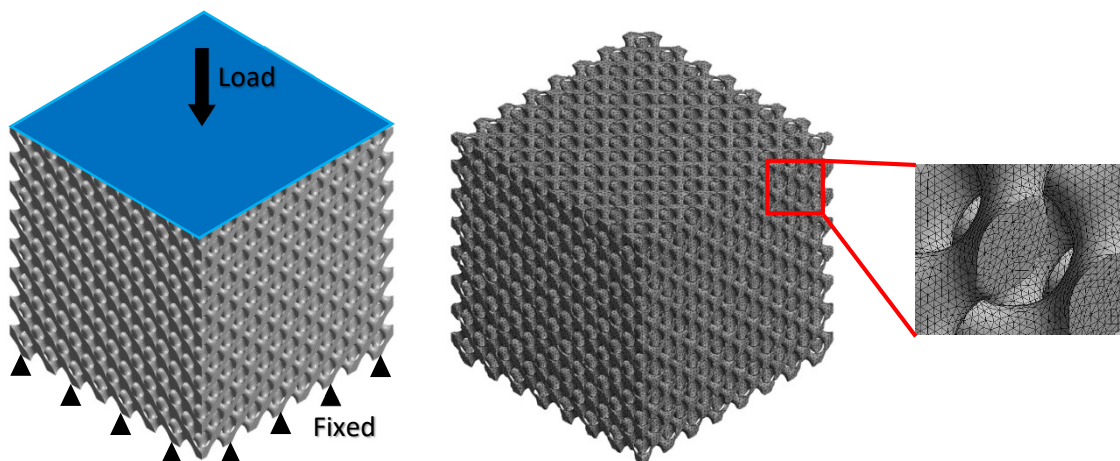


Figure IV.10 Boundary conditions and the finite element mesh of the Lattice structures

Since the lattice structures were completely uniform in the three essential axes ( $X, Y, Z$ ), the elastic modulus of any direction has the following relation ( $E_X = E_Y = E_Z$ ). Thus, described the equivalent elastic modulus  $E_Q$  by the following formula:



$$E_Q = \frac{\sigma}{\varepsilon} = \left(\frac{F_Z}{A}\right) / \left(\frac{\Delta L_Z}{L_Z}\right) \dots\dots\dots (IV.2)$$

Where the A direction and Z is the section-sectional area and the FZ is the Pressure applied to the face [13].

### IV.3.3.2 Predict the Stiffness of the lattice structure of the porous model by using Gibson and Ashby classical method

In previous researchers studied and developed the mechanical properties of porous scaffolds with different porosities with the simple cubic unit cell in order to obtain a porous structure that matches the stiffness of the host bone. Therefore, the relationship between the equivalent modulus of elasticity must be studied quantitatively and porosity. In general, using the porous scaffolds is widely and applicable in several areas due to the mechanical characteristics appropriated to the porosity of the bone structure [170].

In this work, the classical Gibson and Ashby method was adopted as in equation (IV.3) to predict the stiffness of porous scaffolds and compare physical test results with the results of FEA.

$$\frac{E^*}{E_S} = C(\rho^* / \rho_S^S) \dots\dots\dots (IV.3)$$

Where  $E_S$  is the elastic modulus,  $E^*$  is the pore structure's elastic modulus and the geometric proportionality constant is  $C$  approximately 1. The relative density is determined with the porosity as Equation (IV.3) shows; it is the relative density expressed the size of the elastic modulus. The determined relationship is as follows:

$$1 - \theta = (\rho^* / \rho_S) \dots\dots\dots (IV.4)$$

In Equation (IV.4),  $\rho_S$  is the solid density of the material,  $\rho^*$  is the pore density of the structure and the equivalent elastic modulus can be expressed depending on the deformation of Equation (IV.3), as follows:

$$E_e = E_S(1 - \theta)^2 \dots\dots\dots (IV.5)$$

Therefore, used the results of Gibson and Ashby classical method to determine the stiffness of porous structures under applied loads and the results of finite element analysis for the comparative analysis[13].

### IV.3.3.3 Mechanical testing

#### a) Fused Filament Fabrication (FFF) Technology

In the last years, 3D printing is commonly known as additive manufacturing technologies has emerged and faced exceptional growth effectively [2][145]. Where the 3D printing contains several technologies and one of the best AM technologies is FFF technology [163]. Because of several advantages that this technique provides such as cost reduction, the capability of more flexible design, a faster product development cycle and less prototyping time [171]. FFF technology used a continuous filament for the 3D printing process of a thermoplastic material by extruding small beads of molten material from Acrylonitrile butadiene styrene filament (Z-ABS) from a spool to form molten materials layer upon layer and hardens the material layer of the surface after extrusion from the nozzle through a heated, moving printer extruder head [172]. Repeated this process and fused until creating a three-dimensional part completely for the porous scaffold [173].

In this chapter, the proposed lattice structures were fabricated by using the Zortrax M200 plus featuring the FFF manufacturing technique in our laboratory as shown in Figure IV.11 (a). In the first, the 3D models of the proposed lattice structures were exported from Ansys software using the STL file format. Then the STL code from 3D was converted by using the Z-SUIT Zortrax to the Zortrax machine language (G-code) with the layer thickness set to 90  $\mu\text{m}$ , 100% infill density and nozzle diameter 0.4 mm. A part from the proposed lattice structure was printed at 5 times enlargement and 3D enlargements relative to the original model for three different lattice structures (Gyroid, Primitive and Diamond). Whereas, the printing time for the selected parts of the lattice structures with different porosity was an average of 9 hours per part.

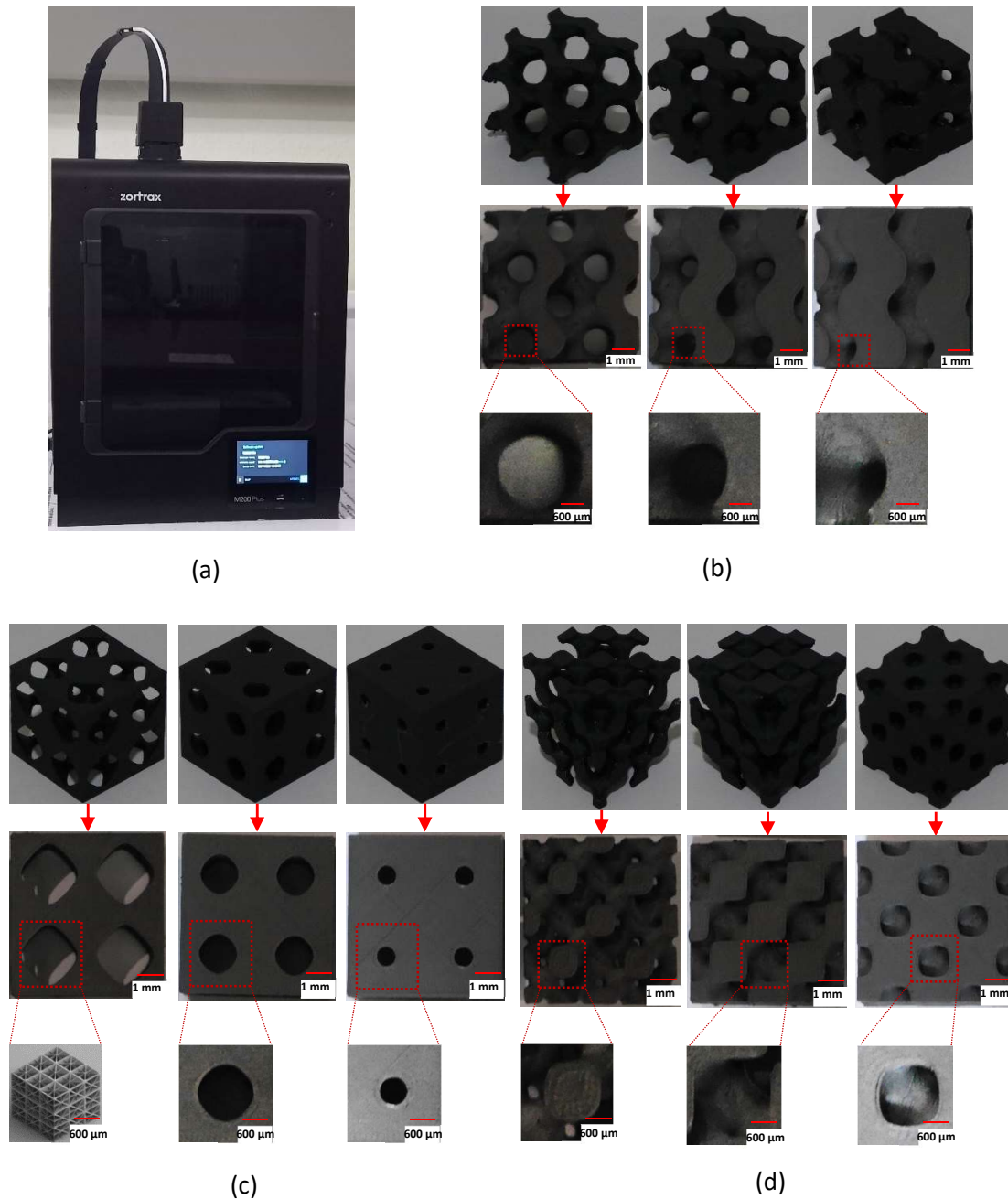


Figure IV.11 (a) 3D printer ZORTRAX M200+, (b) Gyroid, (c) Primitive and (d) Diamond with the porosity 70%, 50% and 30%, respectively for each type

#### b) Stiffness Performance Testing of Lattice Structures

For experimental part, a **Jinan Universal Testing Machine Model WDW-100S** was used to apply a uniaxial compression test with the load capacity of 100 KN, to each type of proposed lattice structure (Gyroid, Primitive and Diamond) manufactured by FFF as illustrated in Figure IV.12. Thus, has been determined the compression performance for the lattice structures where the test speeds are 0.2 mm/min for the manufactured lattice structures.

The displacement was measured for the different lattice structures by the clamp on the extensometer connected to the test machine. As the strain-stress relationship has been calculated based on displacement and force-axial data obtained from the test machine. In the final, the equivalent elastic modulus has been determined by the stress-strain curve.

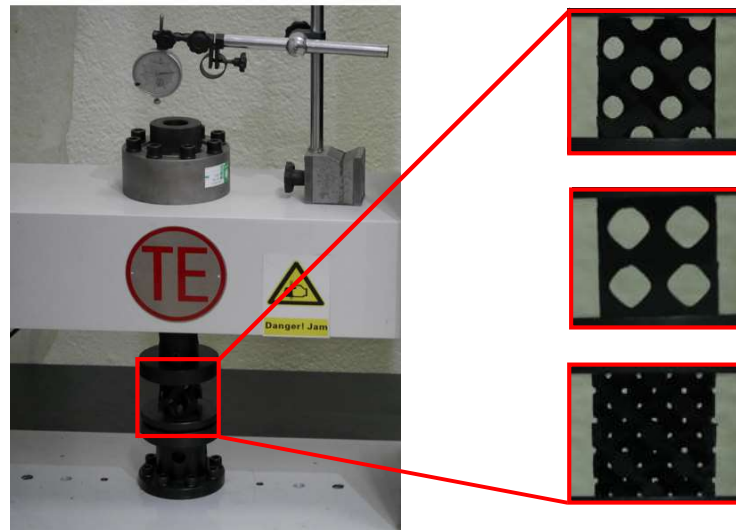


Figure IV.12 The uniaxial compression test machine (Jinan Universal Testing Machine Model WDW-100S)

#### IV.3.4 The effectiveness of the proposed method

The relationship between the effective modulus of elasticity and different porosity ratios of the lattice structures was determined by using three methods to predict the mechanical stiffness:

i) finite element modelling (FEM) simulation, ii) Gibson and Ashby method and iii) a uniaxial compression test after manufacturing the lattice structures by using Fused Filament Fabrication (FFF) technology by three lattice structures from triply periodic minimal surfaces with different ratio porosity.

#### IV.4 Conclusion

In this chapter, we have tried to implement the set of ideas that characterize the proposed approach by focusing on the Lattice structures in two different fields as well as the Topology Optimization. Our approach is well implemented using Topology Optimization and Lattice Structures in the gas turbine blade and the bone cancellous. To demonstrate the efficiency of our approach, all results of the gas turbine blade and bone cancellous from several aspects are presented in the last chapter.

## Chapter V.

# **Numerical and experimental results**



## V.1 Introduction

This chapter describes the validation phase of our proposed approach for the designs of the lattice structures with a different architecture in two different fields (Aerospace, Biomechanical). During this work, numerical simulations have been carried out for gas turbine blades to obtain the deformation and stress values under thermo mechanical loads. On another hand, we applied numerical simulations and experimental tests for bone cancellous to predict the equivalent elastic modulus. Finally, this section presents some results and their interpretations and discuss the results obtained.

## V.2 Aerospace application

### V.2.1 Results and Discussion

#### V.2.1.1 *Designing and Validation*

In this part, we suggest a novel system for designing three different lattice structures that use implicit surfaces modelling derived from TPMS (Diamond, Gyroid and Primitive). These lattice structures are designed by LSTO technique at ANSYS Workbench simulation software to replace the solid internal volume of the turbine blade. The study of numerical simulations of our suggested lattice structures under the influence of the thermo mechanical loads is conducted in three stages shown as follows:

a) *The first stage (the finite element analysis (FEA))*

We generate a mesh for the initial design of the blade as shown in Figure V.1. The used mesh of Tetrahedrons type consists of 40,649 elements and 71,129 nodes with the average size 2 mm.

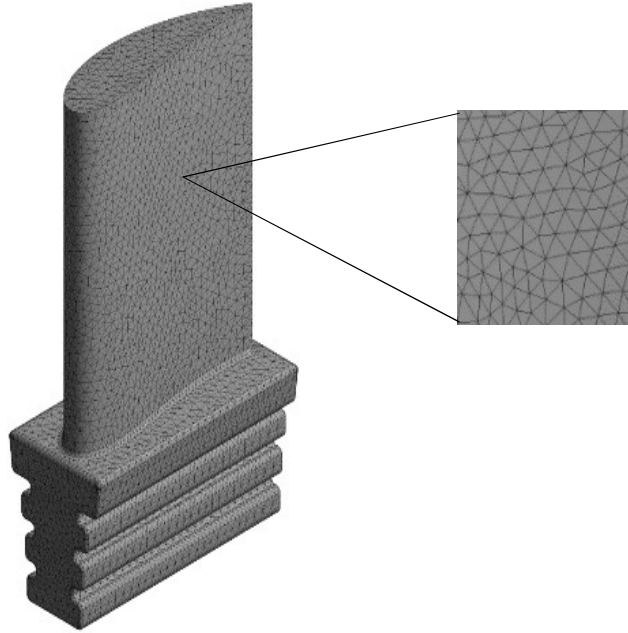


Figure V.1 Finite element mesh of the initial design

The results of the initial design of the blade obtained by using FEA are presented as follow: Total Heat Flux (Min  $2.7294 \times 10^{-17}$  W/mm<sup>2</sup> and Max Heat Flux  $1.0059 \times 10^{-12}$  W/mm<sup>2</sup>), Stress (Min 0.0091739 MPa and Max stresses 8602.3 MPa) and Deformation increases near 0 with a maximum value of 48.15 mm as shown in Figure V.2. The obtained results show that the blade cannot operate in ideal conditions. We have thus suggested a new blade design with graded lattice structures of maximum stiffness and minimum weight.

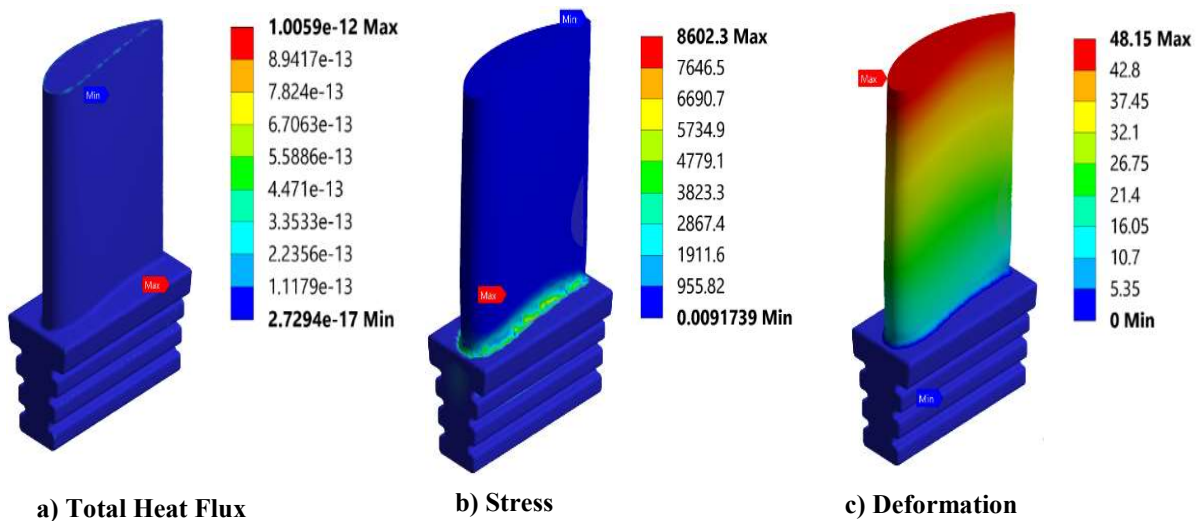


Figure V.2 Distribution of Total Heat Flux, Stress and Deformation in the thermo mechanical state of the initial design



b) *The second stage is a lattice structure topology optimization (LSTO)*

In this stage, the aim of LSTO technique is to determine the optimum distribution of the relative density in the design area based on results obtained from the stage 1. In this stage, we replicated the relative density values' input, which are ranged between 0 to 1. It is found that the best relative density for the blade ranged between 0.2 to 0.9 and at 35% retention rate, and  $\gamma = 1.43$  as safety factor in the safe area. The maximum and minimum density distribution in the blade during the optimization is shown in Figure V.3. The red colour indicates the maximum density of lattice with small pores while blue colour indicates minimum density of lattice with large pores.

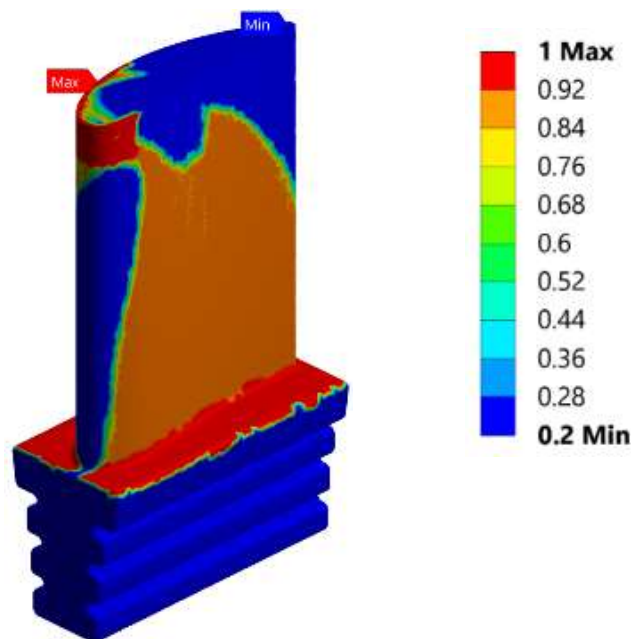
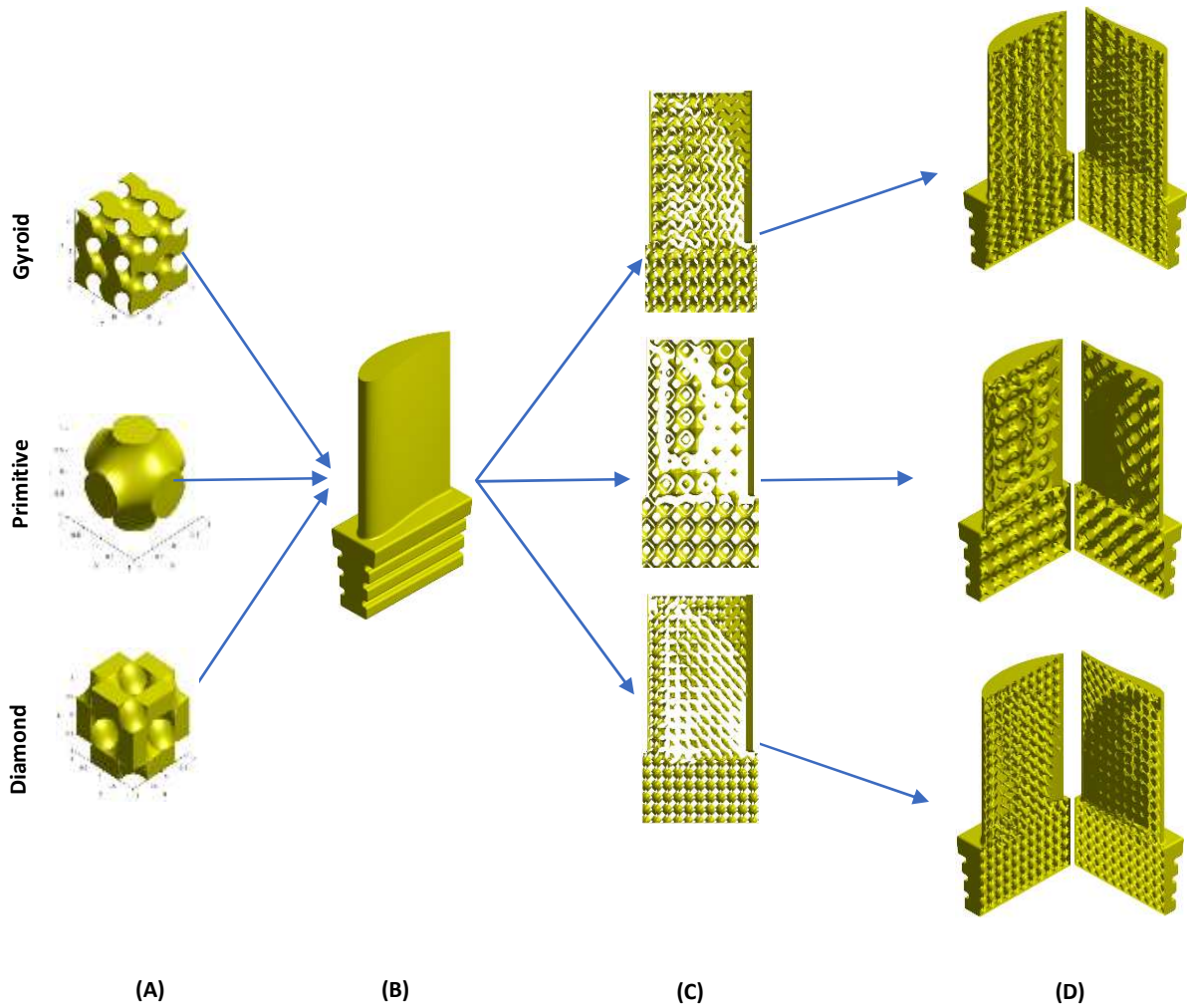


Figure V.3 Optimal density distribution

After getting the optimal distribution of the density within the blade, we replace the solid internal volume of the blade at Space Claim with three lattice structures (Gyroid, Primitive and Diamond) by determining the criterion of fullness at 25% and 1.3 mm for both the thickness of the lattice and outer leather of the blade. Figure V.4. Shows the lattice structures (Gyroid, Primitive and Diamond) used in filling the initial design.



**Figure V.4 (A) The unit cells of each TPMS; (B) The initial design; (C) A different filling densities; (D) The internal blade structure built with lattice structures (Gyroid, Diamond and Primitive)**

*c) The third stage (the finite element validation analysis (FEVA))*

The aim of this stage is to validate the efficiency of the suggested approach by creating an optimized mesh using Tetrahedrons element with the element size average 1.1 mm. The Tetrahedrons element method is used to create a high-fidelity mesh based on the finite element mesh (FEM) to suit both the outer blade's surface and the internal blade structure built from three-dimensional repeatable unit cells, particularly Gyroid, Primitive, Diamond as illustrated in Figure V.5. This mesh consists of (2,482,574 elements 3,796,559 nodes) for final design of the blade with Gyroid, and likewise with both Primitive (271,635 elements 431,675 nodes) and Diamond (630,621 elements 998,323 nodes).

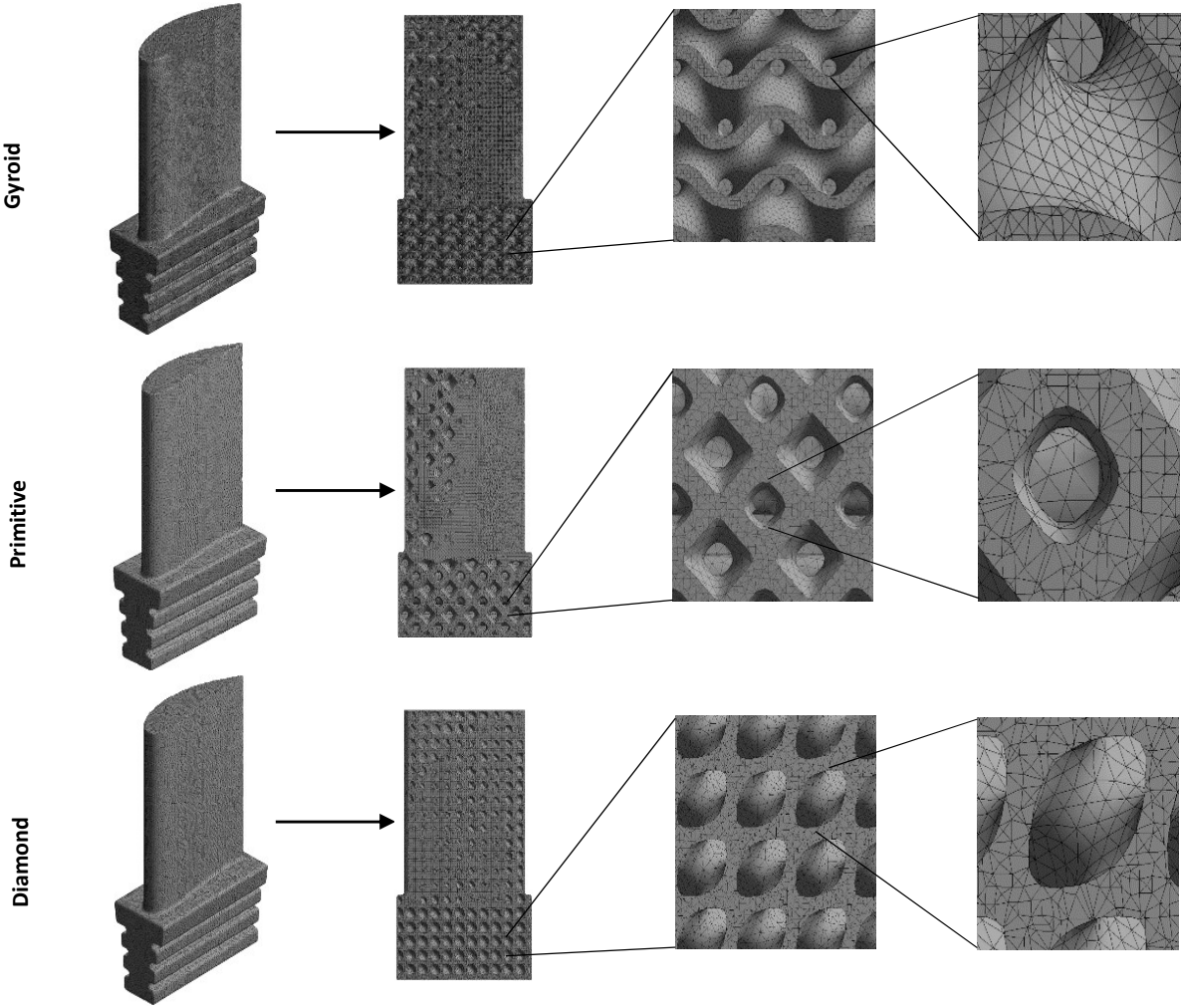
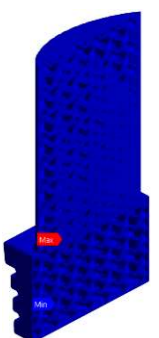
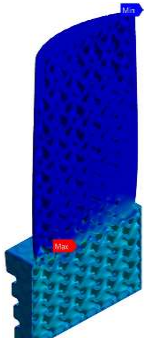
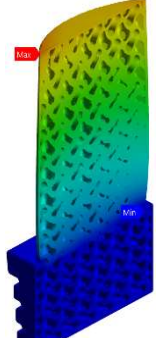
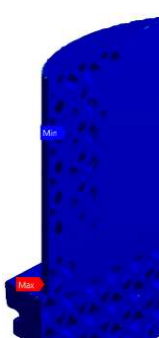

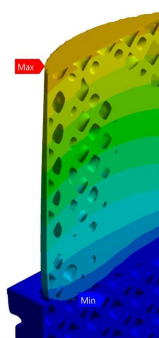
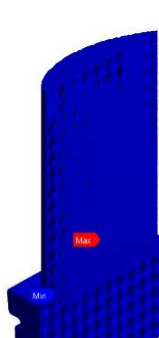
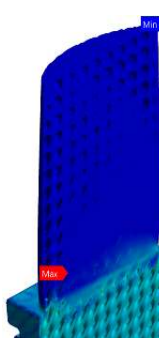
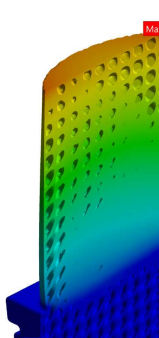


Figure V.5 Finite element mesh of the final optimized designs

At the end of this stage, we applied the same boundary conditions of the first stage to obtain the analysis results for the three optimized blades in term of Total Heat Flux, Stress and Deformation as shown in Table V.1.

Table V.1 Distribution of Total Heat Flux, stress and deformation in the thermo mechanical state of the final optimized designs

	Total Heat Flux ( W/mm <sup>2</sup> )	Stress (MPa)	Deformation (mm)
<b>Gyroid</b>	 <p>2.568e-12 Max 2.3112e-12 2.0544e-12 1.7976e-12 1.5408e-12 1.2841e-12 1.0273e-12 7.7047e-13 5.1368e-13 2.5689e-13 9.9534e-17 Min</p>	 <p>8602.3 7885.4 7168.6 6406.9 Max 5734.9 5018 4301.2 3584.3 2867.4 2150.6 1433.7 716.86 0.0029485 Min</p>	 <p>48.15 44.137 38.722 Max 32.1 28.087 24.075 20.063 16.05 12.037 8.025 4.0125 0 Min</p>
<b>Primitive</b>	 <p>1.0059e-12 8.9414e-13 7.884e-13 Max 6.7062e-13 5.5886e-13 4.471e-13 3.3533e-13 2.2357e-13 1.1181e-13 5.1614e-17 Min</p>	 <p>8602.3 7940.6 7278.9 6617.2 5955.4 5293.7 4425.8 Max 3308.6 2646.9 1985.2 1323.4 661.73 0.015998 Min</p>	 <p>48.15 44.446 39.981 Max 33.335 29.631 25.927 22.223 18.519 14.815 11.112 7.4077 3.7038 0 Min</p>
<b>Diamond</b>	 <p>1.5442e-12 Max 1.3727e-12 1.2011e-12 1.0295e-12 8.5793e-13 6.8635e-13 5.1477e-13 3.4319e-13 1.7162e-13 3.7859e-17 Min</p>	 <p>8602.3 7885.4 7168.6 6451.7 5742.3 Max 5018 4301.2 3584.3 2867.4 2150.6 1433.7 716.87 0.011866 Min</p>	 <p>48.15 44.608 Max 40.125 36.112 32.1 28.087 24.075 20.063 16.05 12.037 8.025 4.0125 0 Min</p>

V.2.1.2 Results discussion

To evaluate the numerical results and highlight the efficiency of the proposed approach, we

make a comparison between final designs and the initial design. The internal volume of the final designs consists of three different lattice structures (Gyroid, Primitive and Diamond). They have also determined criteria (Lightweight, Stress and Deformation) for evaluating the obtained results. The obtained numerical results of the final designs show better results than in the initial design in term of:

- **Lightweight:** this criterion represents the amount of the reduced mass in the turbine blade according to the type of the internal lattice structure. The mass is reduced in varying proportions to reach 40.32% for (blade with Gyroid), 34.07% for (blade with Primitive) and 33.41% for (blade with Diamond) as illustrated in Figure V.6. This difference in values is caused by the difference in the form of the outer surface of the lattice structures used in the blade.

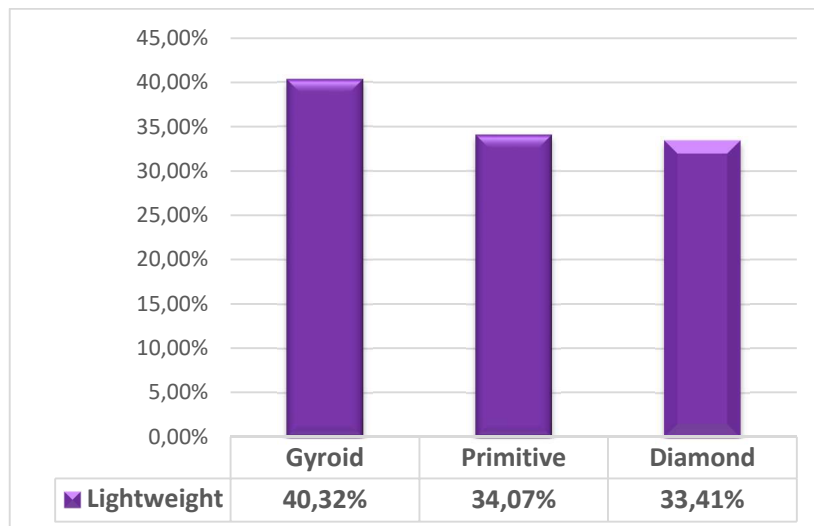


Figure V.6 Rate of reduced weight

- **Stress:** this criterion distinguishes the least stressed design among the initial design and final designs. The analysis results show that the design (blade with Gyroid) is less stressed than the other two final designs while the initial design is weaker than the proposed designs as illustrated in Figure V.7.



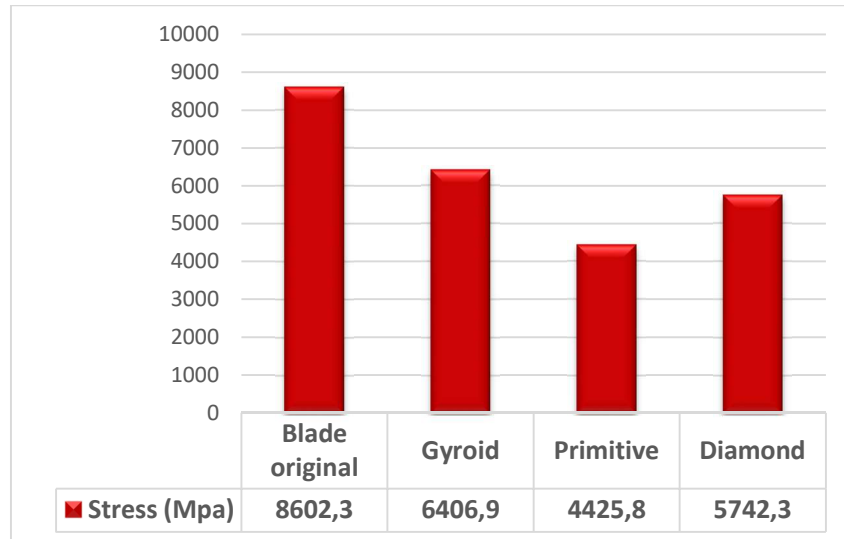


Figure V.7 Rate of Low stress

- Deformation:** this criterion distinguishes the least deformed design among the initial design and the final ones. Results show that (blade with Gyroid) is the least deformed followed by the (blade with Primitive) and (blade with Diamond), respectively while the initial design is the most deformed compared to the proposed designs as illustrated in Figure V.8.

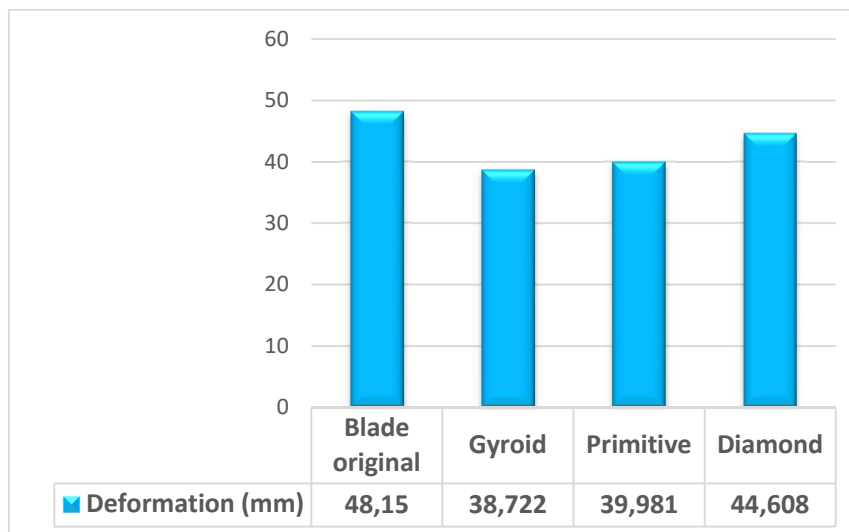


Figure V.8 Rate of Low deformation

## V.3 Biomechanical application

### V.3.1 Results and Discussion

#### V.3.1.1 *Modelling Structural for the proposed lattice Structures*

The cancellous bone is formed in the human body in an irregular geometric shape. In this study, we used miscellaneous geometric structures and a perfect state to simulate the lattice structures with uneven porosities and applied the finite element analysis. The Von Mises Stress distribution and Strain field distribution for each shape of lattice structures and porosity ratio is shown in Figure V.9. The equivalent stress increases when the porosity decreases gradually because of the increase in the diameter of the rib. At the end of this step is evaluated the numerical results of the proposed designs, we do a comparison between the designs in terms of stress and strain in order to get a clear comparison of the stiffness.



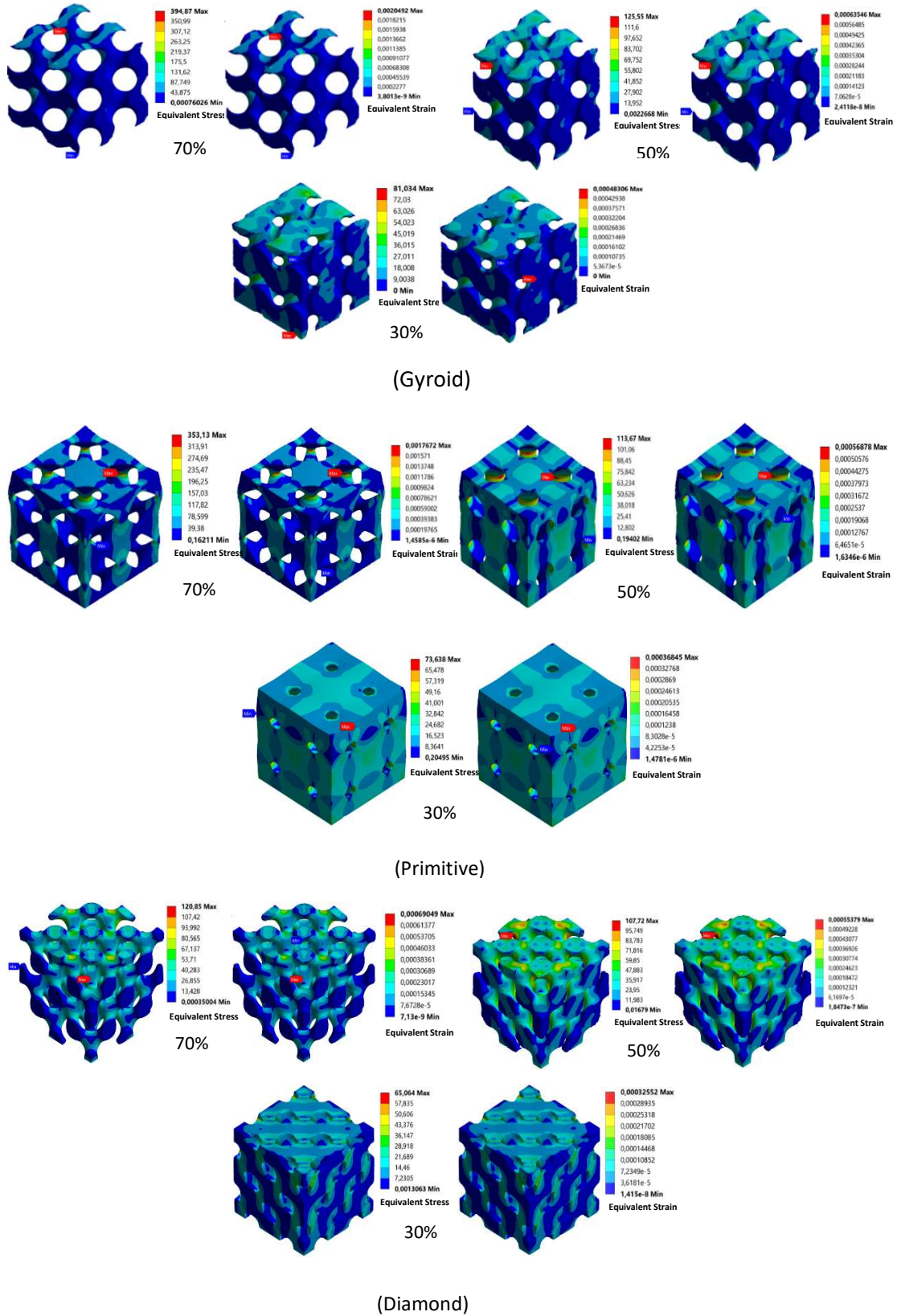


Figure V.9 Distribution of stress and strain in Simulation numerical for the three designs: a) Gyroid, b) Primitive, c) Diamond

## a) Finite Element Simulation Results

Table V.2 Resume of numerical Simulation results

Ratio porosity		70%	50%	30%
Stress Von Mises (MPa)	Gyroid	394.87	125.55	81.034
	Primitive	353.13	113.67	73.638
	Diamond	120.85	107.72	65.064
Strain	Gyroid	2.04 e-3	0.63 e-3	0.48 e-3
	Primitive	1.76 e-3	0.56 e-3	0.36 e-3
	Diamond	0.69 e-3	0.55 e-3	0.32 e-3

As expected Von Mises stress decies with porosity ratio for all lattice structures as illustrated in Table V.2. However, we note that for diamond lattice structures, the maximum Von Mises stress is three times less than the same case for Gyroid or Primitive lattice structures. This means that the particular geometry of a Diamond disperse better the Von Mises Stress than the other structures, also this stress remains relatively constant between 70% and 50% porosity ratio.

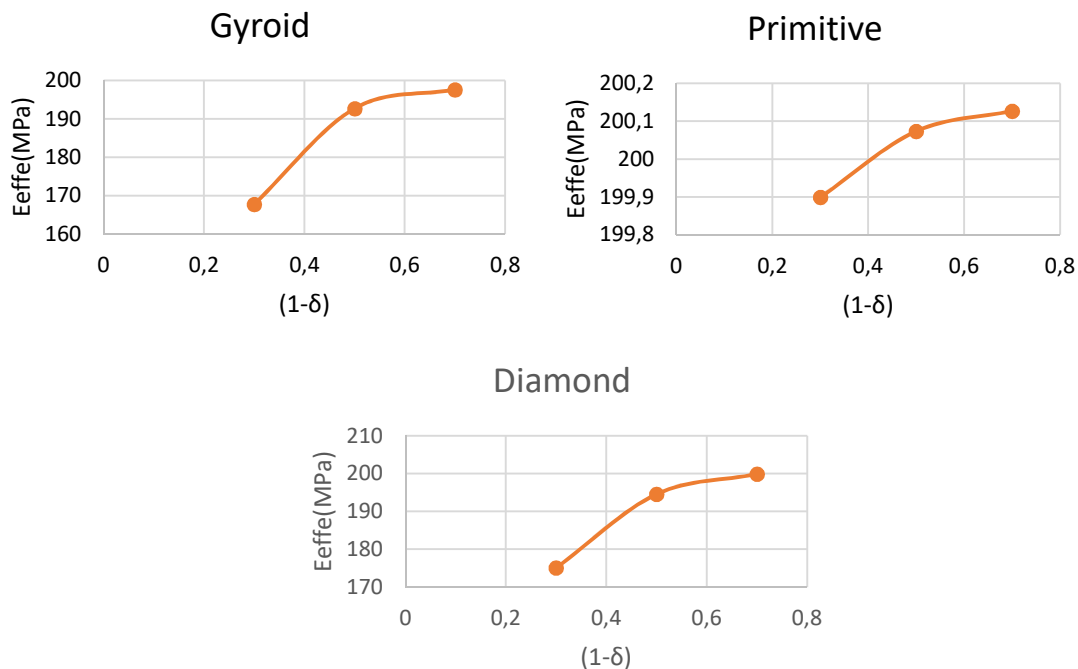


Figure V.10 Variation of equivalent elastic modulus in fact of (1-δ) porosity for the three types of lattice structures

In Figure V.10 we represent the evolution of the effective modulus in fact with porosity ratio for the three Lattice structures', all stiffness values are inside the range of 50–500 MPa, which

is considered satisfactory for human cancellous bone.

The numerical results showed that the relationship between the porosity and the equivalent elastic modulus is a polynomial relationship of the three lattice structures with their different porosity obtained by finite element simulation. Due to the equivalent elastic modulus decreases with the increment of porosity, the relationship between them was studied using the method of polynomial regression analysis.

According to the regression an equation of the lattice structures was used to predict the equivalent elastic modulus as follows:

$$\frac{E_{\text{effe}}}{E_s} = a + b(1 - \delta) - c(1 - \delta)^2 \dots\dots\dots (V.1)$$

Where the porosity is  $\delta$  and the equivalent elastic modulus of Z-ABS is  $E_s$ . Given that (a, b, c) value is 0.0464564, 0.1622588, 0.1250116 respectively and (R<sup>2</sup>) coefficient is the judgement value for the derived expression 0.9983.

While the porosity range used in the literature was greater than 50% [174], the porosity range in this research was ranged between 30% - 70%. From the previous data, it can notice that the equivalent elastic modulus increases with the decrease of the porosity of the lattice structures.

### *V.3.1.2 Result of Effective Stiffness of lattice structures Porous by (Gibson and Ashby) Method*

The equivalent elastic modulus equations of the three lattice structures were predicted using Equation (4). Finite element simulation results showed some similarity with the Gibson and Ashby method in terms of the elastic modulus depending on the porosity ratio of each structure as in Figure V.11. Generally, based on the conclusion reached by most researchers [175], the estimation of the expected value of the stiffness of the structures was close to the finite element simulation results of the three lattice structures compared to the results of the experimental value.

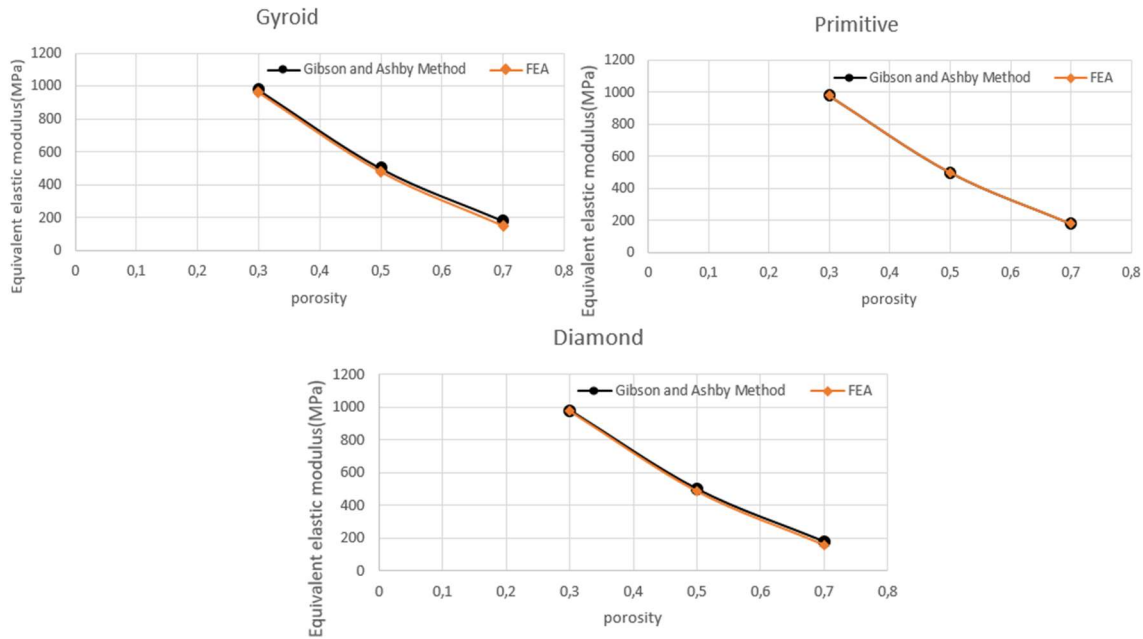
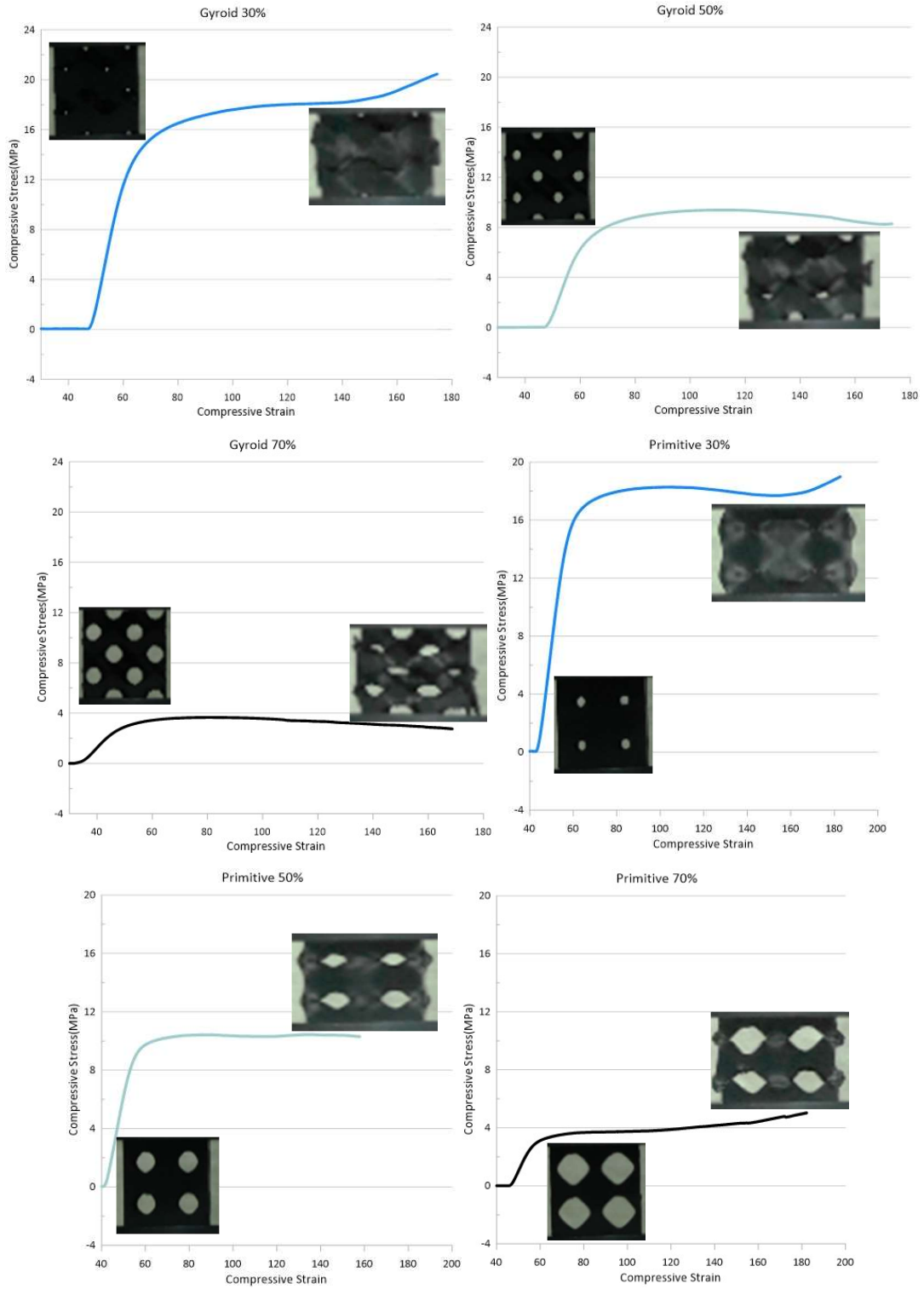
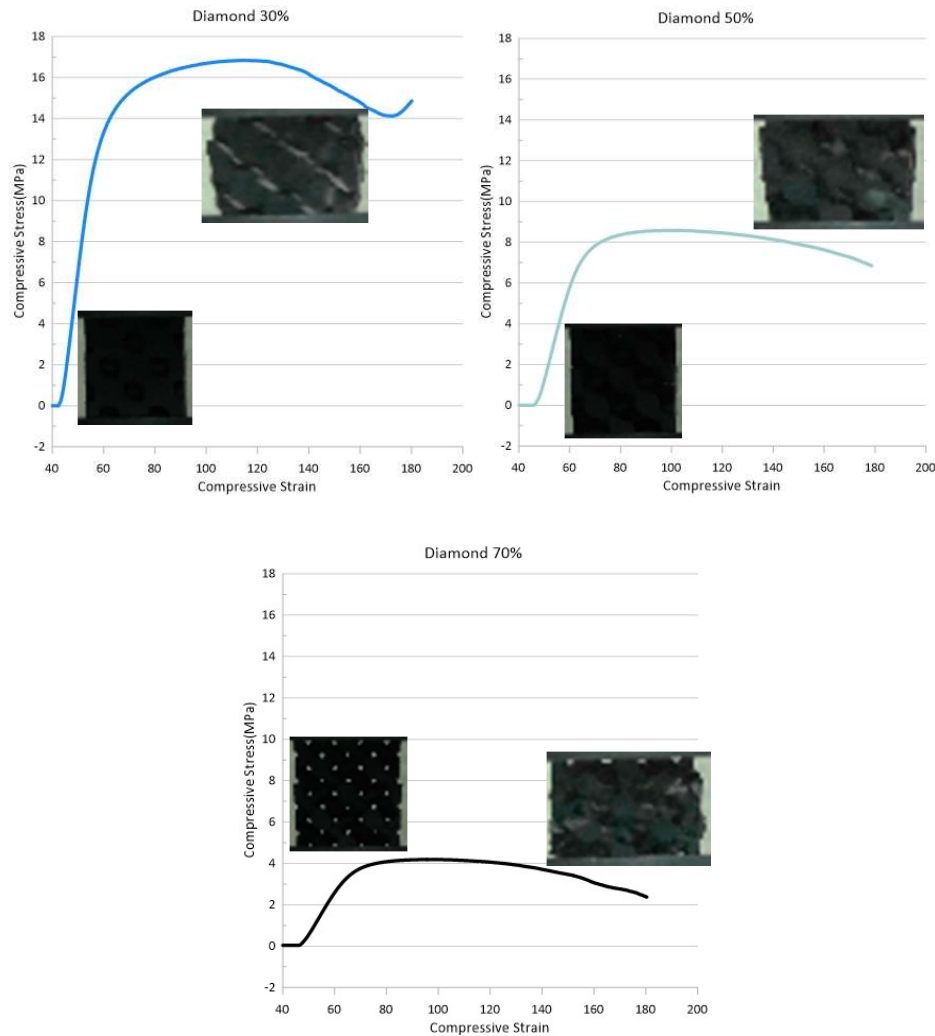


Figure V.11 Comparison of the two methods of the equivalent elastic modulus for the lattice structures

### V.3.1.3 Experimental Method Results

After manufacturing the samples of each type of lattice structure by 3D printer, each one was subjected to a Uniaxial Compression test using standard ISO 604 [176]. According to the force and displacement data in the compression tests, we can represent the average stress-strain curves for each design. The loading was applied in one direction on the different samples that were graded in terms of porosity and form. Because their porosities have differences, the yield strength increase and equivalent elastic modulus with the increase of struts thickness. Due to the large differences in porosity and shape between the proposed designs, the effect of size and porosity in this experiment have fundamentally different stiffness values.





**Figure V.12** The compressive stress-strain curve of three models by the uniaxial compression

The stress-strain curves of three models of lattice structures with different porosity obtained by the uniaxial compression test are shown in Figure V.12. The results show that whatever the shape of the sample, those with the lowest porosity ratio of 30% have more rigidity with a greater elastic modulus and a greater ultimate strength, certainly because there is less material and therefore less ductility. The differences between the results of the experimental for the three proposed designs with different porosity including structural changes and cell body deformation are a result of factors related to the pore size and cell shape and material.

Also, the experimental results showed that the relationship between the porosity and the equivalent elastic modulus is a logarithmic relationship of the three lattice structures with their different porosity obtained by a uniaxial compression test. Figure V.13 shows the stiffness estimation for the three lattice structures with their different porosity depending on the equivalent modulus of elasticity and the uniform porosity of the structures at 30%, 50% and

70%. The relationship between them was studied using the method of logarithmic regression analysis. According to the regression an equation of the lattice structures was used to predict the equivalent elastic modulus as follows:

$$E = a * \ln(\delta) + b \dots\dots\dots (V.2)$$

Where the porosity is  $\delta$  and the (a, b) value is (-88.482108, -12.973509) for the Gyroid and likewise with both Primitive (-113.46381, -13.408052) and Diamond (-111.24868, -18.432903) and (R2) coefficient is the judgment value for the derived expression (0.9999946, 0.9994971 and 0.9992712) respectively.

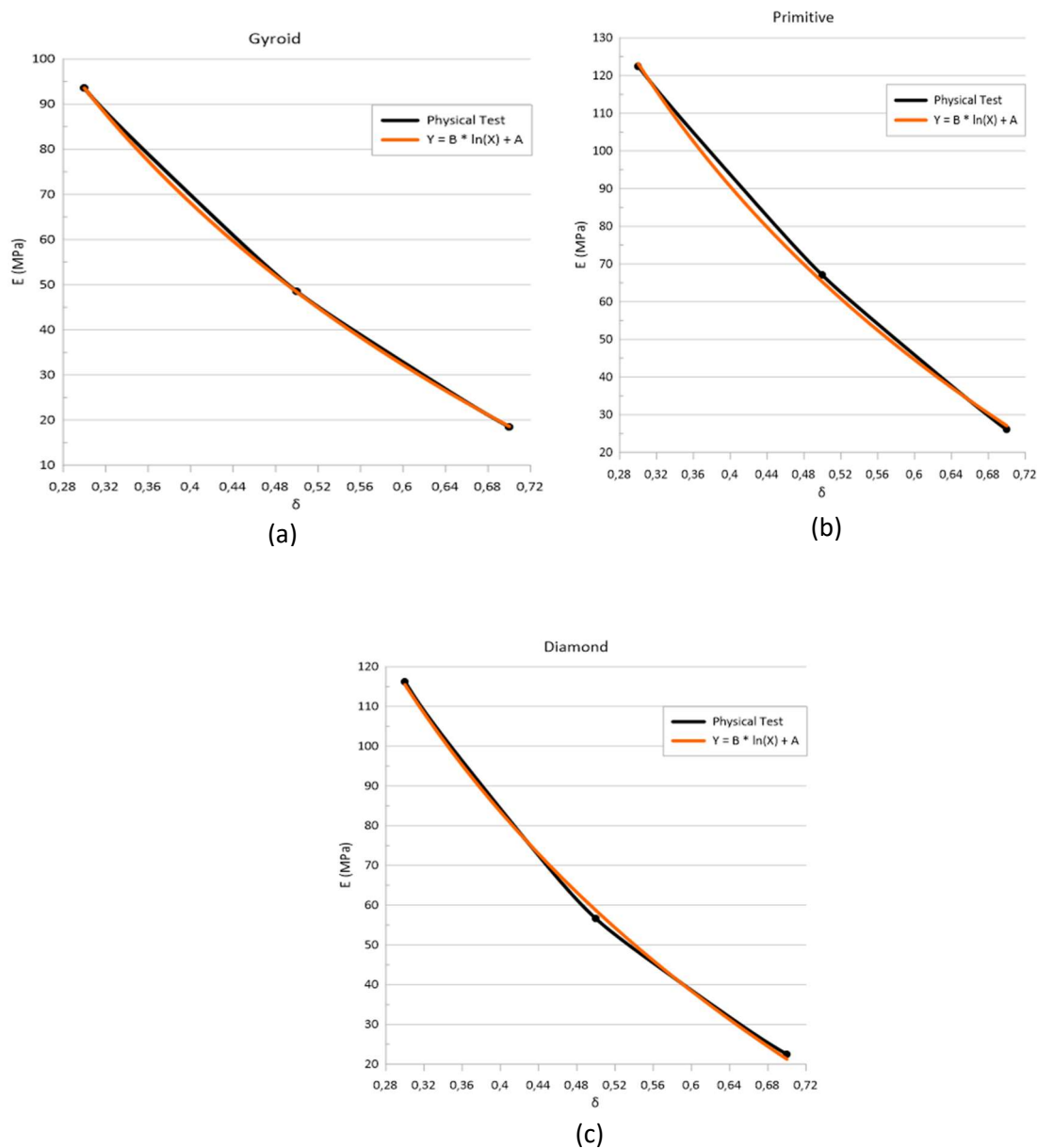


Figure V.13 Effect of ratio porosity on equivalent elastic modulus in the physical test



### V.3.1.4 Results discussion

In this work, to predict the mechanical properties of three lattice structures with different porosity, we used numerical simulation by FEA, Gibson and Ashby method calculation and an experimental uniaxial compression. Figure V.14 illustrates the comparison of the effective stiffness of three lattice structures with porosity ratios at 30%, 50%, and 70%, obtained by three methods (FEA, Gibson and Ashby method and an experimental method). The results of the FEA and Gibson & Ashby method were compatible, whereas there was some difference between them and the experimental results. For the results of the FEA method and the method of Gibson and Ashby, diamond structure in three ratio porosity 30%, 50%, 70% showed a low-stress concentration than the other models, which is advantageous to avoid possible micro-fractures in cancellous bone area. These results showed some similarities with Gibson and Ashby method in terms of the elastic modulus and the porosity ratio of each structure.

While results in the experimental method showed that the relationship between the porosity and the equivalent elastic modulus is a logarithmic relationship of the three lattice structures of different porosity obtained by a uniaxial compression test. In the experimental method, we observe that lattice structures with high porosity ratio had low stiffness and vice versa depending on the homogeneity of lattice structures. Besides, the equivalent elastic modulus of (Z-ABS) primitive lattice structure obtained by a uniaxial compression test had similar stiffness' characteristics to the human vertebral cancellous bone which has a value of 190 MPa [13][177] See Figure 13 (b).

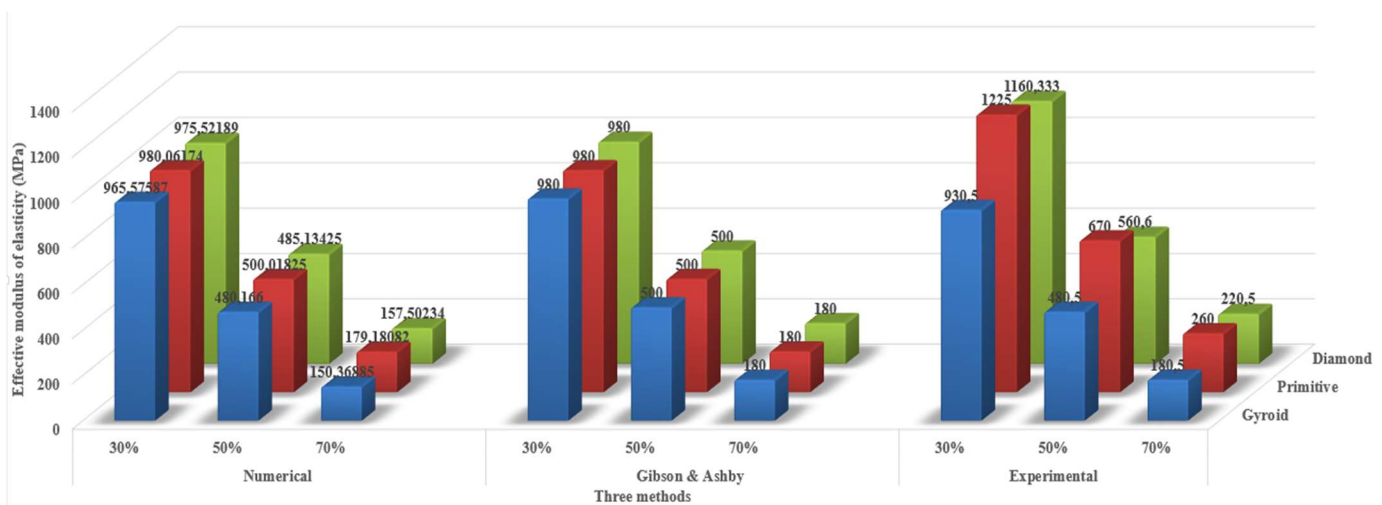


Figure V.14 Comparison of equivalent elastic modulus for the lattice structures by the three methods

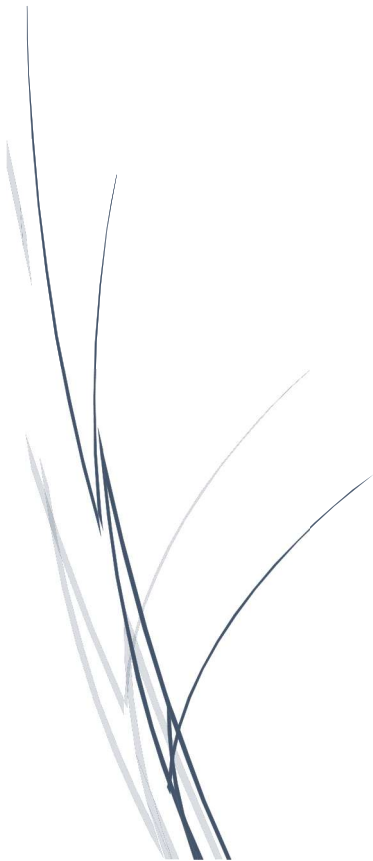
## V.4 Conclusions

In this chapter, we have tried to implement the set of ideas that characterize the proposed approach by focusing on the designs of the lattice structures with a different architecture in two different fields (Aerospace, Biomechanical) as well as the validation the results numerical and experimental. Our architecture is well implemented using Ansys Software, which includes the numerical simulator to simulate the FEM and the Uniaxial Compression test. The effectiveness of the proposed methodology is proved by the results obtained from conducting a simulation of the designs (Gyroid, Diamond and Primitive) in both cases.

For Aerospace application, we evaluated the numerical results and highlight the efficiency of the proposed approach, we make a comparison between the final designs and the initial design. The internal volume of the final designs consists of three different lattice structures (Gyroid, Primitive and Diamond). We have also determined criteria (Lightweight, Stress and Deformation) for evaluating the obtained results that of the final designs show better results than in the initial design.

For Biomechanical application, the results of the FEA and Gibson & Ashby method were compatible, whereas there was some difference between them and the experimental results. These results showed some similarities with Gibson and Ashby method in terms of the elastic modulus and the porosity ratio of each structure. While results in the experimental method showed that, the relationship between the porosity and the equivalent elastic modulus is a logarithmic relationship of the three lattice structures of different porosity obtained by a uniaxial compression test.

# General Conclusion



To keep pace with the development and modernity in the design and manufacture today of complex designs requires sophisticated techniques for into account their manufacturability. Numerous research studies have examined and have led to multiple approaches. It seems that no single approach is sufficient on its own to meet all the challenges faced by designers, so complex is the problem and its diverse aspects. We have come to the conclusion that the Topology Optimization methods with lattice structures are a good idea, provided that there are effective mechanisms that allow it to be implemented by Additive Manufacturing.

The work that has just been presented attempts to consider such an approach in two domains. For the first domain, we designed lattice structures with graded and lightweight forms relying on a homogenization-based Lattice Structure Topology Optimization (LSTO) technique. The effectiveness of the proposed methodology is proved by the results obtained from conducting a simulation of the three final designs (Gyroid, Diamond and Primitive) and comparing them with the initial design under the effects of mechanical and thermal loads. The numerical results show that the efficiency of our approach is manifested in: (1) reducing the weight of the blade rate between (33.41 – 40.32%), (2) reducing stress rate between (25.52 - 48.55%) and (3) reducing the deformation rate between (7.35 - 19.58%).

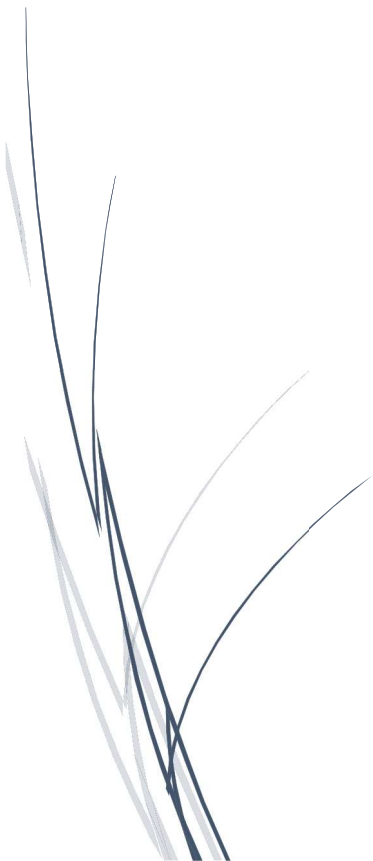
For the second domain, mechanical characteristics of three lattice structures (Gyroid, Diamond and Primitive) with volume porosity 30%, 50% and 70% for each type, and manufactured by Fused Filament Fabrication (FFF) were designed and studied to predict the stiffness of all structures. The results of finite element simulation showed that decreasing the porosity increases the equivalent modulus of elasticity for all lattice structures it was presented as a formula with a polynomial regression relationship to predict the modulus of elasticity with the porosity ratio. Results obtained from FEA and the method of Gibson and Ashby showed that diamonds had less stress in the three porosity ratios 30%, 50%, 70% compared to the other models.

Diamond is therefore advantageous to avoid possible micro-fractures in the cancellous bone area due to its low-stress concentration. While the equivalent elastic modulus was measured by uniaxial compression for the three lattice structures with porosity ratios at 30%, 50%, and 70%, and shows the Primitive stiffness was much more than the other two designs and identical for stiffness characteristics to human vertebral cancellous bone. On the other hand, lattice structures with a low porosity ratio give high rigidity and high friction between organic matter and intercellular lattice. In this work, diamond lattice gave a high porosity ratio (70%), less stress concentration and best blood and organic matter circulation. Blood is supplied to the bone

based on the porosity in the marrow cavity and returned by the periosteal veins through the nutrient arteries. The vascular structure's structure might differ substantially depending on where in the bone it is located, so the porosity helps to facilitate blood circulation because of the difference in structure and give specific arterial inlets that provide nutrients to the bones (such as the periosteal and metaphysical arteries) as well as to the epiphyseal and hypophyseal vessels [178].

In future research, we will be working on enhancing this approach by using more techniques (topology optimization method and additive manufacturing) and optimizing designs by using graded cellular structures under the mechanical and thermal loads. While in the medical domain, it would be interesting to develop our approach using graded lattice structures to enhance osseointegration and the mechanical compatibility of the human bone by distributing structures and the porosity ratio based on the defects of cancellous bone. In addition, the modelling technique also helps optimize structures using the topology optimization method and high-resolution fabrication capacity.

# Bibliography



- 
- [1] Y. Du, H. Li, Z. Luo, and Q. Tian, "Topological design optimization of lattice structures to maximize shear stiffness," *Adv. Eng. Softw.*, vol. 112, pp. 211–221, 2017, doi: 10.1016/j.advengsoft.2017.04.011.
- [2] Y. Du *et al.*, "Laser additive manufacturing of bio-inspired lattice structure: Forming quality, microstructure and energy absorption behavior," *Mater. Sci. Eng. A*, vol. 773, no. November 2019, 2020, doi: 10.1016/j.msea.2019.138857.
- [3] S. Ramtani, H. Bennaceur, and T. Outtas, "Elastic bone-column buckling including bone density gradient effect within the context of adaptive elasticity," *Irbm*, vol. 36, no. 5, pp. 267–277, 2015, doi: 10.1016/j.irbm.2015.07.004.
- [4] S. Pagani *et al.*, "Mechanical and in vitro biological properties of uniform and graded Cobalt-chrome lattice structures in orthopedic implants," *J. Biomed. Mater. Res. - Part B Appl. Biomater.*, no. December 2020, pp. 1–13, 2021, doi: 10.1002/jbm.b.34857.
- [5] Y. Lv *et al.*, "Metal Material, Properties and Design Methods of Porous Biomedical Scaffolds for Additive Manufacturing: A Review," *Front. Bioeng. Biotechnol.*, vol. 9, no. March, pp. 1–16, 2021, doi: 10.3389/fbioe.2021.641130.
- [6] S. Duan, L. Xi, W. Wen, and D. Fang, "Mechanical performance of topology-optimized 3D lattice materials manufactured via selective laser sintering," *Compos. Struct.*, vol. 238, no. January, 2020, doi: 10.1016/j.compstruct.2020.111985.
- [7] G. Dong, Y. Tang, D. Li, and Y. F. Zhao, "Design and optimization of solid lattice hybrid structures fabricated by additive manufacturing," *Addit. Manuf.*, vol. 33, p. 101116, 2020, doi: 10.1016/j.addma.2020.101116.
- [8] Y. Wang, J. Gao, and Z. Kang, "Level set-based topology optimization with overhang constraint: Towards support-free additive manufacturing," *Comput. Methods Appl. Mech. Eng.*, vol. 339, pp. 591–614, 2018, doi: 10.1016/j.cma.2018.04.040.
- [9] L. Mirabella, "DESIGN AND TOPOLOGY OPTIMIZATION OF LATTICE STRUCTURES USING DEFORMABLE IMPLICIT SURFACES FOR ADDITIVE MANUFACTURING," pp. 1–11, 2016.
- [10] J. Niu and H. Leng, "Numerical study on load-bearing capabilities of beam-like lattice structures with three different unit cells," *Int. J. Mech. Mater. Des.*, 2017, doi: 10.1007/s10999-017-9384-3.
- [11] L. Cheng, J. Bai, and A. C. To, "Functionally graded lattice structure topology optimization for the design of additive manufactured components with stress constraints," *Comput. Methods Appl. Mech. Eng.*, vol. 344, pp. 334–359, 2019, doi: 10.1016/j.cma.2018.10.010.
- [12] M. Rajabinezhad, A. Bahrami, M. Mousavinia, S. J. Seyedi, and P. Taheri, "Corrosion-fatigue failure of gas-turbine blades in an oil and gas production plant," *Materials (Basel)*, vol. 13, no. 4, pp. 1–8, 2020, doi: 10.3390/ma13040900.
- [13] X. Chen *et al.*, "Design and mechanical compatibility of nylon bionic cancellous bone fabricated by selective laser sintering," *Materials (Basel)*, vol. 14, no. 8, 2021, doi: 10.3390/ma14081965.
- [14] X. Wang *et al.*, "Topological design and additive manufacturing of porous metals for bone scaffolds and orthopaedic implants: A review," *Biomaterials*, vol. 83, pp. 127–141, 2016, doi: 10.1016/j.biomaterials.2016.01.012.
- [15] D. Hara *et al.*, "Bone bonding strength of diamond-structured porous titanium-alloy implants manufactured using the electron beam-melting technique," *Mater. Sci. Eng. C*, vol. 59, pp. 1047–1052, 2016, doi: 10.1016/j.msec.2015.11.025.
- [16] J. Rivard, V. Brailovski, S. Dubinskiy, and S. Prokoshkin, "Fabrication, morphology and mechanical properties of Ti and metastable Ti-based alloy foams for biomedical applications," *Mater. Sci. Eng. C*, vol. 45, pp. 421–433, 2014, doi: 10.1016/j.msec.2014.09.033.
- [17] M. F. Ashby, "The properties of foams and lattices," *Philos. Trans. R. Soc. A Math. Phys. Eng. Sci.*, vol. 364, no. 1838, pp. 15–30, 2006, doi: 10.1098/rsta.2005.1678.
-



- [18] O. L. A. Harrysson, O. Cansizoglu, D. J. Marcellin-Little, D. R. Cormier, and H. A. West, "Direct metal fabrication of titanium implants with tailored materials and mechanical properties using electron beam melting technology," *Mater. Sci. Eng. C*, vol. 28, no. 3, pp. 366–373, 2008, doi: 10.1016/j.msec.2007.04.022.
- [19] L. E. Murr *et al.*, "Next-generation biomedical implants using additive manufacturing of complex cellular and functional mesh arrays," *Philos. Trans. R. Soc. A Math. Phys. Eng. Sci.*, vol. 368, no. 1917, pp. 1999–2032, 2010, doi: 10.1098/rsta.2010.0010.
- [20] BATACHE Djamel, "Détermination des propriétés mécaniques effectives des milieux hétérogènes, approche par le modèle n+1 phases et validation par l'approche numérique," Université de Batna 2 – Mostefa Ben Boulaïd, 2018.
- [21] X. Liu and V. Shapiro, "Random heterogeneous materials via texture synthesis," *Comput. Mater. Sci.*, vol. 99, pp. 177–189, 2015, doi: 10.1016/j.commatsci.2014.12.017.
- [22] K. S. Basaruddin, R. Daud, Haftirman, A. S. Abdul Rahman, M. J. Aziz Safar, and M. H. M. Som, "Stochastic multiscale modeling of two-phase materials based on first-order perturbation method," *ARPN J. Eng. Appl. Sci.*, vol. 10, no. 20, pp. 9377–9381, 2015.
- [23] S. Torquato, and H. Haslach, *Random Heterogeneous Materials: Microstructure and Macroscopic Properties*, vol. 55, no. 4. Springer, 2002.
- [24] D. I. A. Millar, *Energetic Materials at Extreme Conditions*. 2012.
- [25] D. Ducret, "Elasticité anisotrope et endommagement des matériaux composites : Caractérisation ultrasonore et modélisation micromécanique," Lyon, INSA, 2000.
- [26] B. SAMIR, "Modélisation numérique de la propagation de l'endommagement et de la rupture dans les matériaux composites stratifiés sous sollicitations thermomécaniques et cycliques," l'Université Hadj Lakhdar de Batna2, 2012.
- [27] R. A. Achraf Tafla, "Éléments finis mixtes-hybrides naturels sans facteurs correctifs du cisaillement pour les plaques et les coques composites multicouches," Reims, 2007.
- [28] B. Alemour, O. Badran, and M. R. Hassan, "A review of using conductive composite materials in solving lightning strike and ice accumulation problems in aviation," *J. Aerosp. Technol. Manag.*, vol. 11, pp. 1–23, 2019, doi: 10.5028/jatm.v11.1022.
- [29] Michel ROBERT, "Les composites aéronautiques 40 ans déjà et ce n'est que le début," 2007. [Online]. Available: <https://www.yumpu.com/fr/document/read/7720837/les-composites-aeronautiques-palladium-materiaux-et->
- [30] "No Title." <https://www.turbosquid.com/3d-models/kh-25-missiles-3d-max/1108204>.
- [31] "No Title." <https://www.azom.com/article.aspx?ArticleID=12034>.
- [32] A. G. Dumanli and T. Savin, "Recent advances in the biomimicry of structural colours," *Chem. Soc. Rev.*, vol. 45, no. 24, pp. 6698–6724, 2016, doi: 10.1039/c6cs00129g.
- [33] Z. Hu, V. K. Gadipudi, and D. R. Salem, "Topology Optimization of Lightweight Lattice Structural Composites Inspired by Cuttlefish Bone," *Appl. Compos. Mater.*, vol. 26, no. 1, pp. 15–27, 2019, doi: 10.1007/s10443-018-9680-6.
- [34] S. C. Han, J. W. Lee, and K. Kang, "A New Type of Low Density Material: Shellular," *Adv. Mater.*, vol. 27, no. 37, pp. 5506–5511, 2015, doi: 10.1002/adma.201501546.
- [35] M. MASMOUDI, "Elaboration d'un modele numerique du comportement elasto plastique pour la determination des champs de contraintes et de deformations dans les structures composites," UNIVERSIT\_E BATNA 2, 2017.
- [36] A. Thomas, "Much ado about nothing – a decade of porous materials research," *Nat. Commun.*, vol. 11, no. 1, pp. 11–13, 2020, doi: 10.1038/s41467-020-18746-5.
- [37] T. Fiedler, E. Pesetskaya, A. Öchsner, and J. Grácio, "Calculations of the thermal conductivity of porous materials," *Mater. Sci. Forum*, vol. 514–516, no. PART 1, pp. 754–758, 2006, doi: 10.4028/www.scientific.net/msf.514-516.754.
- [38] B. Biswal, P. E. Øren, R. J. Held, S. Bakke, and R. Hilfer, "Modeling of multiscale porous media," *Image Anal. Stereol.*, vol. 28, no. 1, pp. 23–34, 2009, doi: 10.5566/ias.v28.p23-34.
- [39] M. Dumas and M. P. À, "Modélisation et simulation du comportement d' une tige fémorale

- poreuse par,” 2016.
- [40] M. Ashby, “Designing architected materials,” *Scr. Mater.*, vol. 68, no. 1, pp. 4–7, 2013, doi: 10.1016/j.scriptamat.2012.04.033.
- [41] A. H. Azman, “Method for integration of lattice structures in design for additive manufacturing,” *Hal*, p. 164, 2018.
- [42] H. N. G. Wadley, “Cellular metals manufacturing,” *Adv. Eng. Mater.*, vol. 4, no. 10, pp. 726–733, 2002, doi: 10.1002/1527-2648(20021014)4:10<726::AID-ADEM726>3.0.CO;2-Y.
- [43] L. J. Gibson, “Biomechanics of cellular solids,” *J. Biomech.*, vol. 38, no. 3, pp. 377–399, 2005, doi: 10.1016/j.jbiomech.2004.09.027.
- [44] S. M. Giannitelli, D. Accoto, M. Trombetta, and A. Rainer, “Current trends in the design of scaffolds for computer-aided tissue engineering,” *Acta Biomater.*, vol. 10, no. 2, pp. 580–594, 2014, doi: 10.1016/j.actbio.2013.10.024.
- [45] D. J. Yoo, “New paradigms in cellular material design and fabrication,” *Int. J. Precis. Eng. Manuf.*, vol. 16, no. 12, pp. 2577–2589, 2015, doi: 10.1007/s12541-015-0330-8.
- [46] O. Al-Ketan, M. Adel Assad, and R. K. Abu Al-Rub, “Mechanical properties of periodic interpenetrating phase composites with novel architected microstructures,” *Compos. Struct.*, vol. 176, pp. 9–19, 2017, doi: 10.1016/j.compstruct.2017.05.026.
- [47] A. Safar and L. A. Mihai, “Foam Topology Bending Versus Stretching Dominated Architectures,” *Int. J. Non. Linear. Mech.*, vol. 106, pp. 144–154, 2018.
- [48] B. Liang *et al.*, “Multi-scale modeling of mechanical behavior of cured woven textile composites accounting for the influence of yarn angle variation,” *Compos. Part A Appl. Sci. Manuf.*, vol. 124, no. April, p. 105460, 2019, doi: 10.1016/j.compositesa.2019.05.028.
- [49] V. Brailovski and P. Terriault, *Metallic Porous Materials for Orthopedic Implants: Functional Requirements, Manufacture, Characterization, and Modeling*, no. June 2015. Elsevier Ltd., 2016.
- [50] B. Shi, M. Zhang, S. Liu, B. Sun, and B. Gu, “Multi-scale ageing mechanisms of 3D four directional and five directional braided composites’ impact fracture behaviors under thermo-oxidative environment,” *Int. J. Mech. Sci.*, vol. 155, no. January, pp. 50–65, 2019, doi: 10.1016/j.ijmecsci.2019.02.040.
- [51] S. M. Ahmadi *et al.*, “Mechanical behavior of regular open-cell porous biomaterials made of diamond lattice unit cells,” *J. Mech. Behav. Biomed. Mater.*, vol. 34, pp. 106–115, 2014, doi: 10.1016/j.jmbbm.2014.02.003.
- [52] J. Dirrenberger, S. Forest, D. Jeulin, and C. Colin, “Homogenization of periodic auxetic materials,” *Procedia Eng.*, vol. 10, pp. 1847–1852, 2011, doi: 10.1016/j.proeng.2011.04.307.
- [53] A. Alderson *et al.*, “Elastic constants of 3-, 4- and 6-connected chiral and anti-chiral honeycombs subject to uniaxial in-plane loading,” *Compos. Sci. Technol.*, vol. 70, no. 7, pp. 1042–1048, 2010, doi: 10.1016/j.compscitech.2009.07.009.
- [54] J. C. Álvarez Elipse and A. Díaz Lantada, “Comparative study of auxetic geometries by means of computer-aided design and engineering,” *Smart Mater. Struct.*, vol. 21, no. 10, 2012, doi: 10.1088/0964-1726/21/10/105004.
- [55] J. Dirrenberger, J. D. Propri, and J. Dirrenberger, “Propri ´ et ´ es effectives de mat ´ eriaux architectur ´ es To cite this version : l ´ École Nationale Supérieure des Mines de Paris Propriétés effectives de matériaux architecturés Effective properties of architected materials,” 2013.
- [56] M. P. Bendsøe and O. Sigmund, *Topology Optimization*. 2004.
- [57] S. Broxterman, “Challenge the future Department of Precision and Microsystems Engineering USING TOPOLOGY OPTIMIZATION FOR ACTUATOR PLACEMENT WITHIN MOTION SYSTEMS,” 2017.
- [58] J. D. Deaton and R. V. Grandhi, “A survey of structural and multidisciplinary continuum

- topology optimization: Post 2000,” *Struct. Multidiscip. Optim.*, vol. 49, no. 1, pp. 1–38, 2014, doi: 10.1007/s00158-013-0956-z.
- [59] G. I. N. Rozvany, “Aims, scope, methods, history and unified terminology of computer-aided topology optimization in structural mechanics,” *Struct. Multidiscip. Optim.*, vol. 21, no. 2, pp. 90–108, 2001, doi: 10.1007/s001580050174.
- [60] David S. Richeson, *Euler’s gem: the polyhedron formula and the birth of topology*, vol. 46, no. 06. 2009.
- [61] Z. Xinghua, G. He, and G. Bingzhao, “The application of topology optimization on the quantitative description of the external shape of bone structure,” *J. Biomech.*, vol. 38, no. 8, pp. 1612–1620, 2005, doi: 10.1016/j.jbiomech.2004.06.029.
- [62] F. Mitjana, P. P. Duysinx, P. E. Oudet, and P. C. Bes, “Optimisation topologique de structures sous contraintes de flambage,” 2018.
- [63] Jean-Louis FANCHON, *Guide de mécanique*. 2009.
- [64] G. I. N. Rozvany, M. Zhou, and T. Birker, “Generalized shape optimization without homogenization,” *Struct. Optim.*, vol. 4, no. 3–4, pp. 250–252, 1992, doi: 10.1007/bf01742754.
- [65] P. DUYSINX, “Optimisation topologique: du milieu continu à la structure élastique,” 1996.
- [66] M. P. Bendsøe and N. Kikuchi, “Generating optimal topologies in structural design using a homogenization method,” *Comput. Methods Appl. Mech. Eng.*, vol. 71, no. 2, pp. 197–224, 1988, doi: 10.1016/0045-7825(88)90086-2.
- [67] D. Brackett, I. Ashcroft, and R. Hague, “Topology optimization for additive manufacturing,” *22nd Annu. Int. Solid Free. Fabr. Symp. - An Addit. Manuf. Conf. SFF 2011*, pp. 348–362, 2011.
- [68] F. Riaz, R. Ahmad, K. Alam, and A. S. Abid, *Design optimization of modular bridge structure*, vol. 328. 2013.
- [69] R. Muhammet Gorgularslan, S.-K. Choi, D. W. Rosen, D. L. McDowell, C. J. Saldana, and R. L. Muhanna, “a Multi-Level Upscaling and Validation Framework for Uncertainty Quantification in Additively Manufactured Lattice Structures,” *Georg. Inst. Technol.*, no. December, 2016.
- [70] X. Huang and Y. M. Xie, *Evolutionary Topology Optimization of Continuum Structures: Methods and Applications*. 2010.
- [71] M. P. Bendsøe, O. Sigmund, M. P. Bendsøe, and O. Sigmund, *Topology optimization by distribution of isotropic material*. 2004.
- [72] O. Sigmund, “A 99 line topology optimization code written in matlab,” *Struct. Multidiscip. Optim.*, vol. 21, no. 2, pp. 120–127, 2001, doi: 10.1007/s001580050176.
- [73] D. Jankovics, H. Gohari, M. Tayefeh, and A. Barari, “Developing Topology Optimization with Additive Manufacturing Constraints in ANSYS®,” *IFAC-PapersOnLine*, vol. 51, no. 11, pp. 1359–1364, 2018, doi: 10.1016/j.ifacol.2018.08.340.
- [74] D. J. Munk, D. W. Boyd, and G. A. Vio, *SIMP for Complex Structures*, vol. 846. 2016.
- [75] P. D. Dunning and H. Alicia Kim, *A new hole insertion method for level set based structural topology optimization*, vol. 93, no. 1. 2013.
- [76] Y. L. Hsu, M. S. Hsu, and C. T. Chen, “Interpreting results from topology optimization using density contours,” *Comput. Struct.*, vol. 79, no. 10, pp. 1049–1058, 2001, doi: 10.1016/S0045-7949(00)00194-2.
- [77] M. P. Bendsøe and O. Sigmund, “Material interpolation schemes in topology optimization,” *Arch. Appl. Mech.*, vol. 69, no. 9–10, pp. 635–654, 1999, doi: 10.1007/s004190050248.
- [78] Y. M. Xie and G. P. Steven, “A simple evolutionary procedure for structural optimization,” *Comput. Struct.*, vol. 49, no. 5, pp. 885–896, 1993, doi: 10.1016/0045-7949(93)90035-C.
- [79] Y. M. Xie and G. P. Steven, “A simple approach to structural frequency optimization,” *Comput. Struct.*, vol. 53, no. 6, pp. 1487–1491, 1994, doi: 10.1016/0045-7949(94)90414-6.
- [80] X. Huang and Y. M. Xie, “A further review of ESO type methods for topology

- optimization,” *Struct. Multidiscip. Optim.*, vol. 41, no. 5, pp. 671–683, 2010, doi: 10.1007/s00158-010-0487-9.
- [81] S. Khakalo and J. Niiranen, “Anisotropic strain gradient thermoelasticity for cellular structures: Plate models, homogenization and isogeometric analysis,” *J. Mech. Phys. Solids*, vol. 134, 2020, doi: 10.1016/j.jmps.2019.103728.
- [82] F. Buonamici *et al.*, “A practical methodology for computer-aided design of custom 3D printable casts for wrist fractures,” *Vis. Comput.*, vol. 36, no. 2, pp. 375–390, 2020, doi: 10.1007/s00371-018-01624-z.
- [83] Z. H. Zuo, Y. M. Xie, and X. Huang, “Combining genetic algorithms with BESO for topology optimization,” *Struct. Multidiscip. Optim.*, vol. 38, no. 5, pp. 511–523, 2009, doi: 10.1007/s00158-008-0297-5.
- [84] Y. Luo and Z. Kang, *Topology optimization of continuum structures with Drucker-Prager yield stress constraints*, vol. 90–91, no. 1. 2012.
- [85] M. P. Wolcott, *Cellular solids: Structure and properties*, vol. 123, no. 2. 1990.
- [86] A. Panesar, M. Abdi, D. Hickman, and I. Ashcroft, *Strategies for functionally graded lattice structures derived using topology optimisation for Additive Manufacturing*, vol. 19. 2018.
- [87] A. Armillotta and R. Pelzer, “Modeling of porous structures for rapid prototyping of tissue engineering scaffolds,” *Int. J. Adv. Manuf. Technol.*, vol. 39, no. 5–6, pp. 501–511, 2008, doi: 10.1007/s00170-007-1247-x.
- [88] S. J. Hollister, “Porous scaffold design for tissue engineering,” *Nat. Mater.*, vol. 4, no. 7, pp. 518–524, 2005, doi: 10.1038/nmat1421.
- [89] M. A. Wettergreen, B. S. Bucklen, B. Starly, E. Yuksel, W. Sun, and M. A. K. Liebschner, “Creation of a unit block library of architectures for use in assembled scaffold engineering,” *CAD Comput. Aided Des.*, vol. 37, no. 11, pp. 1141–1149, 2005, doi: 10.1016/j.cad.2005.02.005.
- [90] P. Zhang *et al.*, “Efficient design-optimization of variable-density hexagonal cellular structure by additive manufacturing: Theory and validation,” *J. Manuf. Sci. Eng. Trans. ASME*, vol. 137, no. 2, 2015, doi: 10.1115/1.4028724.
- [91] S. Arabnejad Khanoki and D. Pasini, “Multiscale design and multiobjective optimization of orthopedic hip implants with functionally graded cellular material,” *J. Biomech. Eng.*, vol. 134, no. 3, 2012, doi: 10.1115/1.4006115.
- [92] O. Fryazinov, T. Vilbrandt, and A. Pasko, “Multi-scale space-variant FRep cellular structures,” *CAD Comput. Aided Des.*, vol. 45, no. 1, pp. 26–34, 2013, doi: 10.1016/j.cad.2011.09.007.
- [93] N. Yang and K. Zhou, “Effective method for multi-scale gradient porous scaffold design and fabrication,” *Mater. Sci. Eng. C*, vol. 43, pp. 502–505, 2014, doi: 10.1016/j.msec.2014.07.052.
- [94] O. Fryazinov, M. Sanchez, and A. Pasko, “Shape conforming volumetric interpolation with interior distances,” *Comput. Graph.*, vol. 46, pp. 149–155, 2015, doi: 10.1016/j.cag.2014.09.028.
- [95] I. Gibson, D. Rosen, and B. Stucker, “Additive manufacturing technologies: 3D printing, rapid prototyping, and direct digital manufacturing, second edition,” *Addit. Manuf. Technol. 3D Printing, Rapid Prototyping, Direct Digit. Manuf. Second Ed.*, pp. 1–498, 2015, doi: 10.1007/978-1-4939-2113-3.
- [96] N. Lei, S. K. Moon, and G. Bi, “An Additive Manufacturing resource process model for product family design,” *IEEE Int. Conf. Ind. Eng. Eng. Manag.*, pp. 616–620, 2014, doi: 10.1109/IEEM.2013.6962485.
- [97] V. V. Toropov and S. Y. Mahfouz, “Design optimization of structural steelwork using a genetic algorithm, FEM and a system of design rules,” *Eng. Comput. (Swansea, Wales)*, vol. 18, no. 3–4, pp. 437–459, 2001, doi: 10.1108/02644400110387118.
- [98] D. Brackett, I. Ashcroft, and R. Hague, *Topology optimization for additive manufacturing*.



- 2011.
- [99] I. Campbell, D. Bourell, and I. Gibson, “Additive manufacturing: rapid prototyping comes of age,” *Rapid Prototyp. J.*, vol. 18, no. 4, pp. 255–258, 2012, doi: 10.1108/13552541211231563.
- [100] S. Liu, Y. Xu, X. Shi, Q. Deng, and Y. Li, “Distribution optimization of constrained damping materials covering on typical panels under random vibration,” *Int. J. Acoust. Vib.*, vol. 23, no. 3, pp. 370–377, 2018, doi: 10.20855/ijav.2018.23.31266.
- [101] Juho Halinen, “3D printing-increasing competitiveness in technical maintenance,” p. 71, 2017, [Online]. Available: [www.aalto.fi](http://www.aalto.fi).
- [102] E. Alfredo Campo, “The Complete Part Design Handbook: for Injection Molding of Thermoplastics,” p. 539, 2006.
- [103] S. K. Sharma and A. Mudhoo, “A handbook of applied biopolymer technology,” *A Handb. Appl. Biopolym. Technol.*, pp. 226–227, 2011, [Online]. Available: <http://ebook.rsc.org/?DOI=10.1039/9781849733458>.
- [104] W. E. Frazier, “Metal additive manufacturing: A review,” *J. Mater. Eng. Perform.*, vol. 23, no. 6, pp. 1917–1928, 2014, doi: 10.1007/s11665-014-0958-z.
- [105] I. Gibson, D. Rosen, B. Stucker, and M. Khorasani, *Additive Manufacturing Technologies*. 2021.
- [106] S. H. Khajavi, G. Deng, J. Holmström, P. Puukko, and J. Partanen, “Selective laser melting raw material commoditization: impact on comparative competitiveness of additive manufacturing,” *Int. J. Prod. Res.*, vol. 56, no. 14, pp. 4874–4896, 2018, doi: 10.1080/00207543.2018.1436781.
- [107] ASTM 52921, “Standard Terminology for Additive Manufacturing — Coordinate Systems and Test Methodologies,” *ASTM Int.*, vol. i, pp. 1–13, 2013, [Online]. Available: [www.astm.org](http://www.astm.org).
- [108] Y. Yang, L. Li, Y. Pan, and Z. Sun, “Energy Consumption Modeling of Stereolithography-Based Additive Manufacturing Toward Environmental Sustainability,” *J. Ind. Ecol.*, vol. 21, pp. S168–S178, 2017, doi: 10.1111/jiec.12589.
- [109] C. S. Cabuk Nazim, “3D PRINTERS AND APPLICATION FIELDS 3D Printers And Application Fields,” no. June, pp. 349–355, 2018.
- [110] O. Santoliquido, P. Colombo, and A. Ortona, “Additive Manufacturing of ceramic components by Digital Light Processing: A comparison between the ‘bottom-up’ and the ‘top-down’ approaches,” *J. Eur. Ceram. Soc.*, vol. 39, no. 6, pp. 2140–2148, 2019, doi: 10.1016/j.jeurceramsoc.2019.01.044.
- [111] J. Navarro, M. Din, M. E. Janes, J. Swayambunathan, J. P. Fisher, and M. L. Dreher, “Effect of print orientation on microstructural features and mechanical properties of 3D porous structures printed with continuous digital light processing,” *Rapid Prototyp. J.*, vol. 25, no. 6, pp. 1017–1029, 2019, doi: 10.1108/RPJ-10-2018-0276.
- [112] T. Caffrey, “Additive manufacturing and 3D printing state of the industry annual worldwide progress report,” *Eng. Manag. Res.*, vol. 2, no. 1, pp. 209–222, 2013.
- [113] J. Gonzalez-Gutierrez, S. Cano, S. Schuschnigg, C. Kukla, J. Sapkota, and C. Holzer, “Additive manufacturing of metallic and ceramic components by the material extrusion of highly-filled polymers: A review and future perspectives,” *Materials (Basel)*, vol. 11, no. 5, 2018, doi: 10.3390/ma11050840.
- [114] M. Attaran, “Additive Manufacturing: The Most Promising Technology to Alter the Supply Chain and Logistics,” *J. Serv. Sci. Manag.*, vol. 10, no. 03, pp. 189–206, 2017, doi: 10.4236/jssm.2017.103017.
- [115] A. D. Mazurchevici, D. Nedelcu, and R. Popa, “Additive manufacturing of composite materials by FDM technology: A review,” *Indian J. Eng. Mater. Sci.*, vol. 27, no. 2, pp. 179–192, 2020.
- [116] V. Lang *et al.*, “Process data-based knowledge discovery in additive manufacturing of

- ceramic materials by multi-material jetting (CerAM MMJ),” *J. Manuf. Mater. Process.*, vol. 4, no. 3, 2020, doi: 10.3390/JMMP4030074.
- [117] Y. Bai and C. B. Williams, “The effect of inkjetted nanoparticles on metal part properties in binder jetting additive manufacturing,” *Nanotechnology*, vol. 29, no. 39, 2018, doi: 10.1088/1361-6528/aad0bb.
- [118] H. Fayazfar, F. Liravi, U. Ali, and E. Toyserkani, “Additive manufacturing of high loading concentration zirconia using high-speed drop-on-demand material jetting,” *Int. J. Adv. Manuf. Technol.*, vol. 109, no. 9–12, pp. 2733–2746, 2020, doi: 10.1007/s00170-020-05829-2.
- [119] M. Li, W. Du, A. Elwany, Z. Pei, and C. Ma, “Metal Binder Jetting Additive Manufacturing: A Literature Review,” *J. Manuf. Sci. Eng.*, vol. 142, no. 9, 2020, doi: 10.1115/1.4047430.
- [120] R. Singh *et al.*, “Powder bed fusion process in additive manufacturing: An overview,” *Mater. Today Proc.*, vol. 26, pp. 3058–3070, 2019, doi: 10.1016/j.matpr.2020.02.635.
- [121] M. Galati, F. Calignano, S. Defanti, and L. Denti, “Disclosing the build-up mechanisms of multi jet fusion: Experimental insight into the characteristics of starting materials and finished parts,” *J. Manuf. Process.*, vol. 57, pp. 244–253, 2020, doi: 10.1016/j.jmapro.2020.06.029.
- [122] A. Awad, F. Fina, A. Goyanes, S. Gaisford, and A. W. Basit, “3D printing: Principles and pharmaceutical applications of selective laser sintering,” *Int. J. Pharm.*, vol. 586, 2020, doi: 10.1016/j.ijpharm.2020.119594.
- [123] Y. Guo, W. F. Lu, and J. Y. H. Fuh, “Semi-supervised deep learning based framework for assessing manufacturability of cellular structures in direct metal laser sintering process,” *J. Intell. Manuf.*, 2020, doi: 10.1007/s10845-020-01575-0.
- [124] P. K. Gokuldoss, S. Kolla, and J. Eckert, “Additive manufacturing processes: Selective laser melting, electron beam melting and binder jetting-selection guidelines,” *Materials (Basel)*, vol. 10, no. 6, 2017, doi: 10.3390/ma10060672.
- [125] A. Saboori, A. Aversa, G. Marchese, S. Biamino, M. Lombardi, and P. Fino, “Application of directed energy deposition-based additive manufacturing in repair,” *Appl. Sci.*, vol. 9, no. 16, 2019, doi: 10.3390/app9163316.
- [126] R. P. Mudge and N. R. Wald, “Laser engineered net shaping advances additive manufacturing and repair,” *Weld. J. (Miami, Fla)*, vol. 86, no. 1, pp. 44–48, 2007.
- [127] L. C. Zhang, Y. Liu, S. Li, and Y. Hao, “Additive Manufacturing of Titanium Alloys by Electron Beam Melting: A Review,” *Adv. Eng. Mater.*, vol. 20, no. 5, 2018, doi: 10.1002/adem.201700842.
- [128] D. X. Luong *et al.*, “Laminated Object Manufacturing of 3D-Printed Laser-Induced Graphene Foams,” *Adv. Mater.*, vol. 30, no. 28, 2018, doi: 10.1002/adma.201707416.
- [129] M. Goldin, “Chinese Company Builds Houses Quickly With 3D Printing,” *Mashable. Com*, p. April 29, 2014, 2014, [Online]. Available: <http://mashable.com/2014/04/28/3d-printing-houses-china/#6qFiIuIzJiq6>.
- [130] T. P. Mpofu, C. Mawere, and M. Mukosera, “The Impact and Application of 3D Printing Technology,” *Int. J. Sci. Res.*, vol. 3, no. 6, pp. 2148–2152, 2014, [Online]. Available: [https://www.academia.edu/download/34056587/MDIwMTQ2NzU\\_.pdf%0Ahttps://www.researchgate.net/publication/291975129](https://www.academia.edu/download/34056587/MDIwMTQ2NzU_.pdf%0Ahttps://www.researchgate.net/publication/291975129).
- [131] A. Romero-Torres and D. R. Vieira, “IS 3D printing transforming the project management function in the aerospace industry?,” *J. Mod. Proj. Manag.*, vol. 4, no. 1, pp. 113–119, 2016, doi: 10.3963/jmpm.v4i1.187.
- [132] S. M. Wagner and R. O. Walton, “Additive manufacturing’s impact and future in the aviation industry,” *Prod. Plan. Control*, vol. 27, no. 13, pp. 1124–1130, 2016, doi: 10.1080/09537287.2016.1199824.
- [133] T. Lindström, “Constitutive modelling of an additively manufactured alloy for fatigue lifing in high temperature applications,” 2020.

- 
- [134] A. Rompas, C. Tsirmpas, I. Papatheodorou, G. Koutsouri, and D. Koutsouris, “3D Printing: Basic Concepts Mathematics and Technologies,” *Int. J. Syst. Biol. Biomed. Technol.*, vol. 2, no. 2, pp. 58–71, 2013, doi: 10.4018/ijssbtt.2013040104.
- [135] M. H. Michalski and J. S. Ross, “The shape of things to come: 3D printing in medicine,” *JAMA - J. Am. Med. Assoc.*, vol. 312, no. 21, pp. 2213–2214, 2014, doi: 10.1001/jama.2014.9542.
- [136] R. Opik, A. Hunt, A. Ristolainen, P. M. Aubin, and M. Kruusmaa, “Development of high fidelity liver and kidney phantom organs for use with robotic surgical systems,” *Proc. IEEE RAS EMBS Int. Conf. Biomed. Robot. Biomechatronics*, pp. 425–430, 2012, doi: 10.1109/BioRob.2012.6290831.
- [137] A. Mishra and V. Srivastava, “Effect and Use of 3D Printers Technologies,” *Lect. Notes Mech. Eng.*, pp. 147–155, 2021, doi: 10.1007/978-981-16-0942-8\_13.
- [138] J. Hidalgo, “The future of higher education: Reshaping universities through 3D printing,” *engadget.com*, Oct., vol. 19, 2012.
- [139] C. Ludwig, F. Rabold, M. Kuna, M. Schurig, and H. Schlums, “Simulation of anisotropic crack growth behavior of nickel base alloys under thermomechanical fatigue,” *Eng. Fract. Mech.*, vol. 224, 2020, doi: 10.1016/j.engfracmech.2019.106800.
- [140] X. M. Wang *et al.*, “Mechanics of Materials Direct investigation on high temperature tensile and creep behavior at different regions of directional solidified cast turbine blades,” vol. 136, no. May, 2019.
- [141] D. B. Witkin, D. Patel, T. V Albright, G. E. Bean, and T. McIlouth, “Influence of surface conditions and specimen orientation on high cycle fatigue properties of Inconel 718 prepared by laser powder bed fusion,” *Int. J. Fatigue*, no. November, p. 105392, 2019, doi: 10.1016/j.ijfatigue.2019.105392.
- [142] X. Qiu, X. Cheng, P. Dong, H. Peng, Y. Xing, and X. Zhou, “Sensitivity Analysis of Johnson-Cook Material Constants and Friction Coefficient Influence on Finite Element Simulation of Turning Inconel 718,” 2019.
- [143] R. Nagesh, H. R. Apoorva, and R. Mohan, “Static Structural Analysis of Gas Turbine Blades Comparing the Materials,” vol. 4, no. 7, pp. 29–32, 2017, doi: 10.17148/IARJSET.
- [144] W. Sun *et al.*, “Strategy of incorporating Ni-based braze alloy in cold sprayed Inconel 718 coating,” *Surf. Coatings Technol.*, 2019, doi: 10.1016/j.surfcoat.2018.12.050.
- [145] E. A. A. Alkebsi, H. Ameddah, T. Outtas, and A. Almutawakel, “Design of graded lattice structures in turbine blades using topology optimization,” *Int. J. Comput. Integr. Manuf.*, vol. 34, no. 4, pp. 370–384, 2021, doi: 10.1080/0951192X.2021.1872106.
- [146] E. Tyflopoulos and M. Steinert, “A comparative study between traditional topology optimization and lattice optimization for additive manufacturing,” *Mater. Des. Process. Commun.*, no. November, pp. 1–6, 2019, doi: 10.1002/mdp2.128.
- [147] Y. Tang, A. Kurtz, and Y. F. Zhao, “Bidirectional Evolutionary Structural Optimization (BESO) based design method for lattice structure to be fabricated by additive manufacturing,” *CAD Comput. Aided Des.*, vol. 69, pp. 91–101, 2015, doi: 10.1016/j.cad.2015.06.001.
- [148] J. H. Zhu, W. H. Zhang, and L. Xia, “Topology Optimization in Aircraft and Aerospace Structures Design,” *Arch. Comput. Methods Eng.*, vol. 23, no. 4, pp. 595–622, 2016, doi: 10.1007/s11831-015-9151-2.
- [149] O. Al-Ketan and R. K. Abu Al-Rub, “Multifunctional Mechanical Metamaterials Based on Triply Periodic Minimal Surface Lattices,” *Adv. Eng. Mater.*, vol. 21, no. 10, 2019, doi: 10.1002/adem.201900524.
- [150] L. Cheng, P. Zhang, E. Biyikli, J. Bai, J. Robbins, and A. To, “Efficient design optimization of variable-density cellular structures for additive manufacturing: Theory and experimental validation,” *Rapid Prototyp. J.*, vol. 23, no. 4, pp. 660–677, 2017, doi: 10.1108/RPJ-04-2016-0069.
-



- 
- [151] A. Cutolo, B. Engelen, W. Desmet, and B. Van Hooreweder, “Mechanical properties of diamond lattice Ti–6Al–4V structures produced by laser powder bed fusion: On the effect of the load direction,” *J. Mech. Behav. Biomed. Mater.*, vol. 104, no. September 2019, 2020, doi: 10.1016/j.jmbbm.2020.103656.
- [152] Y. Tang, A. Kurtz, and Y. F. Zhao, “Bidirectional Evolutionary Structural Optimization (BESO) based design method for lattice structure to be fabricated by additive manufacturing,” *CAD Comput. Aided Des.*, vol. 69, pp. 91–101, 2015, doi: 10.1016/j.cad.2015.06.001.
- [153] T. NISHIZU, T. TANITSUGU, A. TAKEZAWA, K. YONEKURA, O. WATANABE, and M. KITAMURA, “Lattice structure design with topology optimization and additive manufacturing,” *Trans. JSME (in Japanese)*, vol. 83, no. 855, pp. 16-00581-16-00581, 2017, doi: 10.1299/transjsme.16-00581.
- [154] A. M. Abou-Ali, O. Al-Ketan, R. Rowshan, and R. Abu Al-Rub, “Mechanical Response of 3D Printed Bending-Dominated Ligament-Based Triply Periodic Cellular Polymeric Solids,” *J. Mater. Eng. Perform.*, vol. 28, no. 4, pp. 2316–2326, 2019, doi: 10.1007/s11665-019-03982-8.
- [155] O. Al-Ketan, R. K. A. Al-Rub, and R. Rowshan, “Mechanical Properties of a New Type of Architected Interpenetrating Phase Composite Materials,” *Adv. Mater. Technol.*, vol. 2, no. 2, pp. 1–7, 2017, doi: 10.1002/admt.201600235.
- [156] Y. Tripathi and M. Shukla, “Triply periodic minimal surface based geometry design of bio-scaffolds,” *2017 Int. Conf. Adv. Mech. Ind. Autom. Manag. Syst. AMIAMS 2017 - Proc.*, pp. 348–350, 2017, doi: 10.1109/AMIAMS.2017.8069237.
- [157] Y. Zhang, M. Xiao, H. Li, L. Gao, and S. Chu, “Multiscale concurrent topology optimization for cellular structures with multiple microstructures based on ordered SIMP interpolation,” *Comput. Mater. Sci.*, vol. 155, no. August, pp. 74–91, 2018, doi: 10.1016/j.commatsci.2018.08.030.
- [158] I. Maskery, A. O. Aremu, L. Parry, R. D. Wildman, C. J. Tuck, and I. A. Ashcroft, “Effective design and simulation of surface-based lattice structures featuring volume fraction and cell type grading,” *Mater. Des.*, vol. 155, pp. 220–232, 2018, doi: 10.1016/j.matdes.2018.05.058.
- [159] H. I. Medellin-Castillo and J. Zaragoza-Siqueiros, “Design and Manufacturing Strategies for Fused Deposition Modelling in Additive Manufacturing: A Review,” *Chinese J. Mech. Eng. (English Ed.)*, vol. 32, no. 1, 2019, doi: 10.1186/s10033-019-0368-0.
- [160] M. Fousová, D. Dvorský, A. Michalcová, and D. Vojtěch, “Changes in the microstructure and mechanical properties of additively manufactured AlSi10Mg alloy after exposure to elevated temperatures,” *Mater. Charact.*, vol. 137, no. January, pp. 119–126, 2018, doi: 10.1016/j.matchar.2018.01.028.
- [161] D. Li, N. Dai, Y. Tang, G. Dong, and Y. F. Zhao, “Design and Optimization of Graded Cellular Structures with Triply Periodic Level Surface-Based Topological Shapes,” *J. Mech. Des. Trans. ASME*, vol. 141, no. 7, 2019, doi: 10.1115/1.4042617.
- [162] A. O. Aremu *et al.*, “A voxel-based method of constructing and skinning conformal and functionally graded lattice structures suitable for additive manufacturing,” *Addit. Manuf.*, vol. 13, pp. 1–13, 2017, doi: 10.1016/j.addma.2016.10.006.
- [163] Y. Tripathi, M. Shukla, and A. D. Bhatt, “Implicit-Function-Based Design and Additive Manufacturing of Triply Periodic Minimal Surfaces Scaffolds for Bone Tissue Engineering,” *J. Mater. Eng. Perform.*, vol. 28, no. 12, pp. 7445–7451, 2019, doi: 10.1007/s11665-019-04457-6.
- [164] T. Maconachie *et al.*, “SLM lattice structures: Properties, performance, applications and challenges,” *Mater. Des.*, vol. 183, 2019, doi: 10.1016/j.matdes.2019.108137.
- [165] K.-H. Leitz, P. Singer, A. Plankensteiner, B. Tabernig, H. Kestler, and L. S. Sigl, “Thermo-fluid Dynamical Simulation of Layer Build-up by Selective Laser Melting of Molybdenum
-

- and Steel,” *BHM Berg- und Hüttenmännische Monatshefte*, vol. 162, no. 5, pp. 172–178, 2017, doi: 10.1007/s00501-017-0588-5.
- [166] C. Panwisawas *et al.*, “Mesoscale modelling of selective laser melting: Thermal fluid dynamics and microstructural evolution,” *Comput. Mater. Sci.*, vol. 126, pp. 479–490, 2017, doi: 10.1016/j.commatsci.2016.10.011.
- [167] K. H. Leitz *et al.*, “Fundamental analysis of the influence of powder characteristics in Selective Laser Melting of molybdenum based on a multi-physical simulation model,” *Int. J. Refract. Met. Hard Mater.*, vol. 72, pp. 1–8, 2018, doi: 10.1016/j.ijrmhm.2017.11.034.
- [168] D. Montoya-Zapata, A. Moreno, J. Pareja-Corcho, J. Posada, and O. Ruiz-Salguero, “Density-sensitive implicit functions using sub-voxel sampling in additive manufacturing,” *Metals (Basel)*, vol. 9, no. 12, pp. 1–25, 2019, doi: 10.3390/met9121293.
- [169] Z. Alomar and F. Concli, “A Review of the Selective Laser Melting Lattice Structures and Their Numerical Models,” *Adv. Eng. Mater.*, vol. 22, no. 12, 2020, doi: 10.1002/adem.202000611.
- [170] F. Li, J. Li, G. Xu, G. Liu, H. Kou, and L. Zhou, “Fabrication, pore structure and compressive behavior of anisotropic porous titanium for human trabecular bone implant applications,” *J. Mech. Behav. Biomed. Mater.*, vol. 46, pp. 104–114, 2015, doi: 10.1016/j.jmbbm.2015.02.023.
- [171] Y. F. Fu, B. Rolfe, L. N. S. Chiu, Y. Wang, X. Huang, and K. Ghabraie, “Design and experimental validation of self-supporting topologies for additive manufacturing,” *Virtual Phys. Prototyp.*, vol. 14, no. 4, pp. 382–394, 2019, doi: 10.1080/17452759.2019.1637023.
- [172] T. Maconachie *et al.*, “The compressive behaviour of ABS gyroid lattice structures manufactured by fused deposition modelling,” *Int. J. Adv. Manuf. Technol.*, vol. 107, no. 11–12, pp. 4449–4467, 2020, doi: 10.1007/s00170-020-05239-4.
- [173] K. Szykiedans and W. Credo, “Mechanical properties of FDM and SLA low-cost 3-D prints,” *Procedia Eng.*, vol. 136, pp. 257–262, 2016, doi: 10.1016/j.proeng.2016.01.207.
- [174] S. Zhang, S. Vijayavenkataraman, W. F. Lu, and J. Y. H. Fuh, “A review on the use of computational methods to characterize, design, and optimize tissue engineering scaffolds, with a potential in 3D printing fabrication,” *J. Biomed. Mater. Res. - Part B Appl. Biomater.*, vol. 107, no. 5, pp. 1329–1351, 2019, doi: 10.1002/jbm.b.34226.
- [175] J. Parthasarathy, B. Starly, S. Raman, and A. Christensen, “Mechanical evaluation of porous titanium (Ti6Al4V) structures with electron beam melting (EBM),” *J. Mech. Behav. Biomed. Mater.*, vol. 3, no. 3, pp. 249–259, 2010, doi: 10.1016/j.jmbbm.2009.10.006.
- [176] B. E. I. 604, “Plastics-Determination of compressive properties. British Standard,” *British Standard*, 1999. .
- [177] I. Diamant, R. Shahar, Y. Masharawi, and A. Gefen, “A method for patient-specific evaluation of vertebral cancellous bone strength: In vitro validation,” *Clin. Biomech.*, vol. 22, no. 3, pp. 282–291, 2007, doi: 10.1016/j.clinbiomech.2006.10.005.
- [178] R. E. Tomlinson and M. J. Silva, “Skeletal Blood Flow in Bone Repair and Maintenance,” *Bone Res.*, vol. 1, pp. 311–322, 2013, doi: 10.4248/BR201304002.

# Annex: Scientific Publications



---

## PUBLICATIONS

1. **Ebrahim Ahmed Ali Alkebsi**, Hacene Ameddah, Outtas Toufik and Abdallah Almutawakel, "Design of graded lattice structures in turbine blades using topology optimization", *International Journal of Computer Integrated Manufacturing*, (February 2021), DOI: [10.1080/0951192X.2021.1872106](https://doi.org/10.1080/0951192X.2021.1872106).
2. **Ebrahim Ahmed Ali Alkebsi**, Outtas Toufik, Abdallah Almutawakel, Hacene Ameddah and Toufik Kanit " *Design of Mechanically Compatible Lattice Structures Cancellous Bone Fabricated by Fused Filament Fabrication of Z-ABS Material*", *Mechanics of Advanced Materials and Structures*, (March 2022), DOI: [10.1080/15376494.2022.2053904](https://doi.org/10.1080/15376494.2022.2053904).
3. **ALKEBSI Ebrahim Ahmed Ali**, AMEDDAH Hacene and Outtas Toufik, "*L'utilisation de la fabrication additive en ingénierie tissulaire pour le cas d'une implantation tissulaire dans le défaut osseux de la jambe*", CAM2019 Congrès Algérien de Mécanique (23-26 février 2020), Ghardaïa- Algérie.
4. AMEDDAH Hacene, **ALKEBSI Ebrahim Ahmed Ali** and Outtas Toufik, "*The use of additive manufacturing for design of 3D scaffolds for bone tissue engineering*", 7th International Conference on Advances in Mechanical Engineering and Mechanics (16-18 December, 2019), Hammamet, Tunisia.
5. **Ebrahim Ahmed Ali Alkebsi**, Hacene Ameddah, Outtas Toufik, Abdallah Almutawakel and Alsamawi Almoutazbellah "*Comparison between Two Materials Used for Gas Turbine Blade Under Thermomechanical Analysis*" Alwaha Scientific Publishing Services SARL (ASPS) (**This paper will be published online in February 2022**)
6. Almoutaz Bellah Alsamawi, Nadir Boumechra, Abdallah Almutawakel, **Ebrahim Alkebsi**, Hamza Basri and Hicham Charrak "*Numerical investigation of fully encased composite columns with web or flange shear connectors under cyclic loading*" Alwaha Scientific Publishing Services SARL (ASPS) (**This paper will be published online in February 2022**)

## "التحسين الطوبولوجي للنمذجة متعددة المقاييس للهياكل المسامية والمعمارية"

ملخص

يركز هذا العمل البحثي على فهم التشكلات الهيكلية على مستويات مختلفة ودراسة سلوكها الميكانيكي في سياق تطوير تحسين الهيكل من خلال الاهتمام بإنشاء وتقييم مواد مسامية ومعمارية جديدة في مجالات الصناعة والفضاء وحتى التطبيقات الطبية. ركزنا على تطوير نهج نمذجة متعددة المقاييس للهياكل المسامية والمعمارية التي تسمح بإنتاج الهيكل عن طريق التصنيع الإضافي لتطبيقات الطيران والطب. لذلك، أظهرنا نهجاً يعتمد على الطباعة ثلاثية الأبعاد لإنتاج الهياكل من خلال عرض النتائج العددية والتجريبية في مجال الطيران والمجال الطبي. أولاً، قدمنا مرحلة التصميم المكافئ لنموذج CAD لشفرة التوربينات المصممة. من خلال تطبيق طريقة تحسين الطوبولوجيا لإيجاد التوزيع الأمثل لكثافة الهياكل الشبكية واختيار التقنية المقترحة لتصنيع الهياكل الشبكية. تم إجراء محاكاة عددية لريش التوربينات الغازية والحصول على قيم التشوه والضغط تحت الأحمال الحرارية الميكانيكية وعرض بعض النتائج ومناقشتها. من ناحية أخرى، تم إنشاء تصميم جديد يعتمد على ثلاثة هياكل شبكية من الأسطح الصغيرة الدورية الثلاثية (TPMS) بمسامية حجم مختلفة لتحل محل العظم الإسفنجي بناءً على التنبؤ بالصلابة الميكانيكية وأخيراً قدم بعض النتائج وتفسيراتها وناقشها.

### "Topological optimization for multi-scale modeling of porous and architectural structures"

Abstract

This research work focuses on understanding structural morphologies at different scales and studying their mechanical behavior in the context of the development of topology optimization by the concern of creation and valuation of new porous and architected materials in fields of industrial, aerospace, and even medical applications. We focused on developing a multi-scale modeling approach of porous and architectural structures allowing the production of the structure by Additive Manufacturing for aeronautical and medical applications. Therefore, we demonstrated an approach based on 3D printing of structure production by displaying the numerical and experimental results in the aerospace and medical field. Firstly, we introduced the design stage of the CAD model equivalent for the designed turbine blade. By applying the method of Topology Optimization for finding the optimal density distribution of lattice structures and selecting the proposed technique for manufacturing the lattice structures. Numerical simulations have been carried out for gas turbine blades and obtaining the deformation and stress values under thermomechanical loads, present some results, and discuss them. On another hand, created a new design based on three lattice structures from triply periodic minimal surfaces (TPMS) with a different volume porosity to replace cancellous bone based on predicting the mechanical stiffness. Finally, present some results and their interpretations and discuss them.

### "Optimisation topologique pour la modélisation multi-échelle de structures poreuses et architecturées"

Résumé

Ce travail de recherche porte sur la compréhension des morphologies structurelles à différentes échelles et l'étude de leur comportement mécanique dans le cadre du développement de l'optimisation topologique par le souci de création et de valorisation de nouveaux matériaux poreux et architecturés dans les domaines des applications industrielles, aérospatiales, voire médicales. Nous nous sommes concentrés sur le développement d'une approche de modélisation multi-échelle des structures poreuses et architecturales permettant la production de la structure par Fabrication Additive pour des applications aéronautiques et médicales. Par conséquent, nous avons démontré une approche basée sur l'impression 3D de la production de structures en affichant les résultats numériques et expérimentaux dans le domaine aérospatial et médical. Tout d'abord, nous avons introduit l'étape de conception du modèle CAO équivalent pour l'aube de turbine conçue. En appliquant la méthode d'optimisation de la topologie pour trouver la distribution de densité optimale des structures en treillis et en sélectionnant la technique proposée pour la fabrication des structures en treillis. Des simulations numériques ont été réalisées pour des aubes de turbines à gaz et l'obtention des valeurs de déformation et de contrainte sous charges thermomécaniques, présente quelques résultats et les discute. D'autre part, a créé une nouvelle conception basée sur trois structures en treillis à partir de surfaces minimales triplement périodiques (TPMS) avec une porosité volumique différente pour remplacer l'os spongieux en fonction de la prédiction de la rigidité mécanique. Enfin, présentez quelques résultats et leurs interprétations et discutez-les.